BEHAVIOUR OF SLOTTED AND FLEXIBLE PERFOBOND RIB SHEAR CONNECTORS

A Thesis

Submitted to the Faculty of Graduate Studies and Research

in Partial Fulfillment of the Requirements

for the Degree of

Master of Science

in the

Department of Civil Engineering

University of Saskatchewan

by

Feeruze Quddusi

Saskatoon, Saskatchewan

1994

COPYRIGHT

ABSTRACT

The perfobond rib connector is a new type of shear connector, first used in the construction of the Third Caroni bridge in Venezuela. Except for a limited number of proprietary tests conducted in Germany, research on perfobond rib shear connectors has been carried out mainly in Canada. Results of earlier experimental investigations at the University of Saskatchewan showed that the perfobond rib connectors performed satisfactorily in both solid slabs and slabs with wide and narrow ribbed metal decks. The load carrying capacity and the overall ductility improved considerably when reinforcing bars were passed through the perfobond rib holes. The overall conclusion drawn from the investigations was that the perfobond rib connector is a viable alternative to the headed studs.

This thesis presents the results of a current investigation which attempts to address some of the minor deficiencies of the perfobond rib connectors identified from earlier tests. Although previous investigation showed that the effect of passing reinforcing bars through the rib holes was an increase in the capacity of the connectors, the task associated with this exercise in an actual construction site may be cumbersome. The earlier test results also showed that the perfobond rib shear connector is not as flexible as headed studs. Lack of flexibility encourages unequal distribution of shear load between the connectors. These minor drawbacks may be rectified by replacing some of the holes with vertical slots. The vertical slots would increase the flexibility of the perfobond connector as well as greatly simplify the task of placing reinforcing bars through the rib holes. Two series of tests involving 24 push-out specimens were carried out to investigate the effectiveness of slotted

perfobond rib connectors in comparison to normal perfobond rib connectors and headed studs.

The flexibility of a perfobond rib connector can also be enhanced by reducing the thickness of the plate. Besides savings in the cost of material, thinner plates would allow punching of holes rather than drilling. Previous investigations at the University of Saskatchewan were limited to a plate thickness of 12 mm. In this research project, the effectiveness of 6 mm thick perfobond rib connectors was investigated by conducting two additional series of tests involving 32 push-out specimens.

In addition to realizing the aforementioned objectives, the test program was designed to provide further information on a number of important issues such as the influence of concrete dowels, concrete strength, and additional transverse reinforcement through the rib openings. The experimental program also included two additional series involving 32 specimens which were tested to investigate the effects of welding a face plate in front of a perfobond rib connector and to study the influence of rectangular openings.

Shank shear was the principal mode of failure in specimens with headed studs. In specimens with perfobond ribs, failure was triggered by the longitudinal splitting of the concrete slab along the line of the shear connector, followed by the crushing of concrete in the bearing zone immediately in front of the perfobond rib. A considerable deformation was observed in the perfobond rib connectors with thin and/or slotted ribs.

The test results indicated that slotted perfobond rib connectors improve the overall ductility of the test specimens. However, the increased concrete

dowel area provided by the slots in the perfobond rib connector tends to offset the increase in flexibility at low load levels. The addition of transverse reinforcement through the slots increases the ultimate load and the load retention capability. The specimens with 6 mm thick perfobond rib connectors exhibited more ductile behaviour than those with 12 mm thick perfobond rib connectors although their ultimate shear capacity was somewhat reduced. This test program confirmed the ability of perfobond rib connectors to retain a substantial portion of the ultimate load in the unloading stage of the load-displacement curve.

As expected, the face plate greatly enhanced the performance of the perfobond rib connector. The increase in the ultimate load capacity was in excess of 30%. There was also a substantial increase in the ductility. However, for these specimens, failure was caused largely due to the crushing of concrete in front of the face plate. Once the concrete crushed, the load retention capability decreased rapidly.

The load-slip behaviour of specimens featuring perfobond rib connectors with square and circular holes of equal area was almost identical. The sharp corners of the square hole did not produce any noticeable detrimental effects.

Finally, the results presented in this thesis indicate that thin and slotted perfobond rib connectors can be effectively used in composite beams with solid slabs .

ACKNOWLEDGEMENTS

My heartfelt thanks and gratitude are reserved for my supervisor, Professor Mel U. Hosain. His very kind, invaluable guidance throughout every stage of the program will remain in my heart forever.

The sincere suggestions and criticisms of Professor Tel Rezansoff and Professor Bruce Sparling during planning and execution of the experimental program is acknowledged with much gratitude.

I also would like to thank the very valuable assistance provided by my good friend Mr. Dan Stott of the Structural Laboratory and by my fellow graduate students and good friends dear Mr. C. Androutsos, Mr. E. Oguejiofor, Mr. S. Gowrishankar, Mr. J. Ju and Mrs. E. Saravanos.

Many thanks and appreciations to the Natural Science and Engineering Research Council of Canada (NSERC) for providing all the required funds needed for the experimental investigation.

Finally, I wish to thank my beloved wife Dr. Sima Quddusi, my loving parents and my parents in-law for their kind support and encouragement throughout the program.

TABLE OF CONTENTS

LIST OF TABLES

LIST OF FIGURES

CHAPTER ONE
INTRODUCTION

1.1 Background

Composite steel-concrete beams have been used for a long time in bridge and building construction. An essential element of a composite beam is the shear connection between the concrete slab and steel section. The shear connection is usually provided by mechanical devices, called shear connectors, which are welded to the steel section and embedded in the concrete. Shear connectors resist the horizontal shear and vertical uplift forces at the steel-concrete interface, hence ensuring that the steel section and concrete slab act together as a composite unit.

The headed stud is the most widely used shear connector in composite construction. Recently, a new type of shear connector called perfobond rib connector was introduced by the German consulting engineering firm, Leonhardt, Andrå and Partners of Stuttgart, during the construction of the Third Caroni Bridge in Venezuela (Zellner 1987). As shown in Fig. 1.1, it is simply a flat plate with a number of holes punched through it. Concrete flows through the rib holes forming dowels that provide resistance in both the vertical and horizontal directions. The advantages of the perfobond rib connector include the fact that it can be installed without the need for an expensive machine. The installation procedure would be similar to that used for beam stiffeners and connection components. Thus, adopting this option eliminates one trade on the job site, the shear connector installation crew, resulting in further savings in construction costs. Inspection procedures such as bending tests required for headed studs may not be necessary for

perfobond type connectors. It is robust and can take rough handling. Only a few perfobond rib connectors will replace a large number of headed studs. This would avoid the clutter usually produced by studs which creates an unsafe workplace.

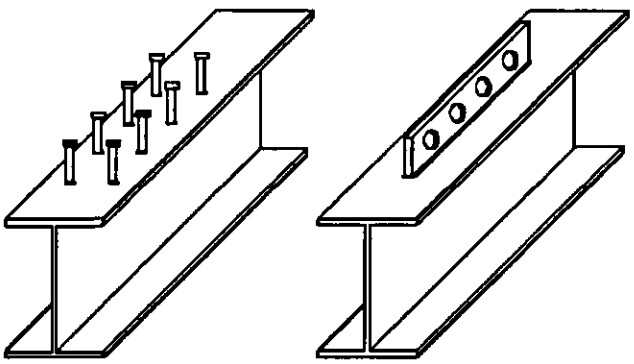

(a) Headed Studs (b) Perfobond Rib Connector

Fig. 1.1 Headed shear studs and perfobond rib shear connectors

Some of the other potential advantages of perfobond rib connectors can be easily recognized (Oguejiofor and Hosain 1993). For example, these connectors can be produced in small fabricating plants, can be easily standardized and mass produced, or custom made for a specific job. If necessary, the shear capacity of the connection at a particular location can be increased by inserting transverse reinforcing bars through the holes of the perfobond rib connectors.

Apart from its use in steel beam-concrete slab shear connection, this connector could also be conveniently applied in connecting floor beams to shear walls in high rise buildings. Other innovative applications are presently being investigated in Australia (Roberts and Heywood 1993).

1.2 Previous Investigation

Except for a limited number of proprietary tests conducted in Germany (Zellner 1987), research on perfobond rib shear connectors has been carried out mainly at the University of Saskatchewan in Saskatoon, Canada. Following a preliminary investigation by Antunes (1988), a comprehensive experimental program was started at the University of Saskatchewan. Four phases of tests have already been completed involving specimens with solid slabs and those with metal deck placed parallel to the beam. The first phase involved 56 push-out specimens (Veldanda and Hosain 1992) while the second phase included 6 full size composite beam specimens (Oguejiofor and Hosain 1992). The objectives of these projects were, among others, to investigate the feasibility of using perfobond rib shear connectors in composite floor systems and to compare their performance vis-a-vis that of headed studs.

Results of the experimental investigations showed that the perfobond rib connectors performed satisfactorily in both solid slabs and slabs with wide and narrow ribbed metal decks. Improved performance was obtained when reinforcing bars were passed through the perfobond rib holes. The overall conclusion drawn from the investigations was that the perfobond rib connector was a viable alternative to the headed studs.

The third and fourth phases involved an extensive investigation of several configurations of the perfobond rib connector using push-out specimens and full size beam specimens. The third phase included 48 push-out specimens (Oguejiofor and Hosain 1994a) while the fourth phase had 6 full size composite beam specimens (Oguejiofor and Hosain 1994b). The test results indicated that the capacity of the perfobond rib connector

increases with an increase in the number of concrete dowels, provided that the dowels have a minimum center to center spacing of two times the diameter of the dowels. Also, the capacity of the shear connection was found to be dependent on the concrete strength and the amount of transverse reinforcement. A semi-empirical expression for predicting the capacity of perfobond rib connectors in a solid slab was formulated. Results of the full size beam specimens confirmed the validity of this expression.

Current focus of research at the University of Saskatchewan is on the modification of the configuration of this connector to enhance its performance and to conduct numerical modeling of its behaviour (Oguejiofor and Hosain 1994c).

1.3 Objectives

Although Veldanda (1991) showed that the effect of passing reinforcing bars through the perfobond rib connector holes was an increase in the capacity of the connectors, the task associated with this exercise in an actual construction site may be cumbersome. The earlier test results also showed that the perfobond rib shear connector is not as flexible as headed studs. Lack of flexibility encourages unequal distribution of shear load between the connectors and causes early formation of cracks in the concrete.

These two minor deficiencies may both be rectified by introducing vertical slots as shown in Fig. 1.2. The vertical slot is expected to increase the flexibility of the connector as well as greatly simplify the task of placing reinforcing bars through the perfobond rib holes. Four series of tests involving 48 push-out specimens were carried out to investigate the

effectiveness of slotted perfobond rib connectors in comparison to normal perfobond rib connectors and headed studs.

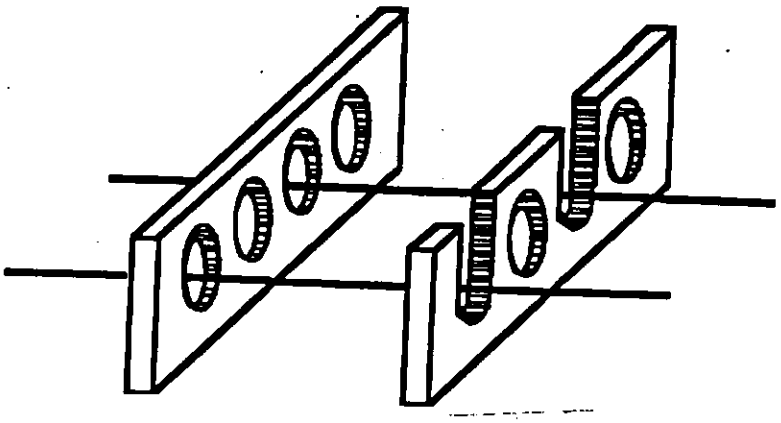

Fig. 1.2 Normal and slotted perfobond rib connectors

The flexibility of a perfobond rib connector can also be enhanced by reducing the thickness of the plate. Besides savings in the cost of material, thinner plates would allow punching of holes rather than drilling which is a more costly operation. Previous investigations (Veldanda and Hosain 1992; Oguejiofor and Hosain 1992) were limited to a plate thickness of 12 mm as shown in Fig. 1.3(a). In this research project, the effectiveness of 6 mm thick perfobond rib connectors was investigated by conducting two more series of tests involving 32 push-out specimens.

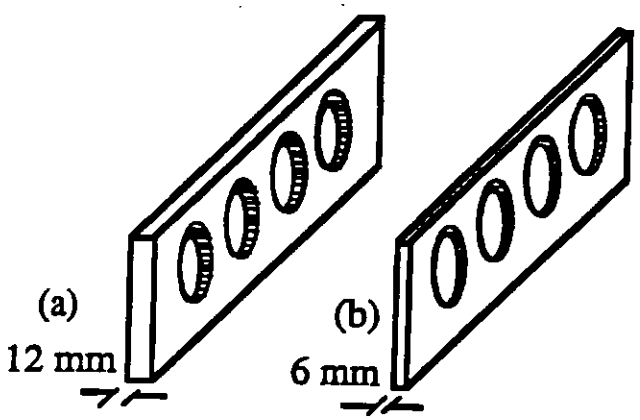

Fig. 1.3 Thick and thin perfobond rib connector

As before, this study included a number of specimens with headed studs to allow comparison.

In addition to realizing the aforementioned objectives, the test program was designed to provide further information on a number of important issues. Specifically, the study focused on the effect of the following parameters on the shear capacity of the connection:

(i) Concrete dowels
(ii) Concrete strength
(iii) Additional transverse reinforcement through the rib openings

According to Veldanda (1991), a significant portion of the ultimate shear resistance of a perfobond rib connector is provided by the concrete dowels. Test results indicated that this additional strength is derived from a double shear failure mechanism. During the course of the present investigation, it was suggested by a member of the thesis advisory committee to investigate the effects of welding a face plate in front of a perfobond rib connector as shown in Fig. 1.4. A suggestion was also received from a consulting engineer in England (Appendix C) to investigate the possibility that load transfer occurs through a cone of compression radiating from the back surface of the hole. This issue can be resolved by testing a number of push-out specimens featuring perfobond rib with circular and rectangular openings of approximately the same cross-sectional areas, as illustrated in Fig. 1.5. If load transfer does occur through radiation, a rectangular hole with the larger contact area than that of a round one should provide higher resistance.

Two additional series of tests involving 32 specimens were carried out to address these two issues.

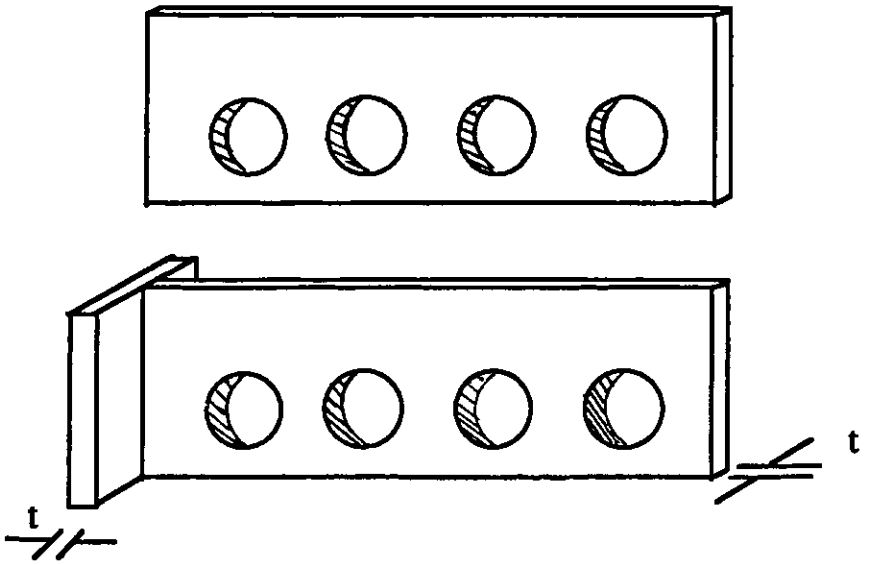

Fig. 1.4 Perfobond rib connector with and without face plate

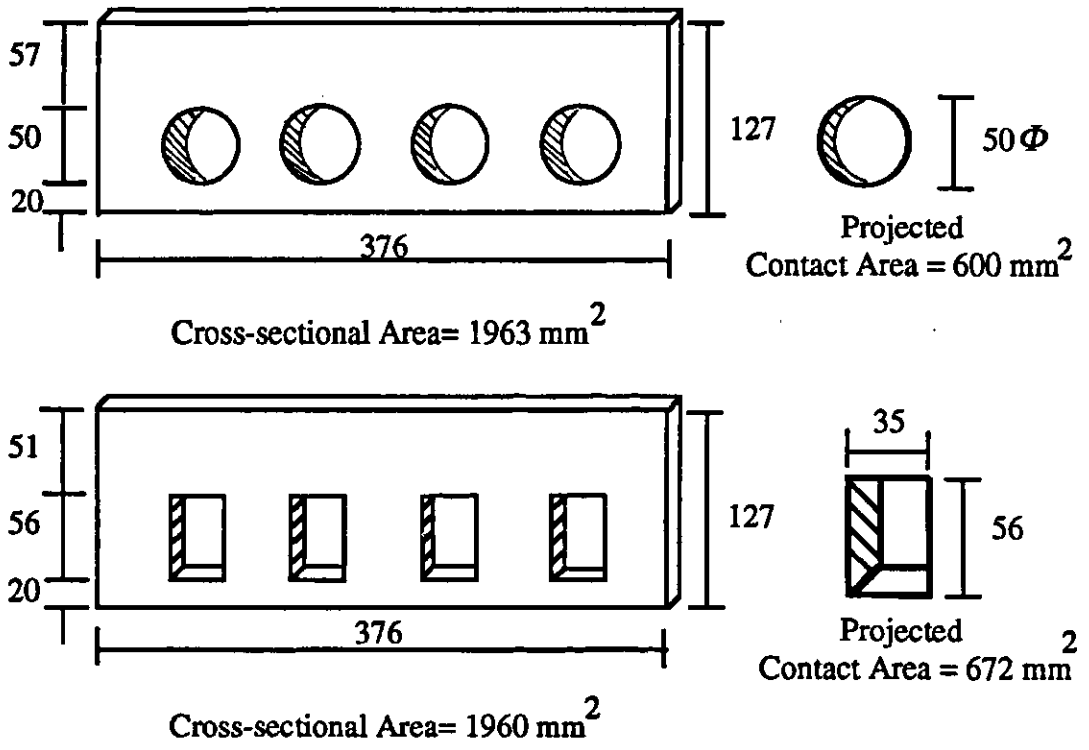

Fig. 1.5 Perfobond rib connector with circular and rectangular openings

In summary, the objectives of this investigation were as follows:

1. To investigate the effectiveness of slotted perfobond rib connectors in comparison to normal perfobond rib connectors and headed studs.

2. To investigate the effectiveness of 6 mm thick perfobond rib connectors in comparison to 12 mm thick perfobond rib connectors and headed studs.

3. To obtain further information on the following issues:

   (i) Contribution of concrete dowels
   (ii) Effect of concrete strength
   (iii) Effect of additional transverse reinforcement through the rib openings

In addition, an attempt was made to address the following topics:

   (i) Behaviour of perfobond rib connectors with face plate
   (ii) Behaviour of perfobond rib connectors with rectangular openings

CHAPTER TWO
EXPERIMENTAL PROGRAM

2.1 Test Program

The test program was divided into two phases. In the first phase, four series of tests involving 48 push-out specimens were carried out to investigate the effectiveness of slotted and thin perfobond rib connectors in comparison to normal perfobond rib connectors as well as headed studs. The second phase consisted of two series of tests involving 32 push-out specimens. These specimens were tested to investigate the effects of welding a face plate in front of a perfobond rib connector and to study the influence of rectangular openings.

As shown in Fig. 2.1, a typical push-out specimen consisted of a short steel beam section held in a vertical position by two identical reinforced concrete slabs. The concrete slabs were attached to the beam flanges by shear connectors. The assembly was subjected to a vertical load which produces shear force along the interface between the concrete slab and the beam flange on both sides. All the specimens had solid reinforced concrete slabs with a thickness of 150 mm. The height and width of the slabs were 712 mm and 530 mm respectively . Within each series, most of the specimens were fabricated with perfobond rib connectors and the rest with 19 mm x 125 mm Nelson headed studs for the purpose of comparison.

In all the specimens, reinforcement was provided using No. 10 reinforcing bars. The longitudinal reinforcement consisted of four bars. A typical arrangement of transverse reinforcement consisted of three

reinforcing bars, two of which were placed 100 mm apart in the area where longitudinal splitting was likely to originate in the loaded end of the slab and the third one was placed on the leeward side as shown in Figs. 2.1 and 2.2. Additional transverse reinforcing bars were passed through the rib holes of some of the specimens. In the specimens with headed studs, the amount of transverse reinforcement was the same as that used in the companion specimens with perfobond rib connectors.

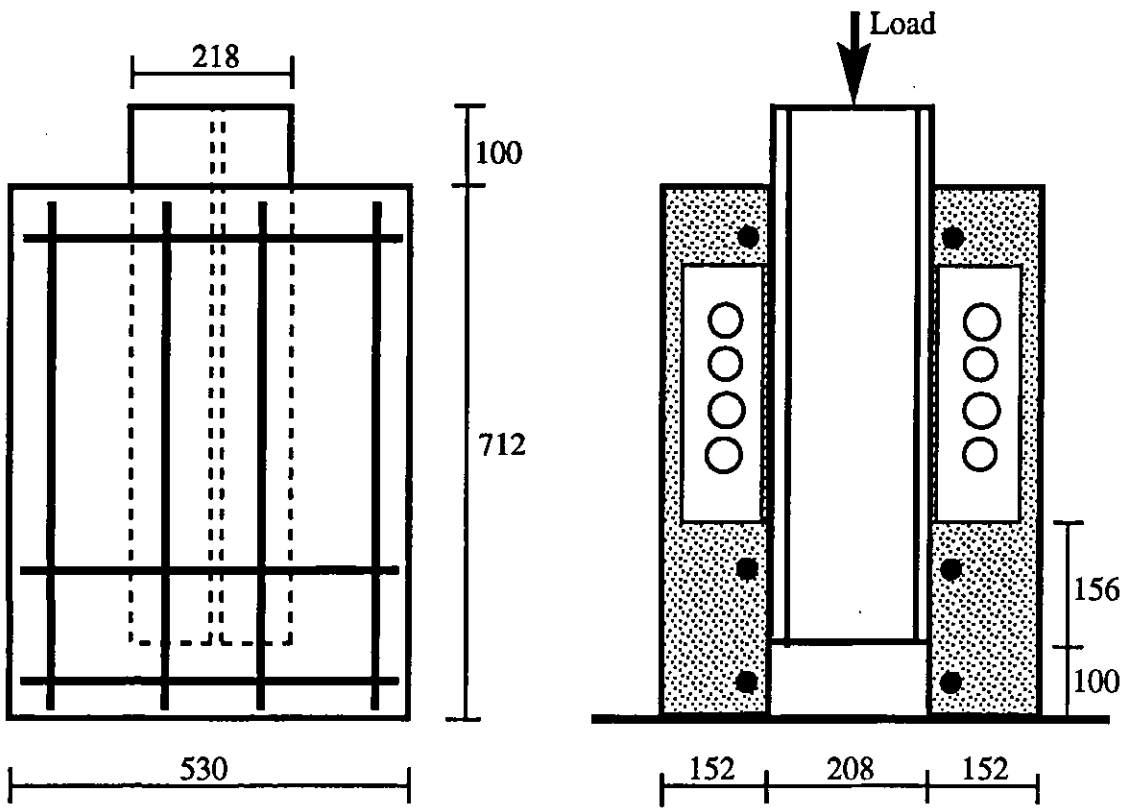

Fig. 2.1 Dimensions of the push-out test specimens (mm)

In addition to the transverse reinforcement, a single layer of 152 x 152 x MW 18.7 x MW 18.7 welded wire mesh was used in the slab of all specimens except those in Series 1.

The number of studs in the companion specimens were chosen on the assumption that one hole in a perfobond rib connector was equivalent to one headed stud of the same height as the perfobond rib connector. This was done to provide a basis for comparison.

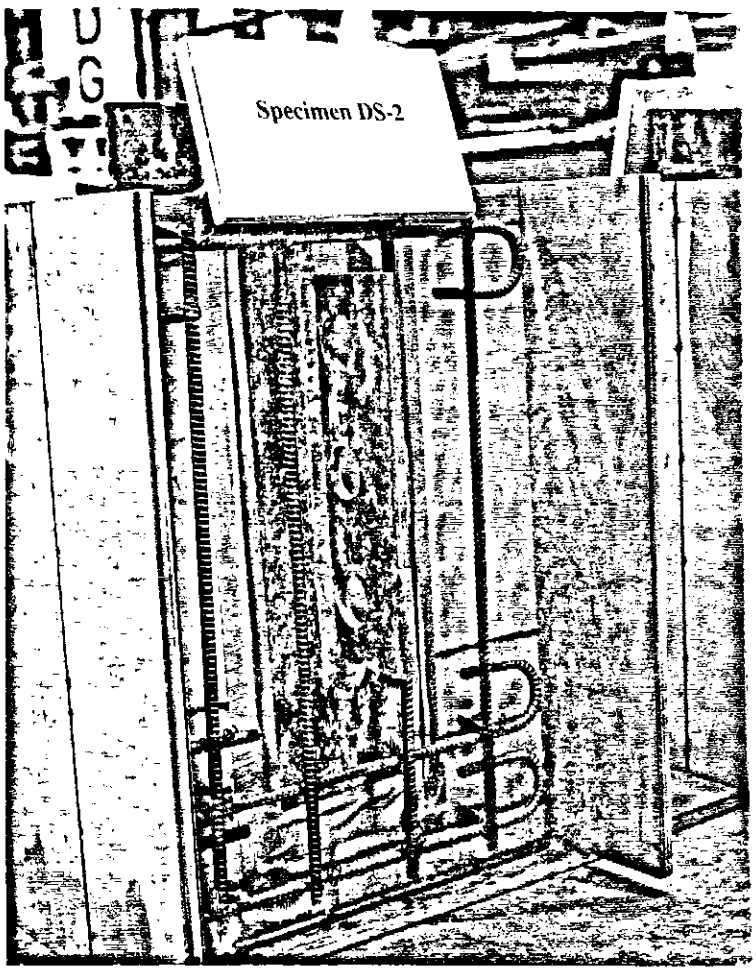

Fig. 2.2 Typical position of reinforcement

2.2 Experimental parameters

The test program was divided into two phases. The first phase consisted of four series of tests while two series of tests were included in phase two. A summary of the geometric properties of the specimens is included in Tables

2.1 to 2.6 which are presented at the end of this chapter. Each series was designed to study the influence of a specific set of test parameters.

PHASE ONE

In the first phase, the test parameters were the types of perfobond rib connectors, the plate thickness, the amount and location of transverse reinforcement and the compressive strength of concrete. Six different types of perfobond rib connectors were investigated. The dimensions of these perfobond rib connectors are shown in Fig. 2.3.

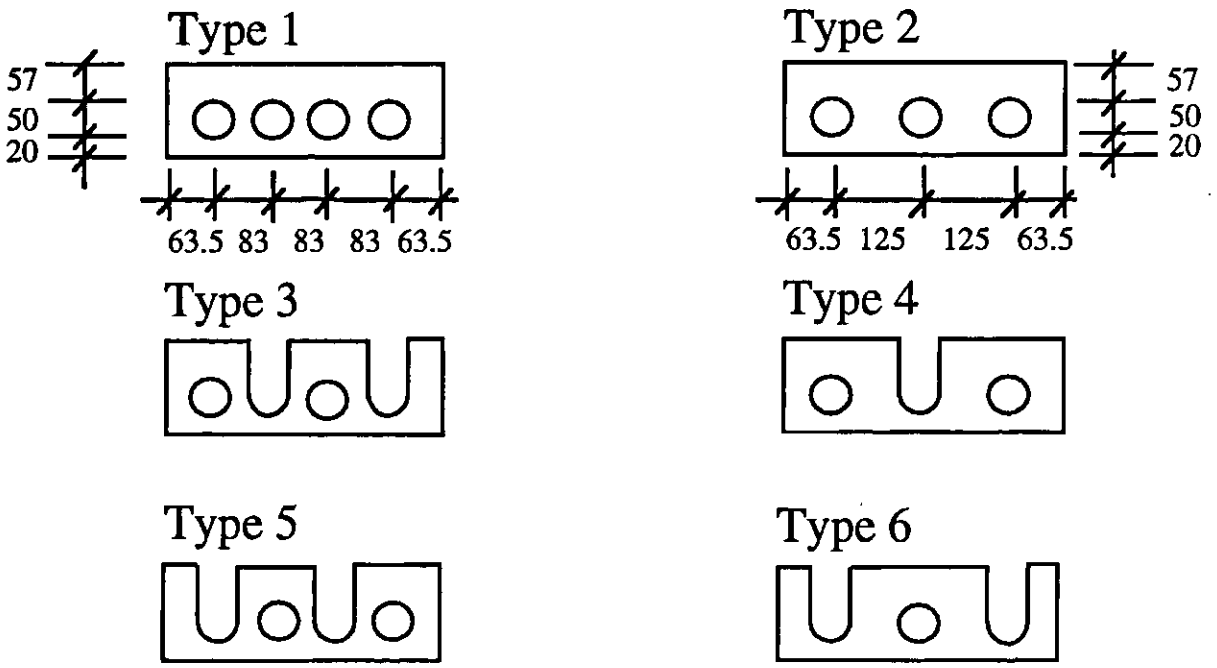

Fig. 2.3 Types of perfobond rib connectors

The first two types, with four and three holes respectively, were investigated by Veldanda and Hosain (1992) in an earlier study. These two will be referred to as "normal" perfobond rib connectors. Type 3 and Type 5 slotted perfobond rib connectors are companions of the Type 1 connector. Likewise, Type 4 and Type 6 slotted perfobond rib connectors are

companions of the Type 2 connector. Two different plate thicknesses, 12 mm and 6 mm, were used. Forty one specimens had 12 mm thick plates, while twenty nine specimens had 6 mm thick plates. In ten specimens, 19 mm x 125 mm headed studs were used. Photographs of some of the perfobond rib connectors are presented in Fig. 2.4(a) and (b). Individual characteristics of each series are described in detail in the following sections.

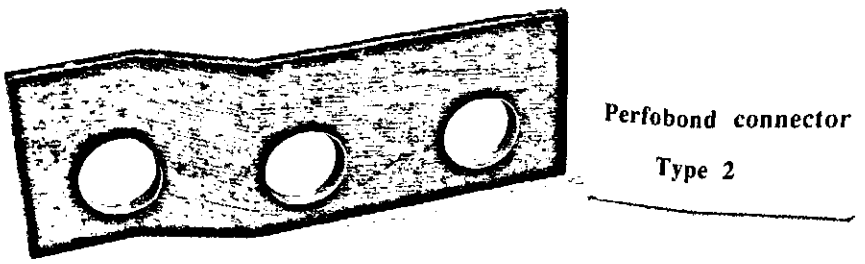

a) Type 2 perfobond rib connector

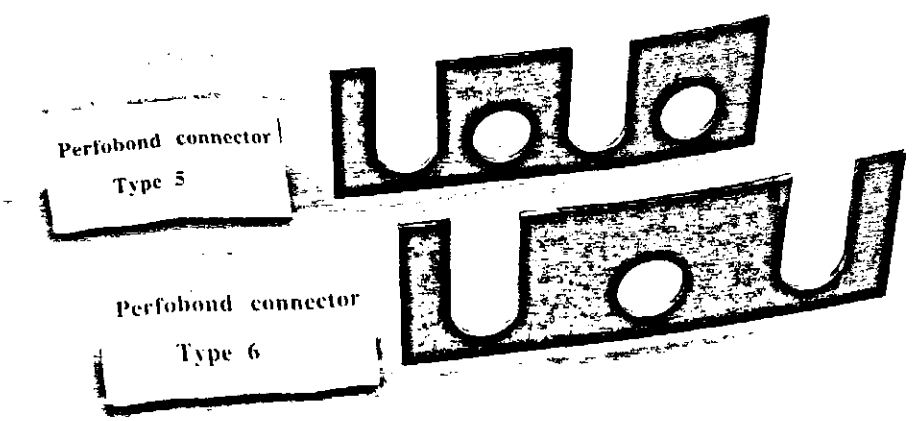

(b) Types 5 and 6 perfobond rib connectors

Fig. 2.4 Photographs of some perfobond rib connectors

2.2.1 Test Series 1

The characteristics of individual specimens in Series 1 are shown schematically in Table 2.1. The purpose of this initial test series was to explore the feasibility of using slotted perfobond rib connectors. All ten specimens in this series featured 12 mm thick perfobond rib connectors. The first two specimens, AS-1 and AS-2, were control specimens and featured Type 1 and Type 2 normal perfobond rib connectors, respectively. Their performance was compared with that of specimens using slotted perfobond rib connectors. As indicated earlier, the main objective was to ascertain if the slotted perfobond rib connector enhances the ductility. Specimens AS-7 and AS-9, featuring Type 3 and Type 5 slotted perfobond rib connectors respectively, were companions of control specimen AS-1. Similarly, specimens AS-3 and AS-5, featuring Type 4 and Type 6 slotted perfobond rib connectors, respectively, were companions of control specimen AS-2.

Series 1 also included four additional specimens which were tested to evaluate the influence of the reinforcing bars placed through the slots of the connectors. These four specimens were AS-4, AS-6, AS-8 and AS-10. While specimens AS-8 and AS-10 were the companion specimens of the control specimen AS-1, specimens AS-4 and AS-6 were the companion specimens of the control specimen AS-2.

2.2.2 Test Series 2

In this series, a total of twelve specimens were tested as listed in Table 2.2. The first 10 specimens, BS-1 to BS-10, were identical to specimens AS-1 to AS-10 of Series 1 except that a layer of 152 x 152 x MW 18.7 x MW 18.7 welded wire mesh was used in their slabs. In the two additional specimens, BS-11 and BS-12, 19 mm x 125 mm Nelson headed studs were

used for the purpose of comparison. These two specimens had three and four studs, respectively, in order to serve as companion specimens of the control specimens BS-1 and BS-2.

2.2.3 Test Series 3

The purpose of this test series was to investigate if the ductility of the perfobond rib connector could be improved by reducing the plate thickness.

As shown in Table 2.3, a total of twelve specimens were tested. The first 10 specimens, CS-1 to CS-10, were identical to specimens BS-1 to BS-10 of Series 2 except that the plate thickness was 6 mm instead of 12 mm. Specimens CS-11 and CS-12, featuring headed studs, were identical to BS-11 and BS-12, respectively.

2.2.4 Test Series 4

The main purpose of this test series was to study the effects of plate thickness on the shear capacity of unslotted perfobond rib connectors. A total of fourteen specimens were tested (Table 2.4). Four specimens featured 12 mm thick Type 1 and Type 2 perfobond rib connectors, four specimens had 6 mm Type 1 and Type 2 perfobond rib connectors and in four specimens Nelson studs were used. In order to evaluate the contribution of the concrete dowels, two specimens (DS-5 and DS-10) contained unperforated plate connectors. In four specimens (DS-3, DS-4, DS-8 and DS-9), additional transverse reinforcements were passed through the rib holes.

PHASE TWO

In this phase, a total of 32 specimens were tested to address two additional issues: the use of face plates and the effectiveness of rectangular

openings. The main objective was to study the effects of using a narrow plate in front of the perfobond rib connector as shown in Fig. 2.5. By distributing the bearing pressure over a larger area, the plate was expected to reduce the susceptibility to splitting as well as to improve the ductility. These advantages must of course be weighed against the expected additional costs.

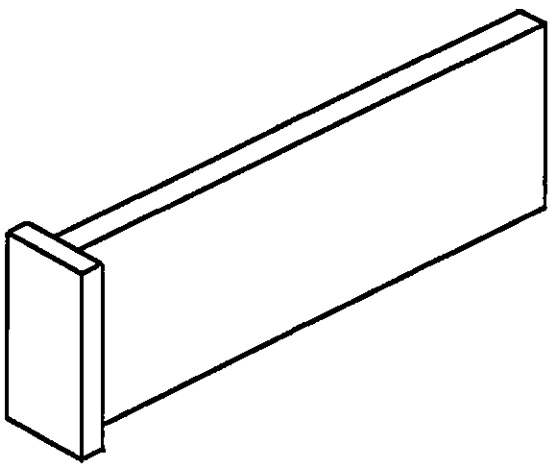

Fig. 2.5 Perfobond rib connector with face plate

One of the objectives of this investigation was to study the shear transfer mechanism between the perfobond rib connector and the concrete slab. Referring to Fig. 2.6, a part of the total shear load is transferred by a bearing against the plate tip. Previous tests showed that the rest of the shear load is carried by the concrete dowels which are subjected to double shear. However, there is the possibility of shear transfer through radiation against the projected wall area of each hole as illustrated in Figs. 2.7(a) and 2.7(b). If the load transfer is through radiation, a rectangular opening with the longer side oriented vertically would be more effective than a circular opening with the same cross-sectional area since the rectangular opening would have a larger contact area. Unfortunately, when the perfobond rib

connectors for these tests were fabricated the heights of the rectangular openings were inadvertently made equal to the hole diameter of the companion specimens. With the same projected contact areas, these specimens were not suitable to study the shear transfer mechanism. However, they were tested to study the difference in the behaviour of rectangular and circular holes.

Individual characteristics of Series 5 and 6 specimens are described in detail in the following sections.

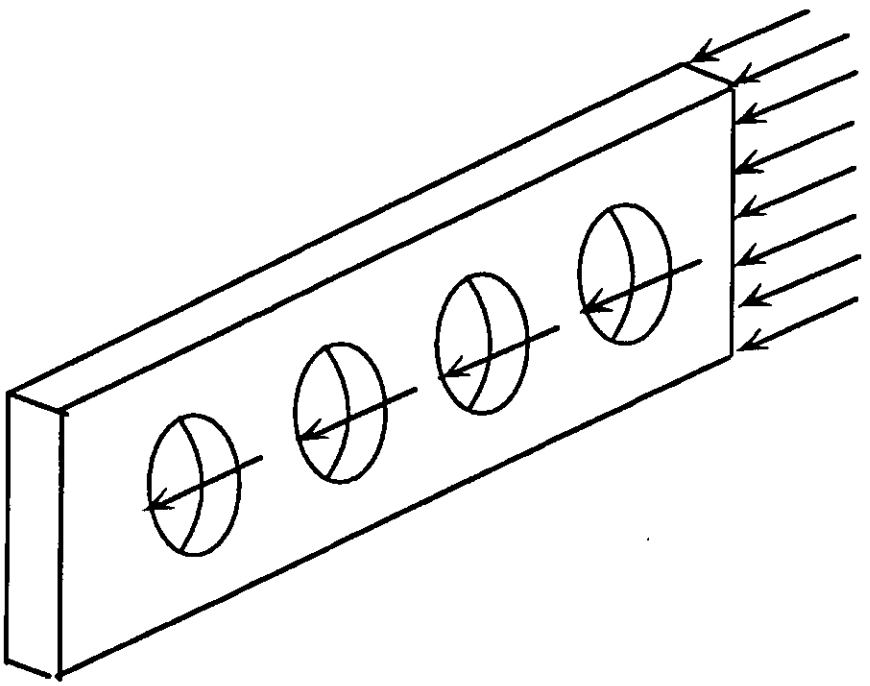

Fig. 2.6 Shear transfer in plate tip

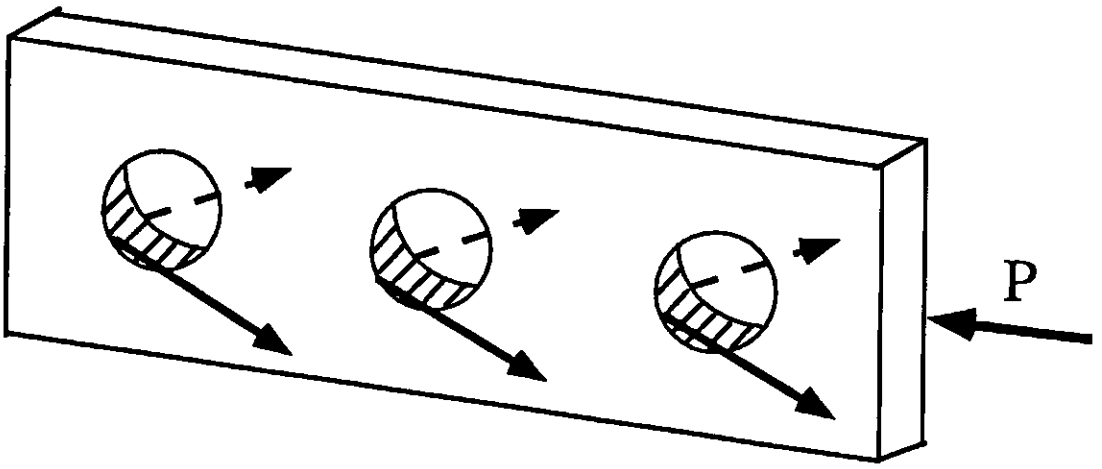

(a) Shear transfer in circular openings

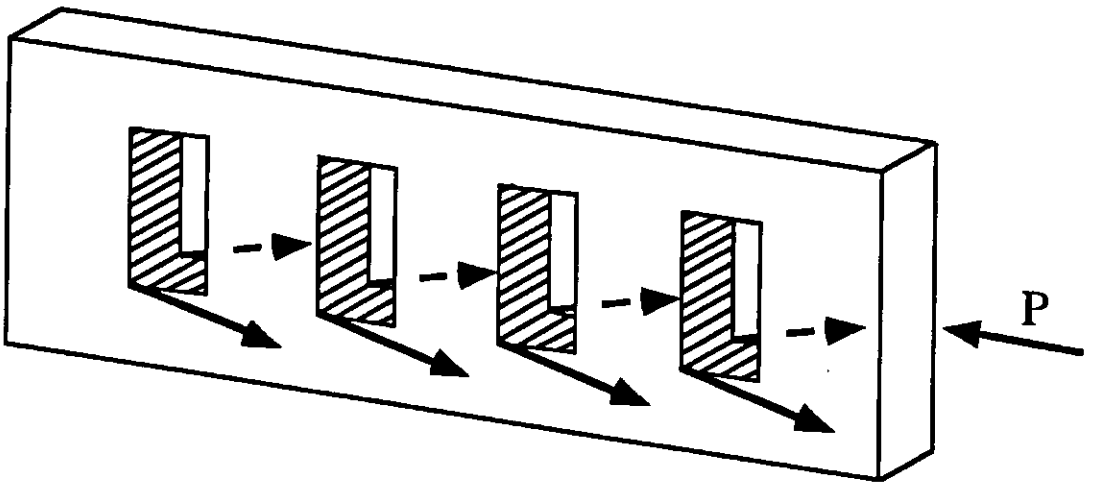

(b) Shear transfer in rectangular openings

Fig. 2.7 Shear transfer mechanisms

2.2.5 Test Series 5

The characteristics of individual specimens in Series 5, which included sixteen specimens, are shown schematically in Table 2.5. In specimens ES-15 and ES-16, headed studs were used. The other fourteen specimens featured 6 mm thick perfobond rib connectors. Ten specimens were tested, five with and five without face plates, to study the effects of using a narrow plate in front of the perfobond rib connector. Fig. 2.8 shows a photograph of the companion specimens ES-1 and ES-5.

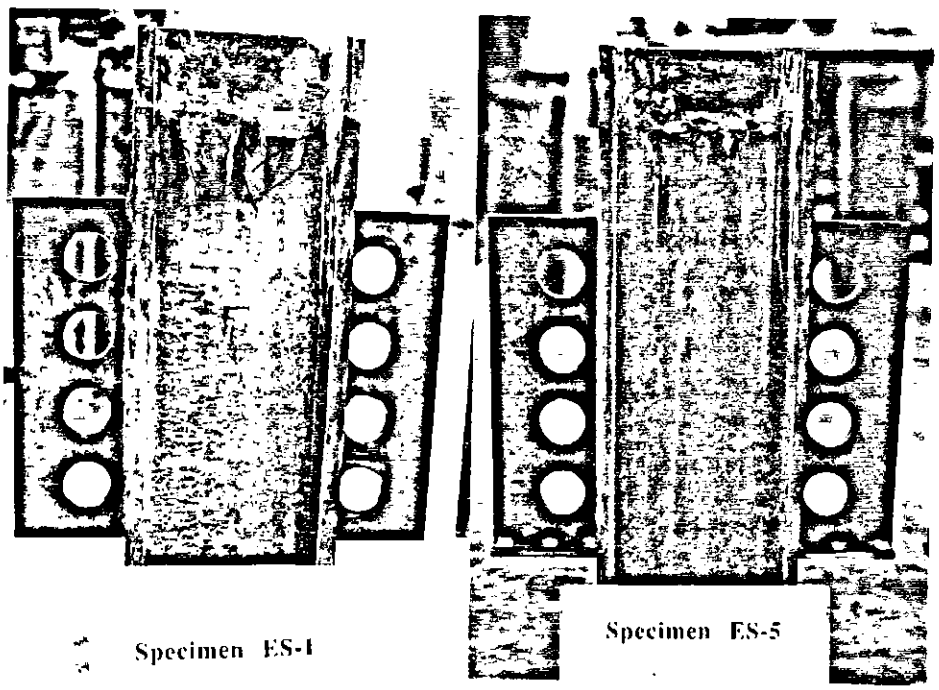

Fig. 2.8 Type 1 perfobond rib connectors with and without face plate

Specimen ES-1 featured Type 1 perfobond rib connector. Type 1 perfobond rib connector was also used in specimen ES-5, but a 50 mm wide by 127 mm high steel plate was welded on to the edge facing the thrust from the concrete slab. The thickness of the plate was 6 mm, the same as that of the connector. Referring to Table 2.5, specimens ES-6, ES-7, ES-8 and ES-10 served as companion specimens to ES-2, ES-3, ES-4 and ES-9,

respectively. As shown in Fig. 2.9, companion specimens ES-9 and ES-10 featured unperforated plate connectors. These specimens were tested to evaluate the contribution of the concrete dowels.

Four specimens had perfobond rib connectors with rectangular openings instead of circular holes and rounded slots. The dimensions of these specimens together with those of the companion specimens ES-1 and ES-2 are presented in Fig. 2.10.

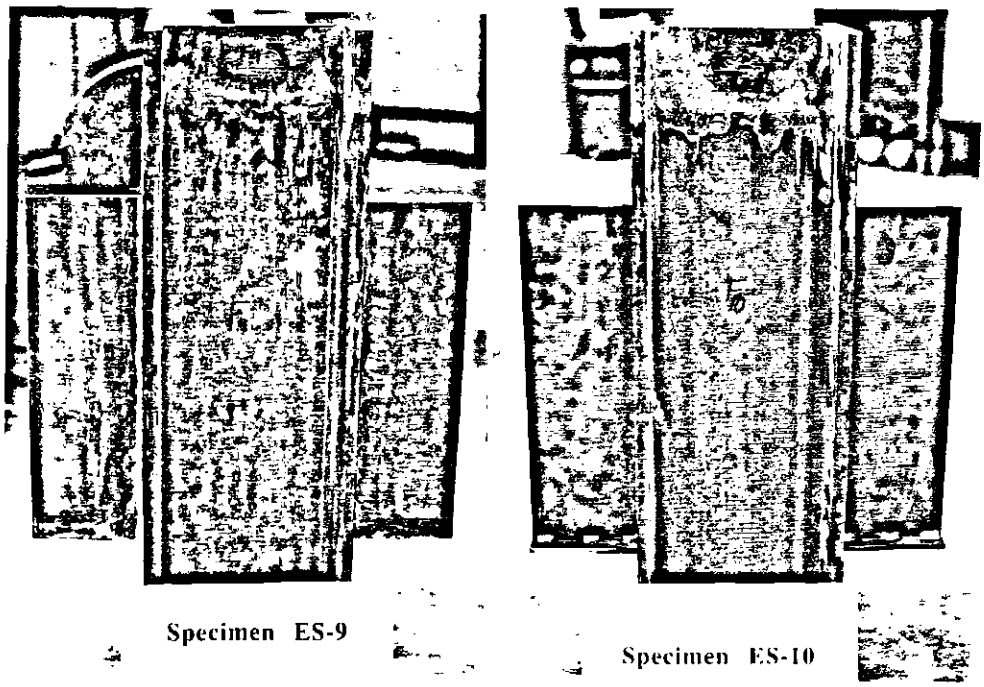

Fig. 2.9 Unperforated perfobond with and without face plate

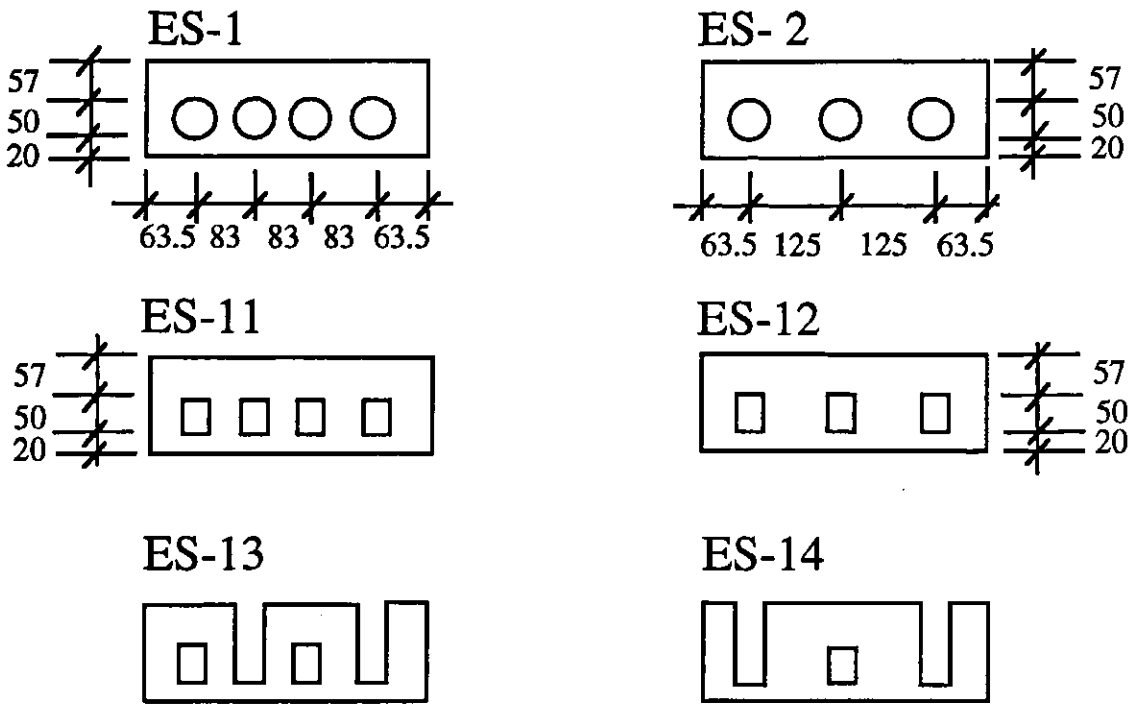

Fig. 2.10 Perfobond with circular and rectangular openings

A photograph of specimens ES-11 and ES-13 is shown in Fig. 2.11. As before, two specimens with headed studs were tested for comparison.

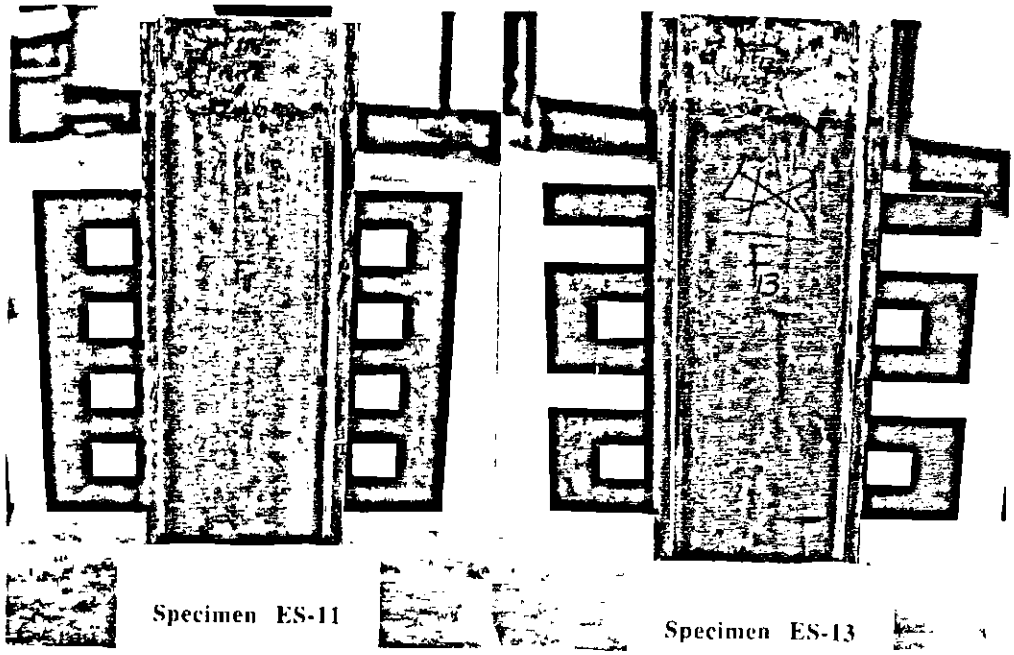

Fig. 2.11 Perfobond rib connectors with rectangular openings

2.2.6 Test Series 6

This series included sixteen specimens. The first 14 specimens were identical to those of Series 5 except that the thickness of the plate was 12 mm. As shown in Fig. 2.12, the last two specimens, FS-15 and FS-16, featured 75 mm and 100 mm wide face plates, respectively.

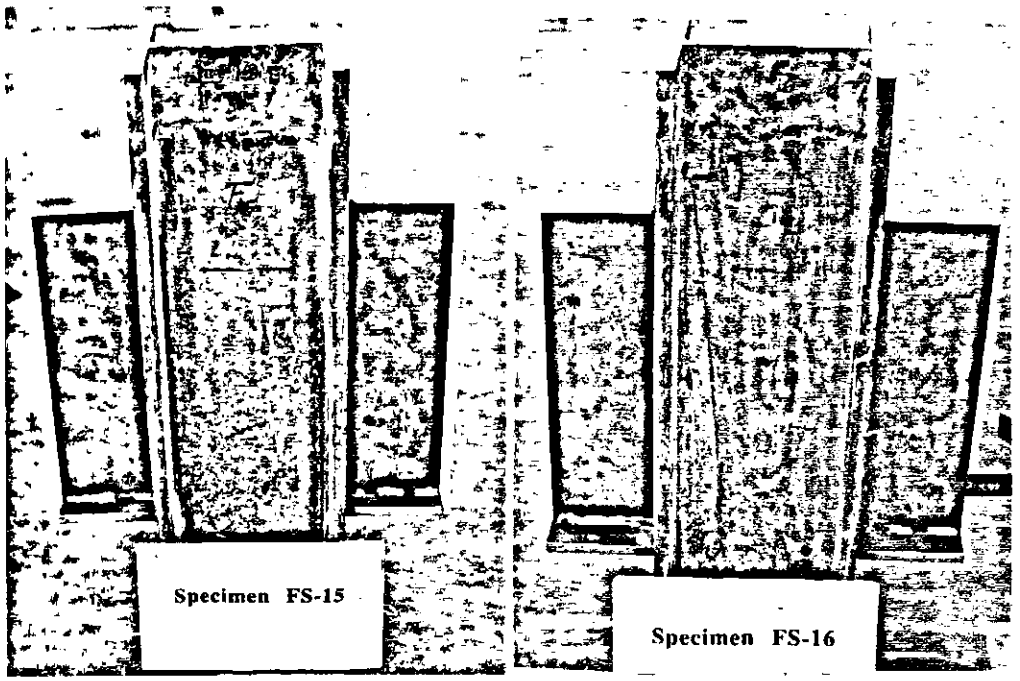

Fig. 2.12 Unperforated perfobond with face plate

2.3 Fabrication of the test specimens

A 6100 mm long W200 X 59 beam section, conforming to G40.21M-300W, was cut into twelve 712 mm long pieces. The perfobond ribs were fabricated in the engineering shops by cutting 12 mm and 6 mm thick flat plates and drilling holes in the individual pieces. Vertical slots were provided in some of the perfobond rib connectors. The perfobond ribs were welded to the beam flanges by a qualified welder. The headed studs were installed using a welding gun connected to a TR 2400 stud welding system.

2.4 Test setup and instrumentation

As shown in Fig. 2.13, the test setup was similar to that used for earlier push-out tests (Veldanda 1991). Loads were applied using an Amsler Hydraulic Testing Machine with a capacity of 2000 kN. Before placing the specimen in the machine, a 25 mm thick steel plate was placed on the loading frame to serve as a base plate for the specimen. Two dial gages of an accuracy of 0.0254 mm were installed on either side of the specimen to measure the slip at the interface. All the specimens were tested under monotonic loading. Initially, the load was applied in increments of 50 kN; when the load-slip curve started to deviate from a straight line, the load increment was reduced to 20 kN.

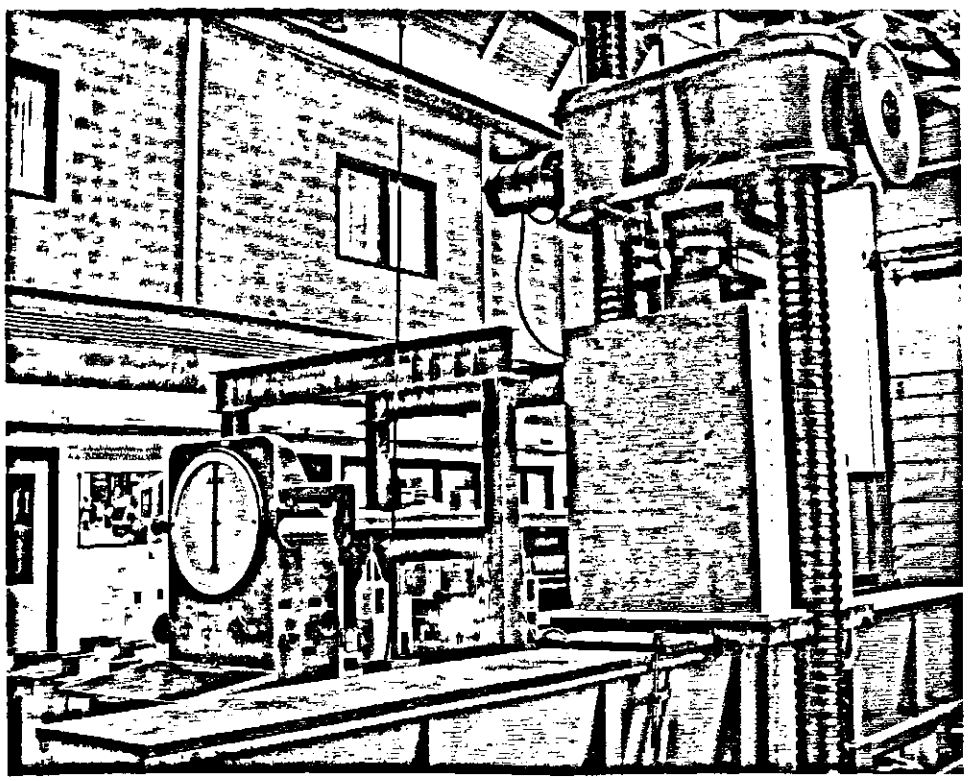

Fig. 2.13 Test setup

2.5 Material properties:

At the time of casting each series of test specimens, 305 mm x 152 mm concrete cylinders were made and cured in water. On the day of testing the specimens, three concrete cylinders were tested in a Baldwin compression tester, as shown in Fig. 2.14, and their average compressive and tensile splitting strengths were determined. The test results are listed in Table 2.7.

Samples of reinforcing bars used were tested in tension using an Amsler universal testing machine with a capacity of 300 kN to determine their yield and ultimate strengths. The test results are summarized in Table 2.8. A limited number of Nelson headed studs used were tested in tension. The results are summarized in Table 2.9 and the test details are provided in Appendix D.

Tension coupons were prepared from the flat plates used as perfobond rib connectors. These coupons were also tested in tension using an Amsler universal testing machine. Their yield and ultimate strengths are given in Table 2.10.

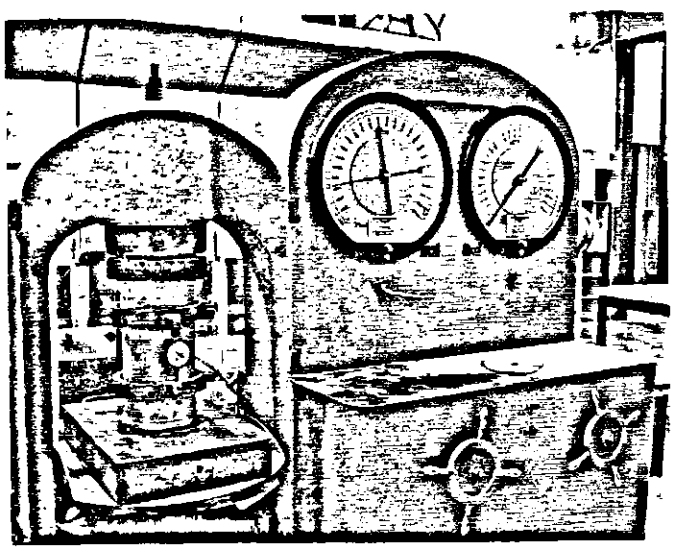

Fig. 2.14 Baldwin compression tester

Table 2.1 Physical Properties of Specimens - Series 1
$f'c = 26.3$ MPa, $f'_{ct} = 3.14$ MPa, slab without wire mesh

Specimen	Connector Geometry	Connector Type	Dimension (mm)
AS-1	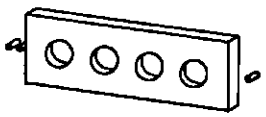	1	376x127x12
AS-2	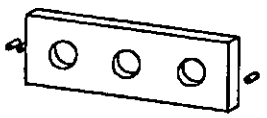	2	376x127x12
AS-3	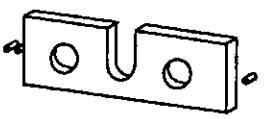	4	376x127x12
AS-4	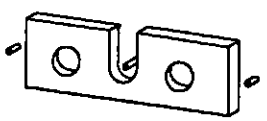	Type 4 with rebar	376x127x12
AS-5	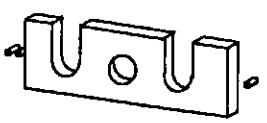	6	376x127x12
AS-6	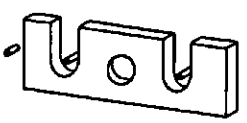	Type 6 with rebar	376x127x12
AS-7		3	376x127x12
AS-8	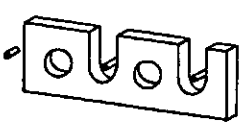	Type 3 with rebar	376x127x12
AS-9	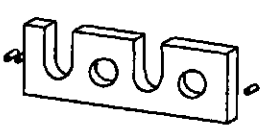	5	376x127x12
AS-10	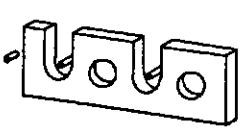	Type 5 with rebar	376x127x12

Table 2.2 Physical Properties of Specimens - Series 2
f'_c = 27.2 MPa, f'_{ct} = 3.20 MPa, slab with wire mesh

Specimen	Connector Geometry	Connector Type	Dimension (mm)
BS-1	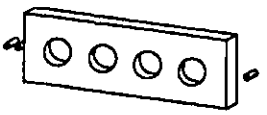	1	376x127x12
BS-2	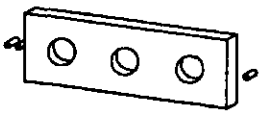	2	376x127x12
BS-3	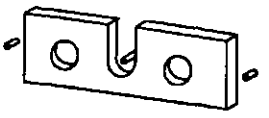	Type 4 with rebar	376x127x12
BS-4	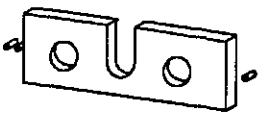	4	376x127x12
BS-5	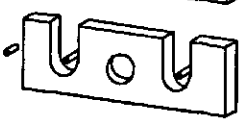	Type 6 with rebar	376x127x12
BS-6	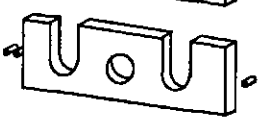	6	376x127x12
BS-7	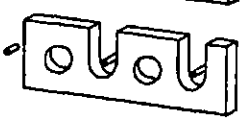	Type 3 with rebar	376x127x12
BS-8		3	376x127x12
BS-9	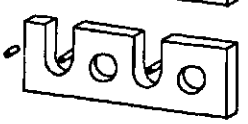	Type 5 with rebar	376x127x12
BS-10	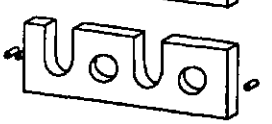	5	376x127x12
BS-11		Studs	19x125
BS-12		Studs	19x125

Table 2.3 Physical Properties of Specimens - Series 3
$f'c = 25.2$ MPa, $f'_{ct} = 3.05$ MPa, slab with wire mesh

Specimen	Connector Geometry	Connector Type	Dimension (mm)
CS-1	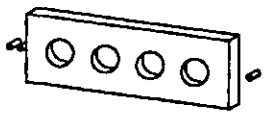	1	376x127x6
CS-2	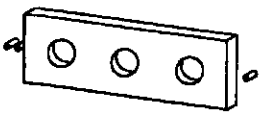	2	376x127x6
CS-3	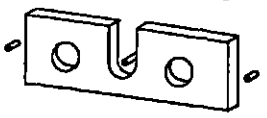	Type 4 with rebar	376x127x6
CS-4	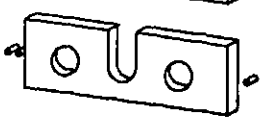	4	376x127x6
CS-5	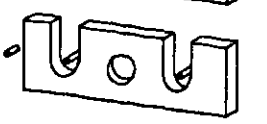	Type 6 with rebar	376x127x6
CS-6		6	376x127x6
CS-7		Type 3 with rebar	376x127x6
CS-8		3	376x127x6
CS-9		Type 5 with rebar	376x127x6
CS-10	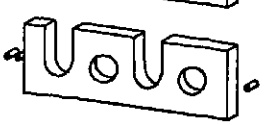	5	376x127x6
CS-11		Studs	19x125
CS-12		Studs	19x125

Table 2.4 Physical Properties of Specimens - Series 4
f'_c = 20.6 MPa, f'_{ct} = 2.80 MPa, slab with wire mesh

Specimen	Connector Geometry	Connector Type	Dimension (mm)
DS-1	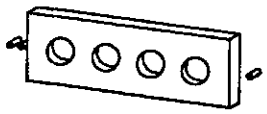	1	376x127x12
DS-2	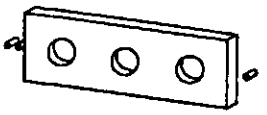	2	376x127x12
DS-3	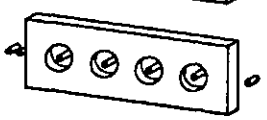	Type 1 with rebar	376x127x12
DS-4	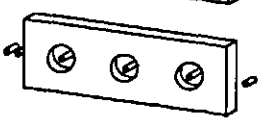	Type 2 with rebar	376x127x12
DS-5		Solid	376x127x12
DS-6		1	376x127x6
DS-7	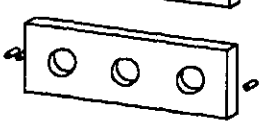	2	376x127x6
DS-8		Type 1 with rebar	376x127x6
DS-9	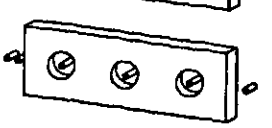	Type 2 with rebar	376x127x6
DS-10		Solid	376x127x6
DS-11		Studs	19x125
DS-12		Studs	19x125
DS-13		Studs	19x125
DS-14		Studs	19x125

Table 2.5 Physical Properties of Specimens - Series 5
f'_c = 26.2 MPa, f'_{ct} = 3.11 MPa, slab with wire mesh

Specimen	Connector Geometry	Connector Type	Dimension (mm)
ES-1	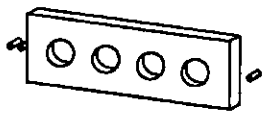	1	376x127x6
ES-2	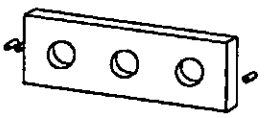	2	376x127x6
ES-3		3	376x127x6
ES-4	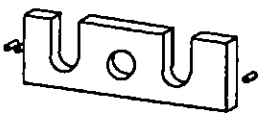	6	376x127x6
ES-5	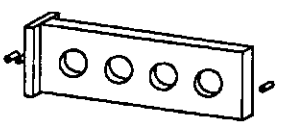	Type 1 with face plate	376x127x6 (50x127 face plate)
ES-6	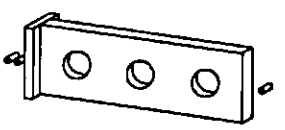	Type 2 with face plate	376x127x6 (50x127 face plate)
ES-7	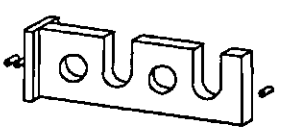	Type 3 with face plate	376x127x6 (50x127 face plate)
ES-8	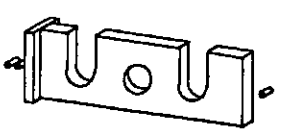	Type 6 with face plate	376x127x6 (50x127 face plate)

Table 2.5 (Cont'd.) Physical Properties of Specimens - Series 5
f'_c = 26.2 MPa, f'_{ct} = 3.11 MPa, slab with wire mesh

Specimen	Connector Geometry	Connector Type	Dimension (mm)
ES-9	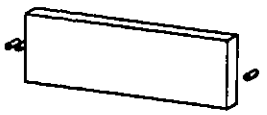	Solid	376x127x6
ES-10	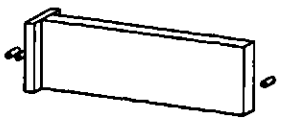	Solid with face plate	376x127x6 (50x127 face plate)
ES-11	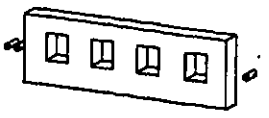	Type 1 with rectangular openings	376x127x6
ES-12	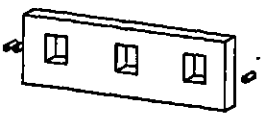	Type 2 with rectangular openings	376x127x6
ES-13	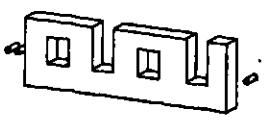	Type 3 with rectangular openings	376x127x6
ES-14	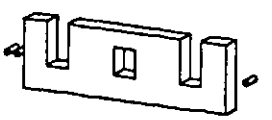	Type 6 with rectangular openings	376x127x6
ES-15		Studs	19x125
ES-16		Studs	19x125

Table 2.6 Physical Properties of Specimens - Series 6
f'_c = 25.84 MPa, f'_{ct} = 2.93 MPa, slab with wire mesh

Specimen	Connector Geometry	Connector Type	Dimension (mm)
FS-1	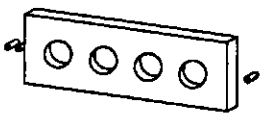	1	376x127x12
FS-2	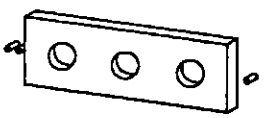	2	376x127x12
FS-3		3	376x127x12
FS-4	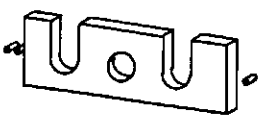	6	376x127x12
FS-5	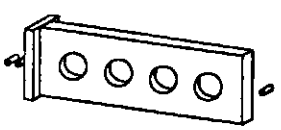	Type 1 with face plate	376x127x12 (50x127 face plate)
FS-6	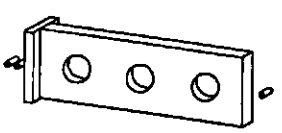	Type 2 with face plate	376x127x12 (50x127 face plate)
FS-7	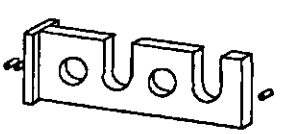	Type 3 with face plate	376x127x12 (50x127 face plate)
FS-8	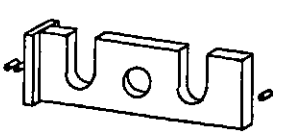	Type 6 with face plate	376x127x12 (50x127 face plate)

Table 2.6 (Cont'd.) Physical Properties of Specimens - Series 6
$f'_c = 25.84$ MPa, $f'_{ct} = 2.93$ MPa, slab with wire mesh

Specimen	Connector Geometry	Connector Type	Dimension (mm)
FS-9	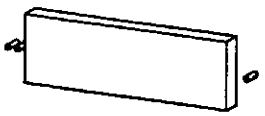	Solid	376x127x12
FS-10	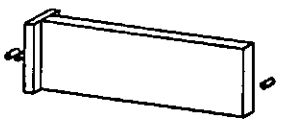	Solid with face plate	376x127x12 (50x127 face plate)
FS-11	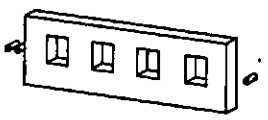	Type 1 with rectangular openings	376x127x12
FS-12	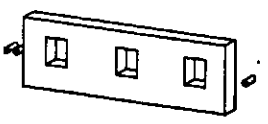	Type 2 with rectangular openings	376x127x12
FS-13	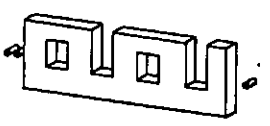	Type 3 with rectangular openings	376x127x12
FS-14	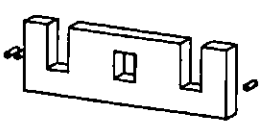	Type 6 with rectangular openings	376x127x12
FS-15	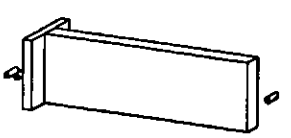	Solid with face plate	376x127x12 (75x127 face plate)
FS-16	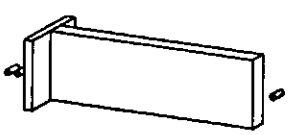	Solid with face plate	376x127x12 (100x127 face plate)

Table 2.7 Concrete properties

Test series	Compressive strength f'_c (MPa)	Tensile strength f'_{ct} (MPa)
One (AS)	26.30	3.14
Two (BS)	27.20	3.20
Three (CS)	25.20	3.05
Four (DS)	20.60	2.80
Five (ES)	26.20	3.11
Six (FS)	25.84	2.93

Table 2.8 Reinforcement properties

Test series	Yield stress Fy (MPa)	Ult. stress Fu (MPa)	Elongation e %	Reduction in area %
One (AS)	410.00	611.70	19.00	45.80
Two (BS)	426.00	639.00	18.60	42.60
Three (CS)	402.00	604.20	18.85	45.70
Four (DS)	402.00	604.20	18.85	45.70
Five (ES)	405.00	620.00	18.80	41.70
Six (FS)	405.00	620.00	18.80	41.70

Table 2.9 Material properties of studs

Test series	Yield stress Fy (MPa)	Ult. stress Fu (MPa)	Elongation e %	Reduction in area %
One (AS)	No studs	-	-	-
Two (BS)	419.50	541.95	18.40	60.35
Three (CS)	419.50	541.95	18.40	60.35
Four (DS)	379.90	468.80	23.40	63.70
Five (ES)	379.90	468.80	23.40	63.70
Six (FS)	No studs	-	-	-

Table 2.10 Material properties of perfobond rib connectors

Test series	Yield stress Fy (MPa)	Ult. stress Fu (MPa)	Elongation e %	Reduction in area %
One(AS,12 mm)	347.83	562.85	27.00	52.00
Two(BS,12 mm)	347.83	562.85	27.00	52.00
Three(CS,6 mm)	373.50	545.60	25.98	53.87
Four(DS,6 mm)	373.50	545.60	25.98	53.87
Four(DS,12 mm)	347.83	562.85	27.00	52.00
Five(ES,6 mm)	376.00	549.00	25.50	52.30
Six(FS,12 mm)	356.00	556.00	27.95	54.00

CHAPTER THREE

EXPERIMENTAL RESULTS : PHASE ONE

3.1 Failure Mechanisms

In the specimens with perfobond rib connectors, failure was triggered by the longitudinal splitting of the concrete slab, followed by the crushing of concrete in front of the perfobond rib. Fig. 3.1 shows specimen BS-2 after failure and illustrates a typical failure mechanism of specimens with perfobond rib connectors.

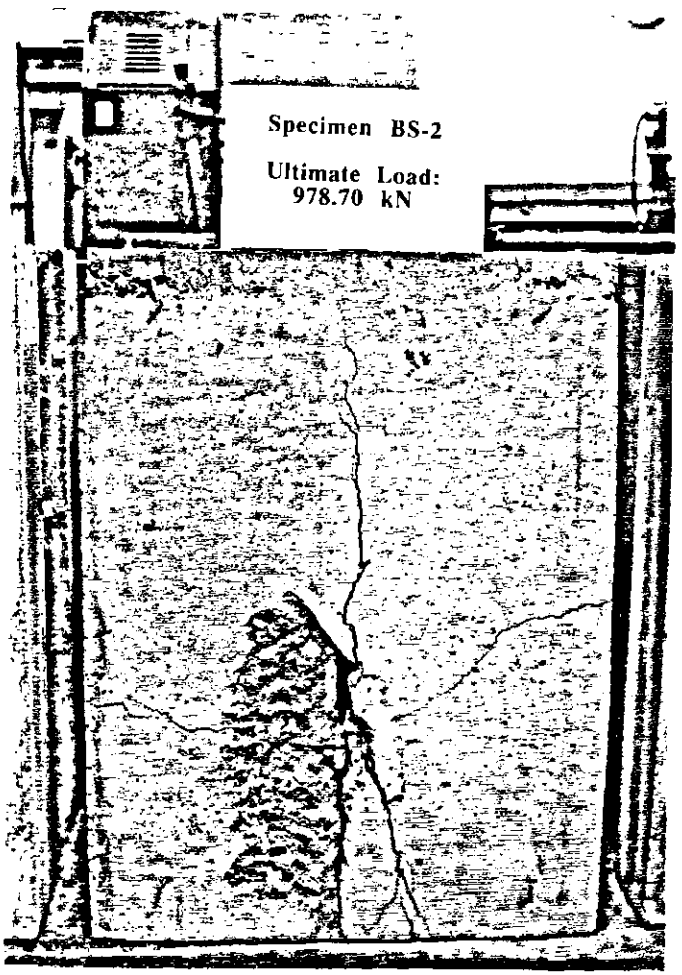

Fig. 3.1 Failure mechanism: specimen BS-2

The load-slip curve for specimen BS-2 is shown in Fig. 3.2. A description of the perfobond rib connector is provided in the inset. The specimen behaved linearly in the initial stage of the test. The first sign of longitudinal splitting crack was observed on the concrete surface in front of perfobond rib connector when the applied load was 797 kN. As the applied load was increased, the longitudinal splitting became more prominent. When the applied load reached 994 kN, the concrete in front of the perfobond rib connector crushed and the load carrying capacity of the specimen started to decrease. The specimen continued to maintain a large portion of the ultimate load due to shear resistance provided by aggregate interlock along the split surface.

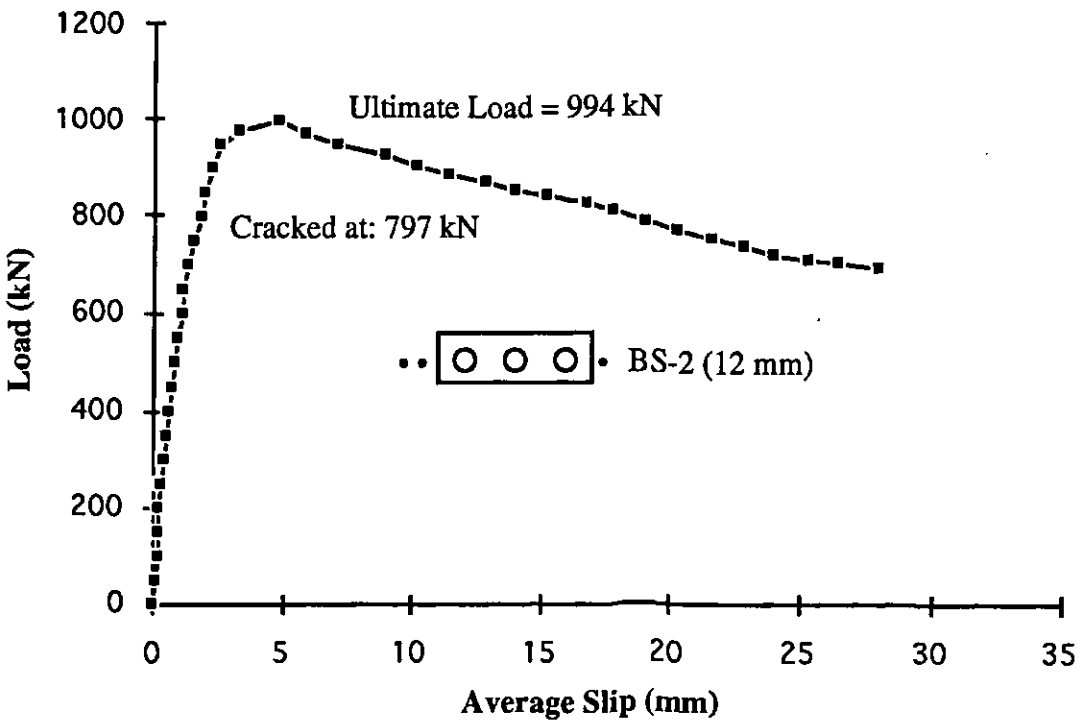

Fig. 3.2 Load-slip relationship of specimen BS-2

In Fig. 3.2 and all subsequent graphs, the ordinate represents the total load carried by the specimen and the abscissa represents the average slip at the interface between the concrete slab and the steel flange. The slip measurements do not include the shortening of the concrete slab duetotheapplied load. In this thesis, the recorded peak load will be referred to as the ultimate load. The ultimate load value of 994 kN shown in Fig. 3.2 was obtained after the recalibration of the Amsler Testing Machine which was carried out on the completion of testing the first three series. This is the reason why there is a slight difference in the ultimate load value shown in the photographs of the test specimens of Series 1, 2 and 3. The observed ultimate load values of all the specimens in phase 1 are listed in Tables 3.1 to 3.4 which are placed at the end of the chapter.

Figure 3.3 shows a 12 mm normal perfobond rib connector after the test. The thick plates remained virtually intact. In fact, none of the 12 mm normal perfobond rib connectors showed any sign of deformation and were reused several times.

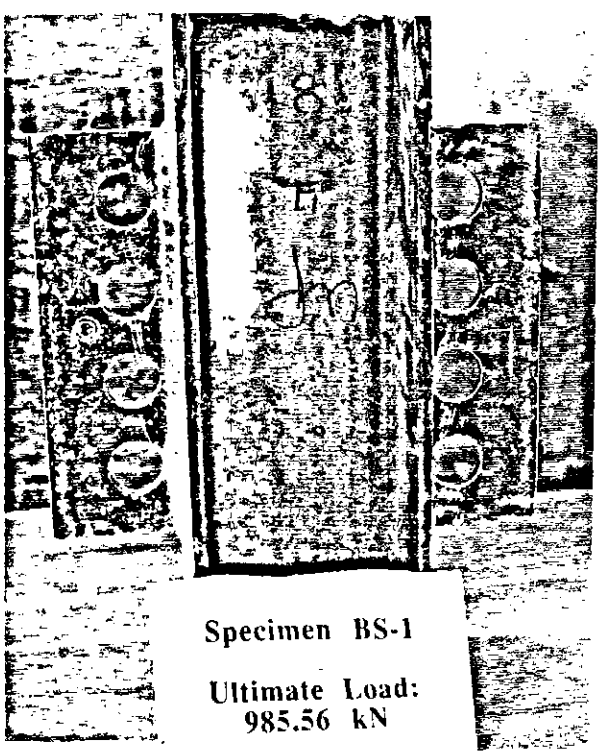

Fig. 3.3 Type 1 perfobond rib connector after test: specimen BS-1

The load-slip curve for the specimen CS-2 is shown in Fig. 3.4. As described in the inset, this specimen featured a 6 mm thick perfobond rib connector with three holes. Fig. 3.5 shows the specimen after the test. The structural behavior of this specimen was similar to that of specimen BS-2 except that specimen CS-2 exhibited a higher overall ductility. Moreover, as can be seen in Fig. 3.6, the 6 mm plate deformed considerably. None of the 6 mm normal perfobond rib connectors could be reused.

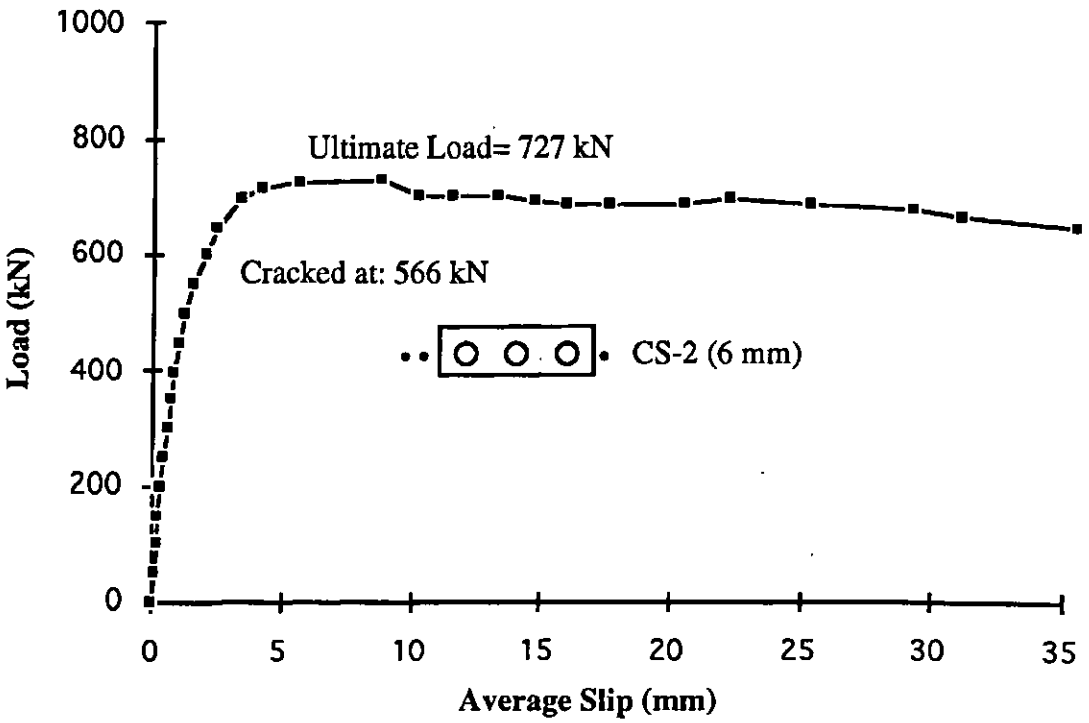

Fig. 3.4 Load-slip relationship of specimen CS-2

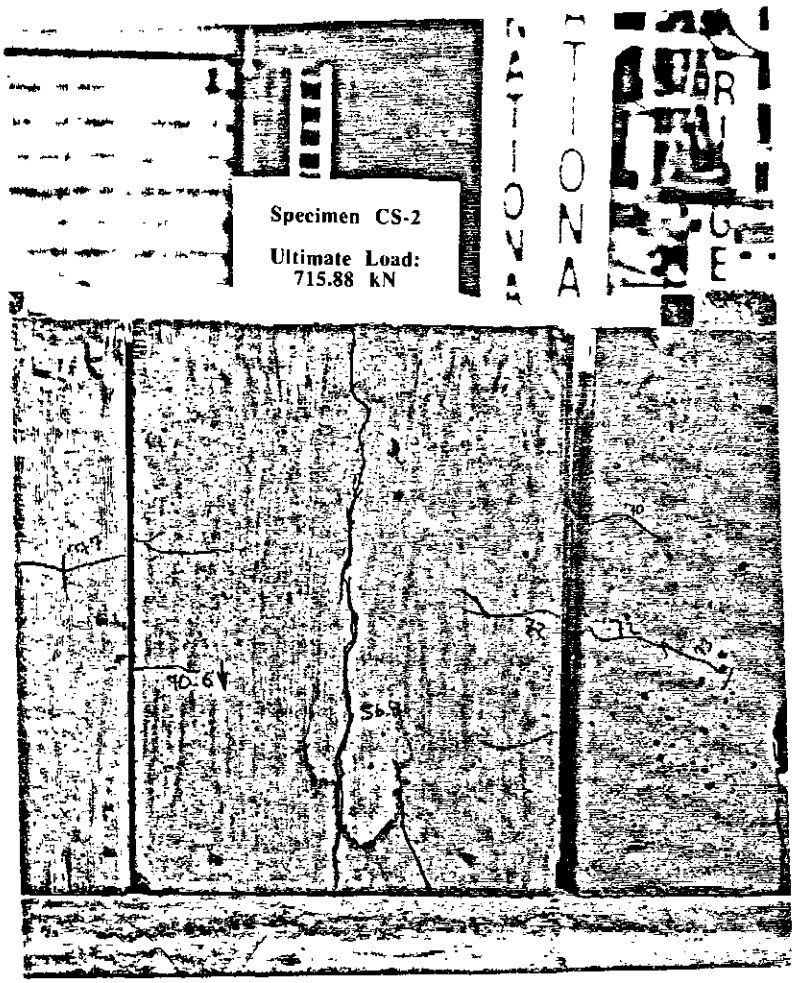

Fig. 3.5 Failure mechanism: specimen CS-2

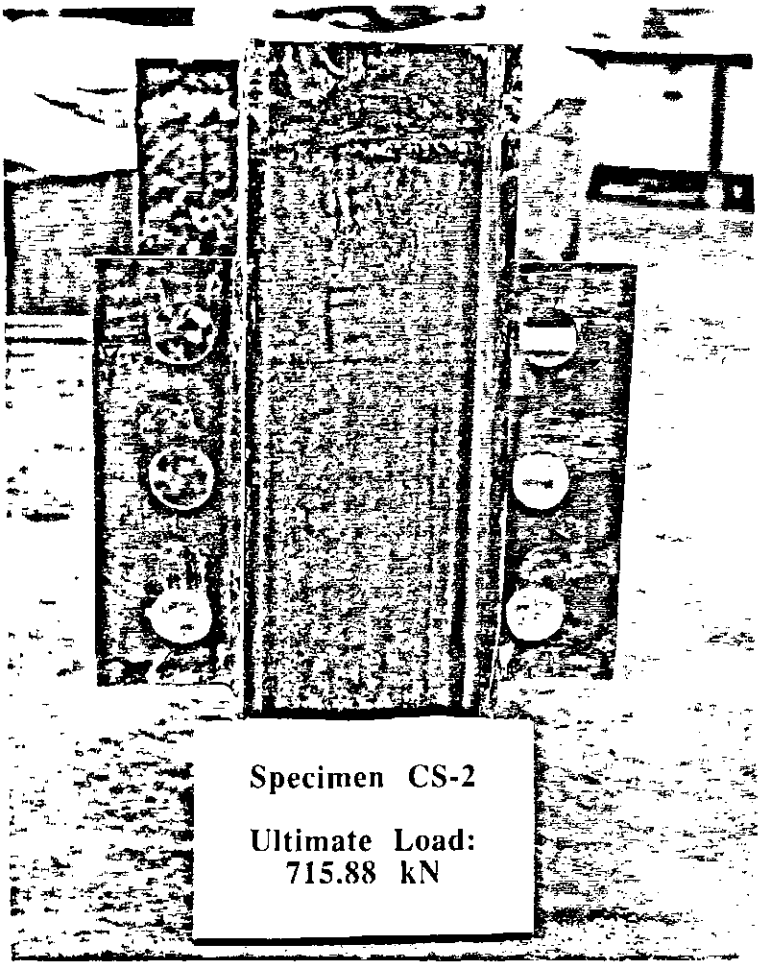

Fig. 3.6 Deformation of 6 mm thick normal perfobond rib connector

The load-slip curve for specimen BS-8 is shown in Fig. 3.7 and its failure mechanism is illustrated in Fig. 3.8(a). As before, failure was triggered by the longitudinal splitting of the concrete slab, followed by the crushing of concrete in front of the perfobond rib. However, the slotted perfobond rib connector showed considerable deformation as shown in Fig. 3.8(b). Specimen BS-10 featured the same slotted perfobond rib connector in a reversed position (Type 5). The deformation pattern of this connector is

shown in Fig. 3.9. Most of the 12 mm slotted perfobond rib connectors deformed and could not be reused.

All 6 mm slotted perfobond rib connectors suffered extensive damage. Figs. 3.10 and 3.11 present two of the typical deformations. In Fig. 3.11 there is a clear sign of fracture of the plate. Photographs of other specimens from Series 3 are in Appendix B.

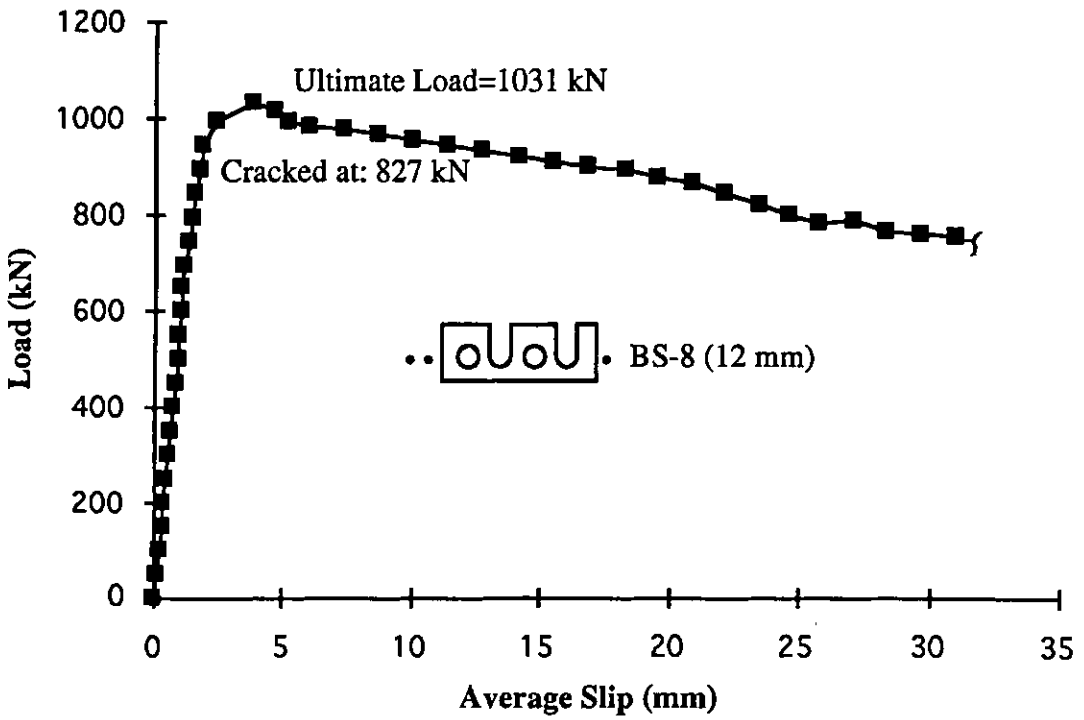

Fig. 3.7 Load-slip relationship of specimen BS-8

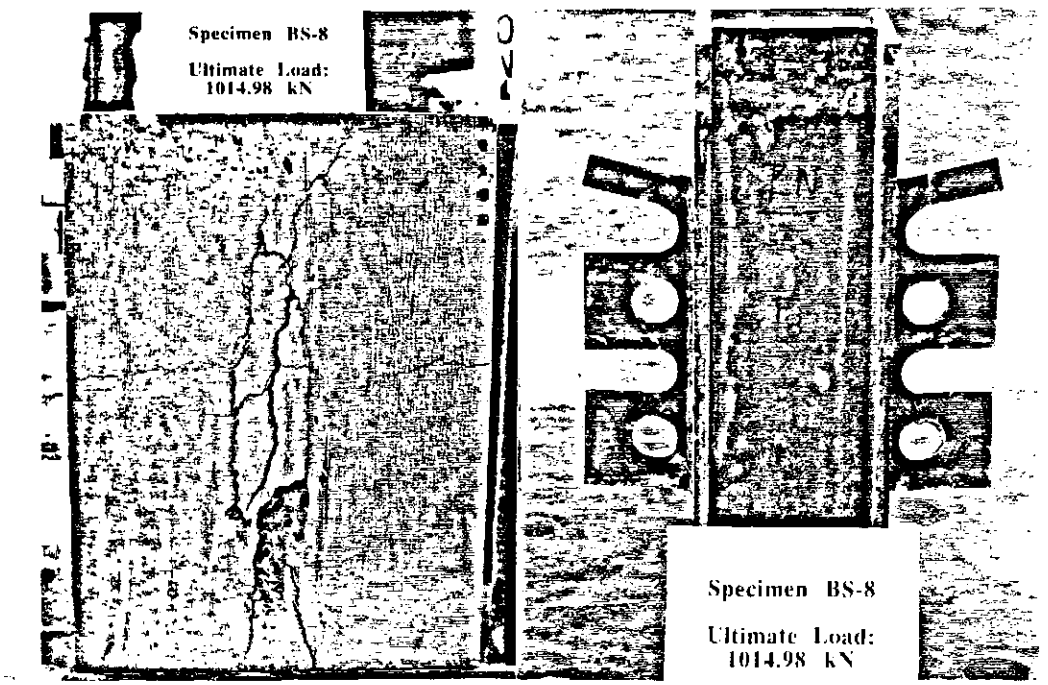

(a) View of slab

(b) Deformation of perfobond rib connectors

Fig. 3.8 Specimen BS-8 after testing

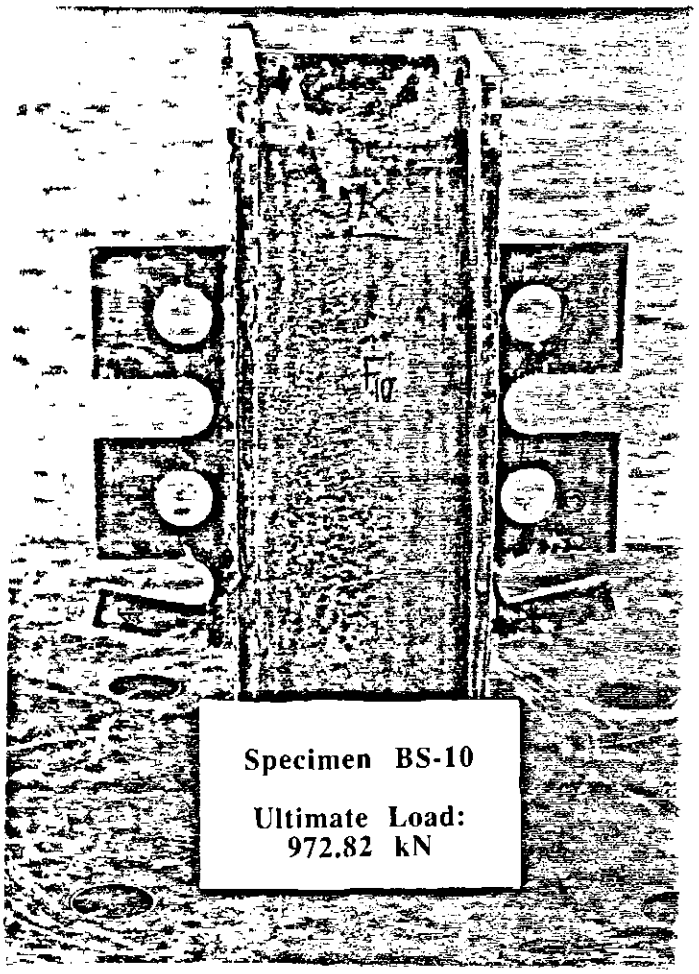

Fig. 3.9 Type 5 perfobond rib connector after testing: specimen BS-10

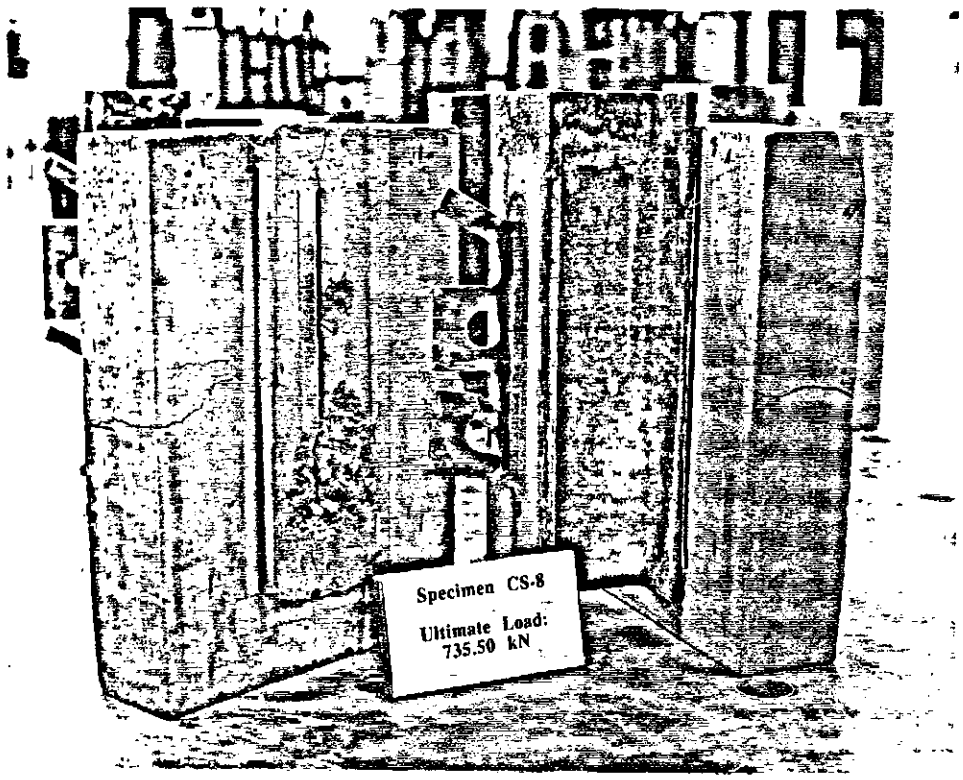

Fig. 3.10 Deformation of 6 mm thick Type 3 perfobond rib connector: specimen CS-8

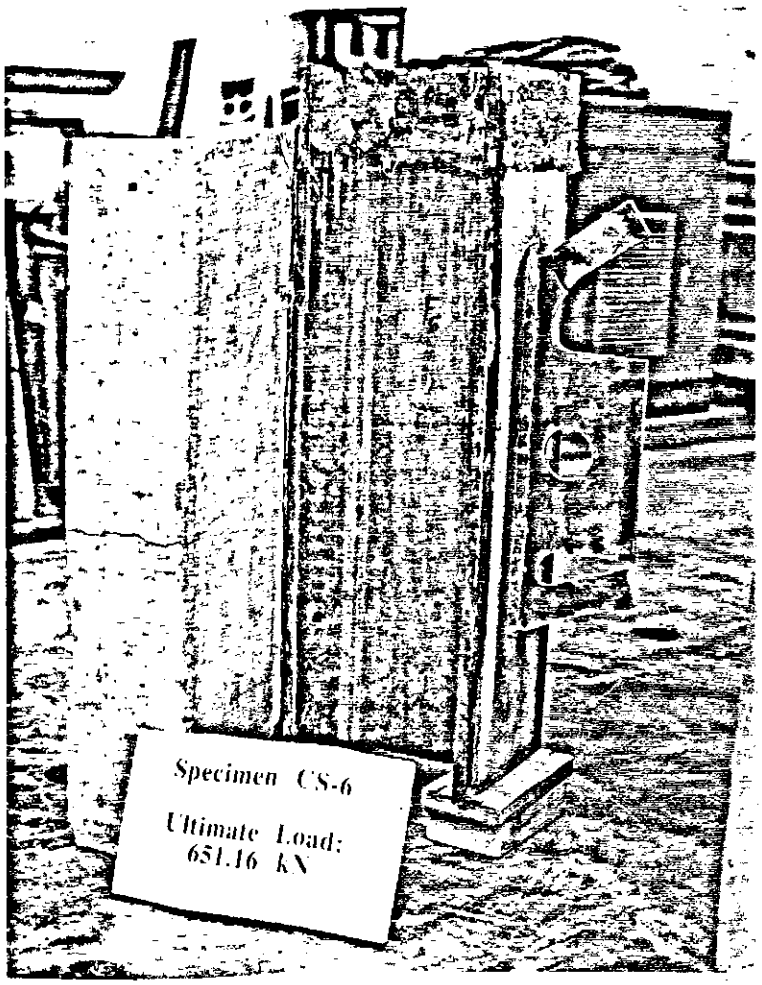

Fig. 3.11 Failure mechanism: Type 6 perfobond rib connector, specimen CS-6

Shank shear was the principal mode of failure in specimens with headed studs. Fig. 3.12 shows the shank shear failure of the studs in specimen DS-13. There are signs of localized crushing of the concrete in front of the stud prior to the failure of the studs. However, the concrete slab remained intact with just a few surface cracks, as shown in Fig. 3.13. In specimens with concrete of higher strength, no surface cracks were observed. Fig. 3.14 shows the concrete slab of specimen BS-11 which failed by shank shear of

the studs. The strength of concrete for this specimen was 27.2 MPa compared to 20.6 MPa for specimen DS-13.

Fig. 3.12 Shank shear failure of headed studs: specimen DS-13

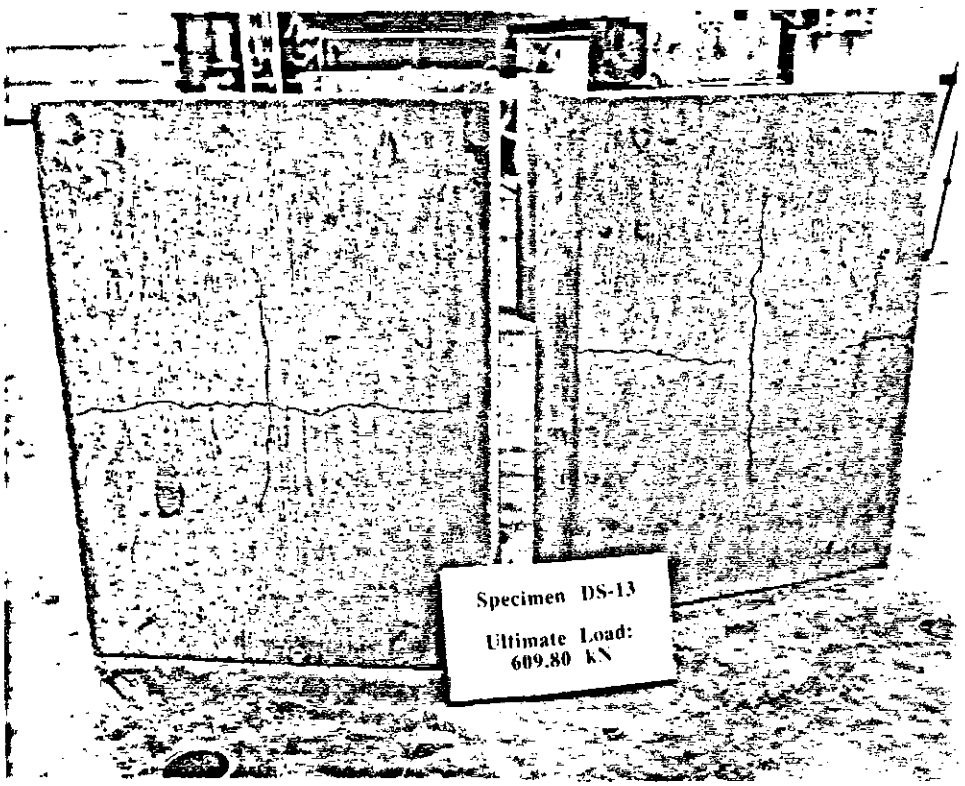

Fig. 3.13 Failure mechanism: specimen DS-13

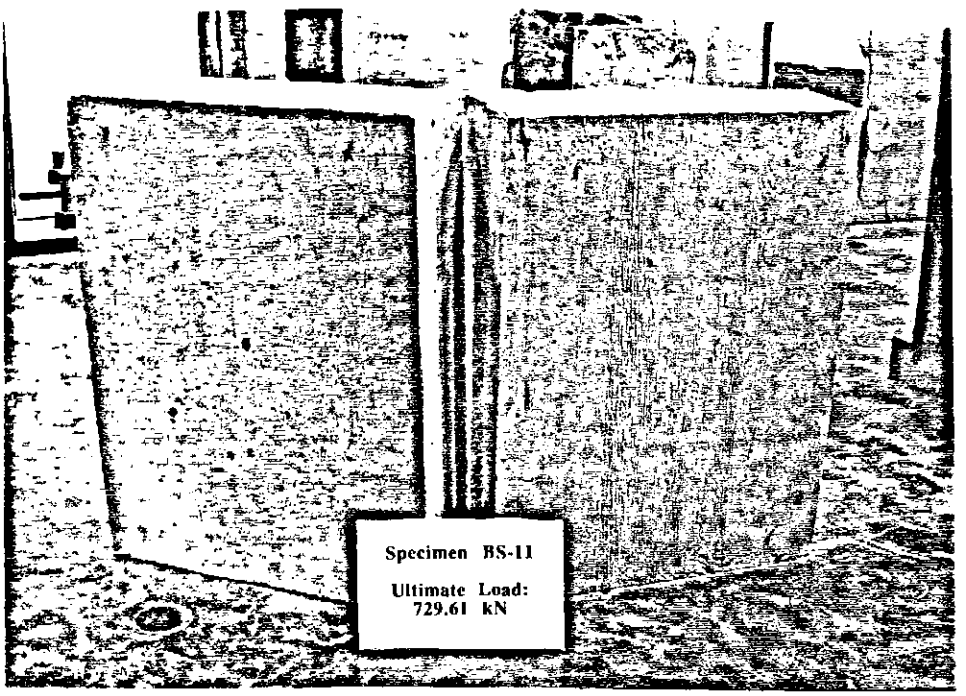

Fig. 3.14 Failure mechanism: specimen BS-11

3.2 Comparison of Performance

3.2.1 Slotted Vs Normal Perfobond Rib Connectors

As indicated earlier, one of the reasons for introducing slots was to improve the flexibility of the perfobond rib connector in order to ensure an even distribution of shear load between the connectors in a composite beam. In this thesis, the slope of the linear portion of the load-slip curve will be used as a measure of the flexibility of the connector.

The load-slip curves for push-out specimens BS-1, BS-7 and BS-8, all from Series 2, with 12 mm thick perfobond rib connectors, are presented in Fig. 3.15. The load-slip curve for specimen BS-11, with four headed studs, is also included in this figure. The inset to this curve shows the configurations of the perfobond rib connectors used in these specimens. A comparison of the load-slip curves for specimens BS-1 and BS-8 indicates no improvement in the flexibility of specimen BS-8 although it featured slotted perfobond rib connectors. It appears that the increased concrete dowel area provided by the slots in the perfobond rib connector of specimens BS-8 offsets the effects of the flexible slotted connector. However, the beneficial effects of the slotted perfobond rib connector is apparent by an increase in the ductility of specimen BS-8. The addition of transverse reinforcement through the slots increased the ultimate load of specimen BS-7 but, once again, there was no improvement in flexibility. All three specimens demonstrated the remarkable ability of perfobond rib connectors to retain a substantial portion of the ultimate load in the unloading stage.

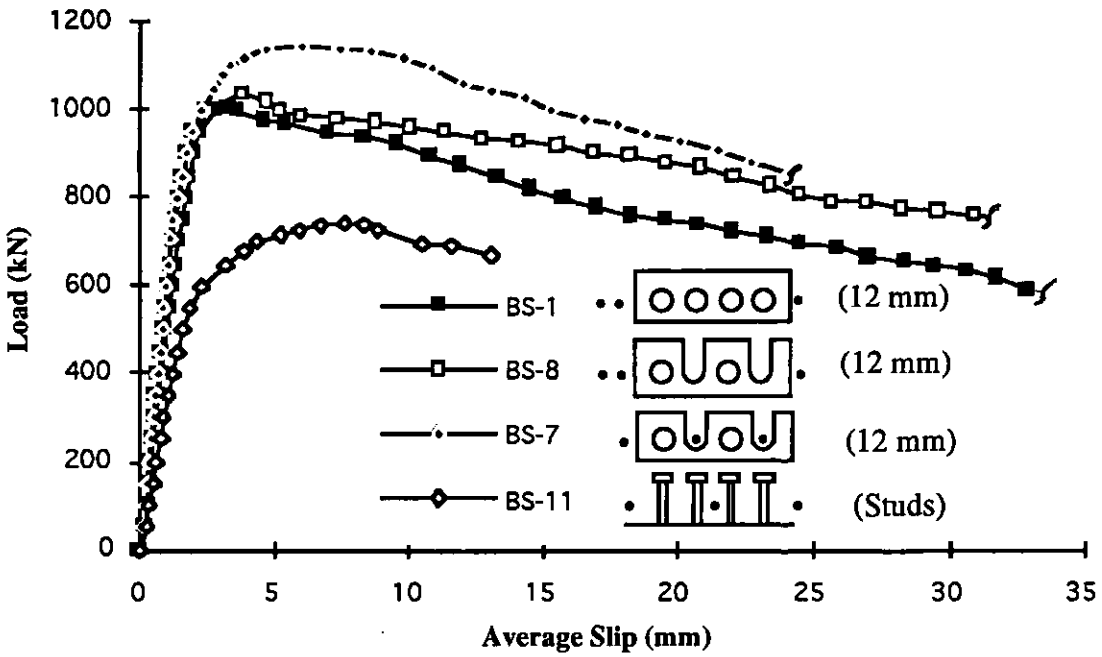

Fig. 3.15 Load-slip relationship of specimens BS-1, BS-8, BS-7 and BS-11

The load-slip curves for specimens BS-1 and BS-8 are presented again in Fig. 3.16 together with that of specimen BS-10. As shown in the inset, specimens BS-8 and BS-10 featured Types 3 and 5 perfobond rib connectors, respectively. Specimen BS-10, with only a narrow strip of metal facing the load, was expected to demonstrate a more flexible behaviour. However, Fig. 3.16 indicates only a marginal increase in flexibility for specimen BS-10.

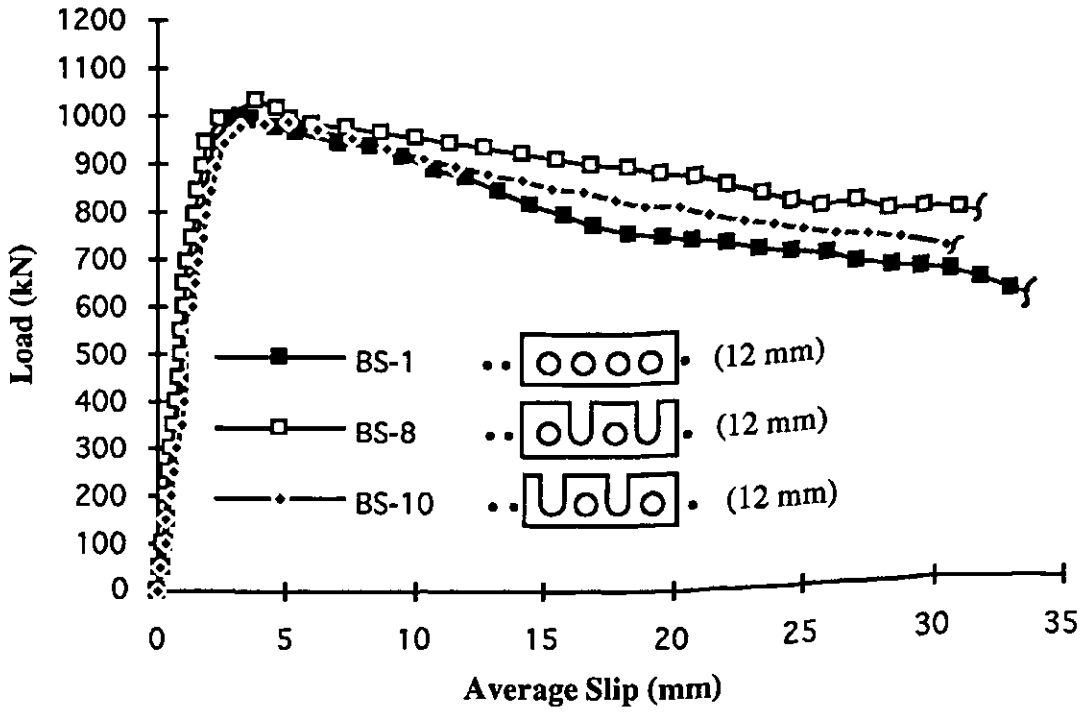

Fig. 3.16 Load-slip relationship of specimens BS-1, BS-8 and BS-10

The load-slip curves for specimens BS-2, BS-4, BS-3 and BS-12, also from Series 2, are presented in Fig. 3.17. The first three specimens feature 12 mm perfobond rib connectors with three holes and/or slots. As before, specimen BS-3 with reinforced slotted perfobond rib connectors carried the maximum load. However, the relative flexibility of the three specimens with perfobond rib connectors can not be ascertained from this figure.

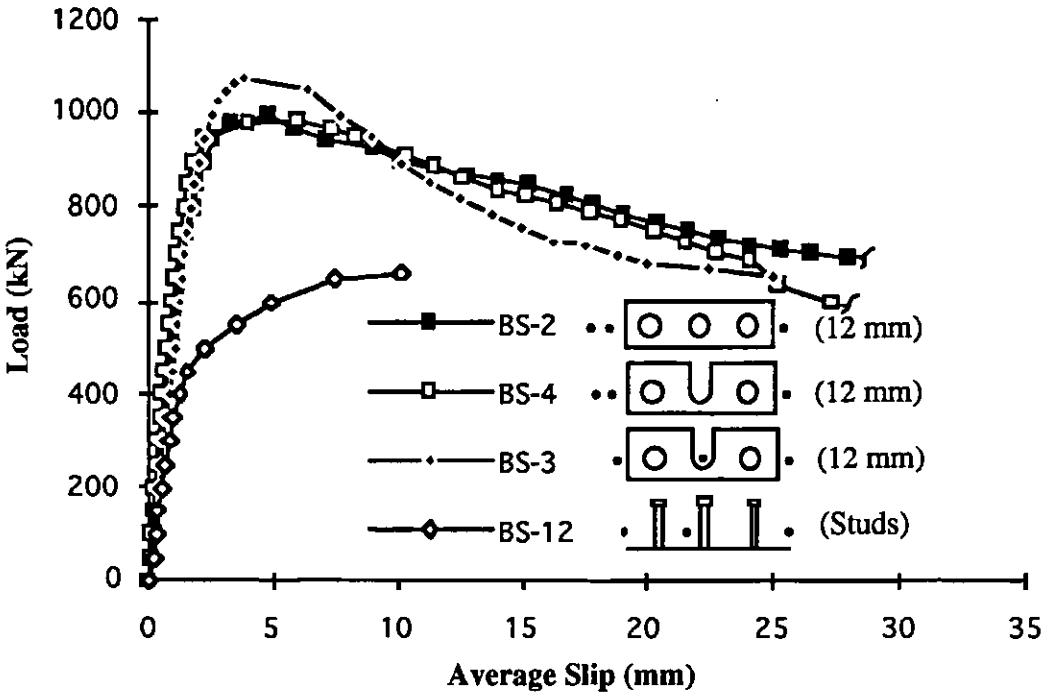

Fig. 3.17 Load-slip relationship of specimens BS-2, BS-4, BS-3 and BS-12

The load-slip curve of specimen BS-4 with an enlarged horizontal scale is shown in Fig. 3.18 together with that of specimens BS-2 and BS-12. It is clear from this figure that specimen BS-4, with a slotted hole in the middle, is stiffer than specimen BS-2. As explained earlier, this is probably due to the larger size of the concrete dowel created by the slot.

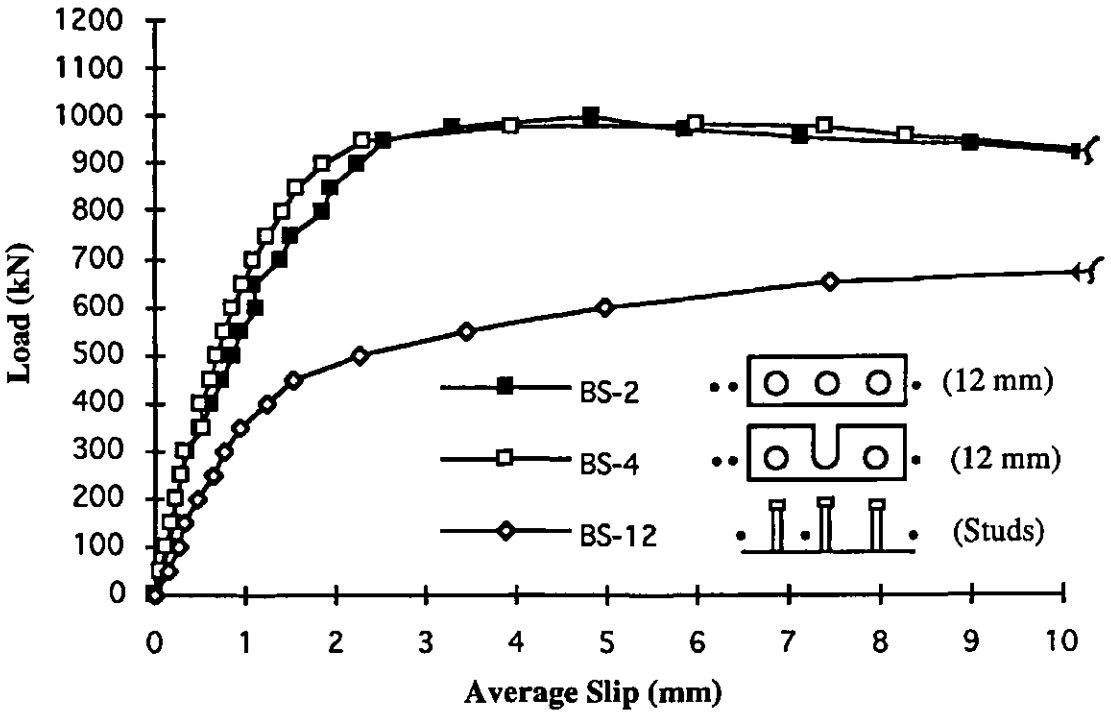

Fig. 3.18 Load-slip relationship of specimens BS-2, BS-4 and BS-12

The load-slip curves for specimens BS-2, BS-5, BS-6 and BS-12, all from Series 2, are presented in Fig. 3.19. Once again, the slotted specimens did not provide any significant increase in flexibility. Specimen BS-6 with two slotted openings exhibited slightly more ductile behavior although its ultimate shear capacity was somewhat reduced compared to that of Specimen BS-2 which had three holes.

The load-slip curves for specimens BS-4 and BS-6, plotted with an enlarged horizontal scale, are presented in Fig. 3.20. In spite of larger concrete dowel area, Specimen BS-6 appears to be more flexible. As illustrated in this figure, the perfobond rib connector used in specimen BS-6 is more flexible than that of specimen BS-4 because of its configuration.

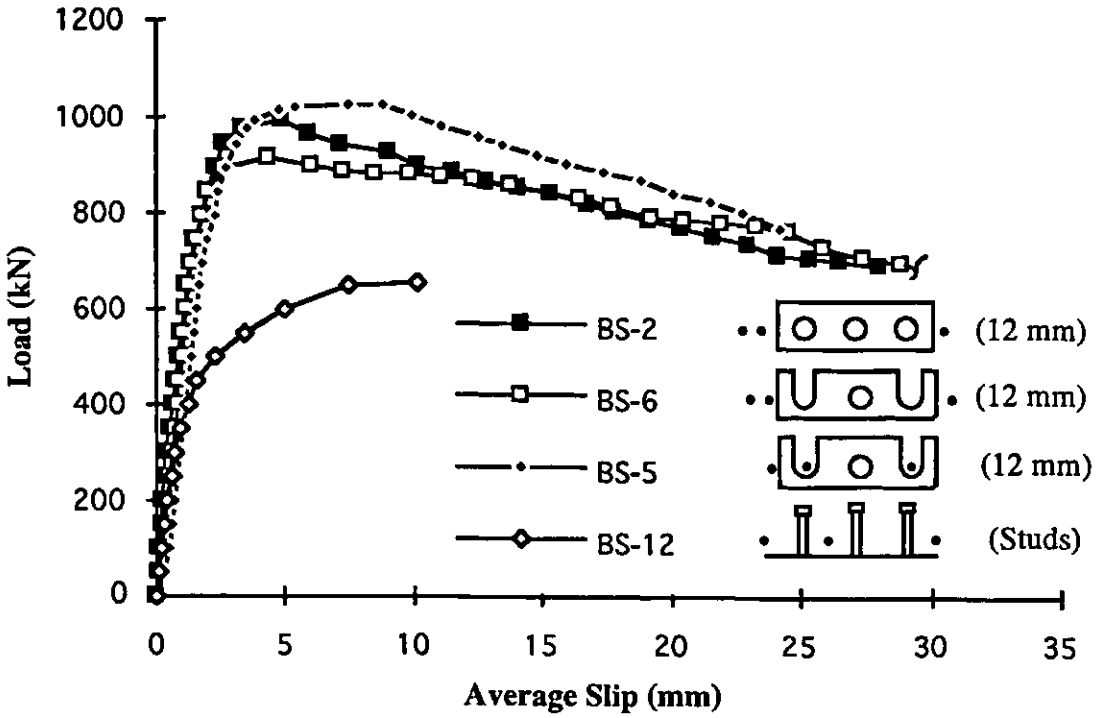

Fig. 3.19 Load-slip relationship of specimens BS-2, BS-6, BS-5 and BS-12

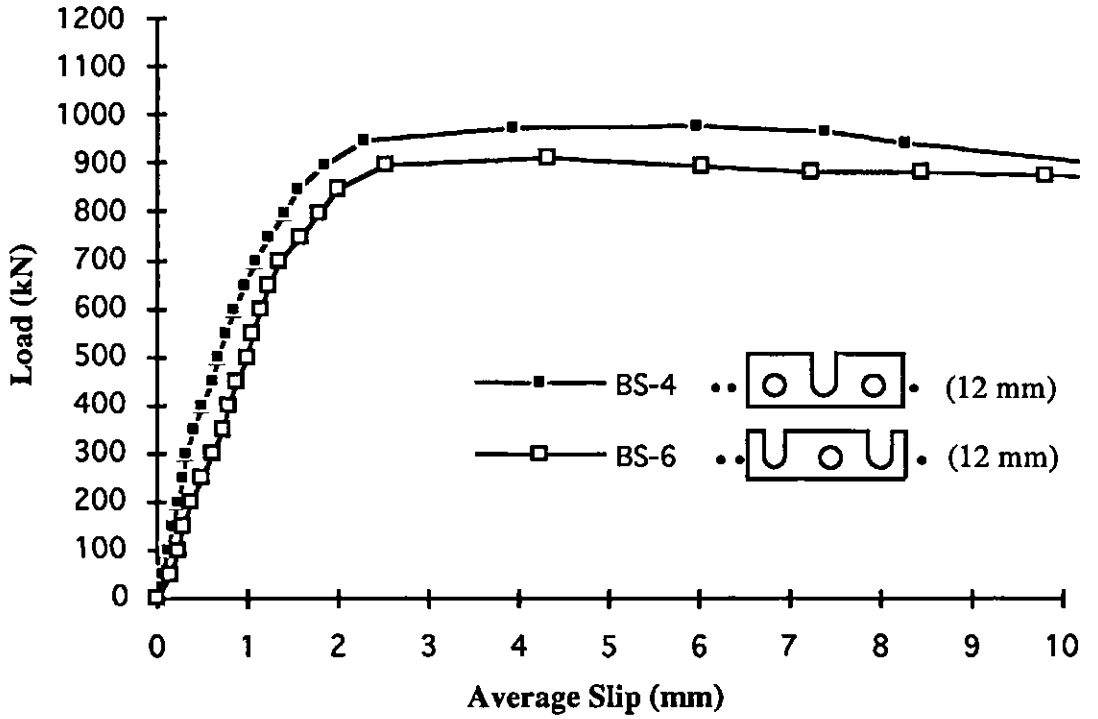

Fig. 3.20 Load-slip relationship of specimens BS-4 and BS-6

Comparison of load-slip curves for 6 mm perfobond rib connectors are shown in Figs. 3.21 and 3.22. The load-deformation curves for specimens CS-1, CS-7, CS-8 and CS-11, all from Series 3, are shown in Fig. 3.21. Specimen CS-8, with two slots, is slightly stiffer than specimen CS-1 with four holes. It carried a slightly higher ultimate load and it is more ductile. The behaviour of a perfobond rib connector with a slot adjacent to the loading face is compared in Fig. 3.22 where the load-slip curves of four specimens from Series 3 are presented. There is no significant difference in the stiffness characteristics. Similar behavior was also observed for the specimens featuring perfobond rib connectors with three openings. The load-slip curves for these specimens are included in Appendix A.

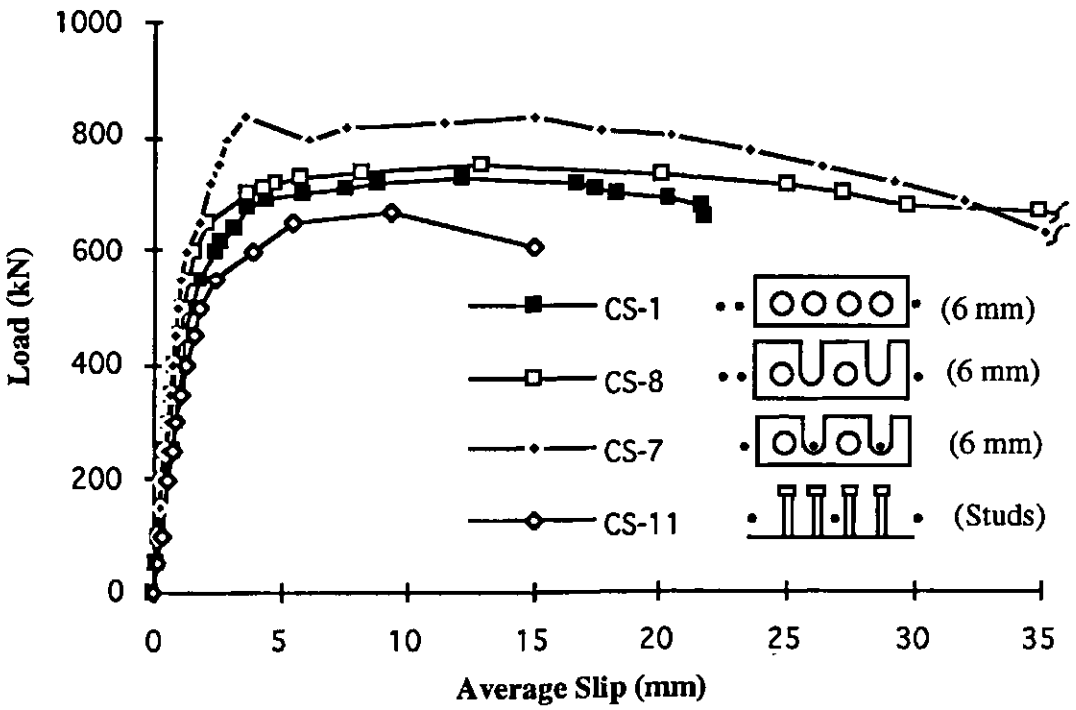

Fig. 3.21 Load-slip relationship of specimens CS-1, CS-8, CS-7 and CS-11

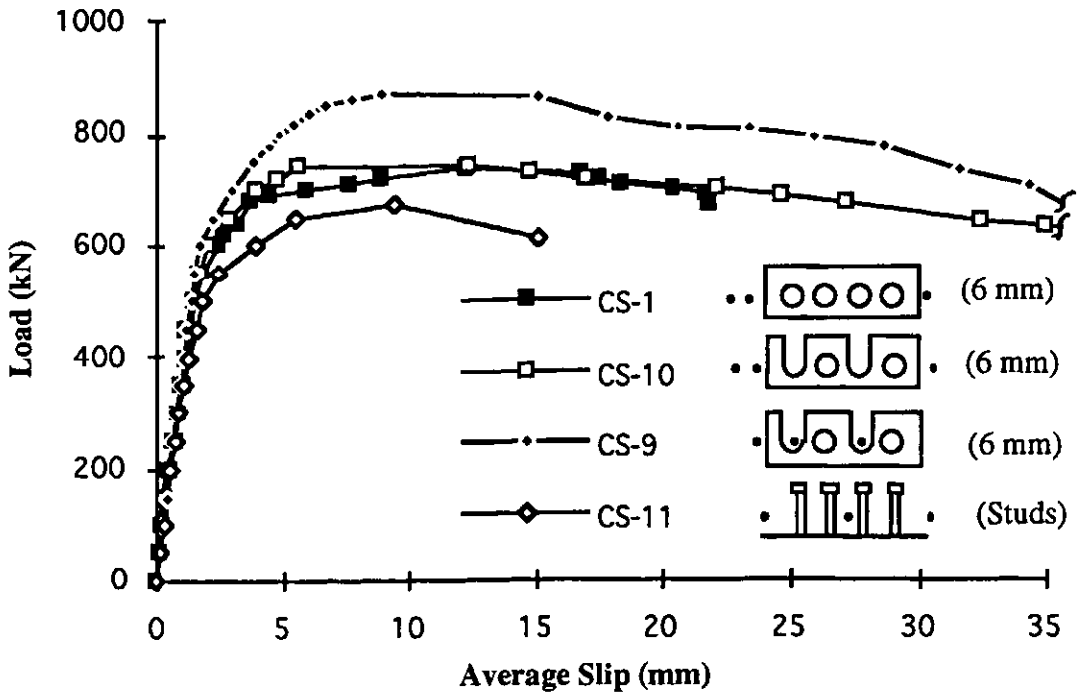

Fig. 3.22 Load-slip relationship of specimens CS-1, CS-10, CS-9 and CS-11

3.2.2 Thick Perfobond Connectors Vs Thin Perfobond Connectors

Fig. 3.23 presents the load-slip curves for specimens DS-2 and DS-7 which were exactly the same in every respect except that the perfobond rib connectors in specimen DS-2 were 12 mm thick whereas those in specimen DS-7 were 6 mm thick. As indicated in the inset, both specimens featured Type 2 perfobond rib connectors with three holes. The load-slip curve for specimen DS-12, featured three headed studs in each slab. As expected, specimen DS-7 with the thinner perfobond rib connectors exhibited a slightly higher flexibility. This specimen is also considerably more ductile although its ultimate shear capacity was somewhat reduced. The ultimate capacity of specimen DS-7 was 719 kN compared to 833 kN for specimen

for specimen DS-2. This reduction in strength is approximately 14%. The stiffness of the specimen with the thinner perfobond rib connector was almost identical to that of the specimen with headed studs.

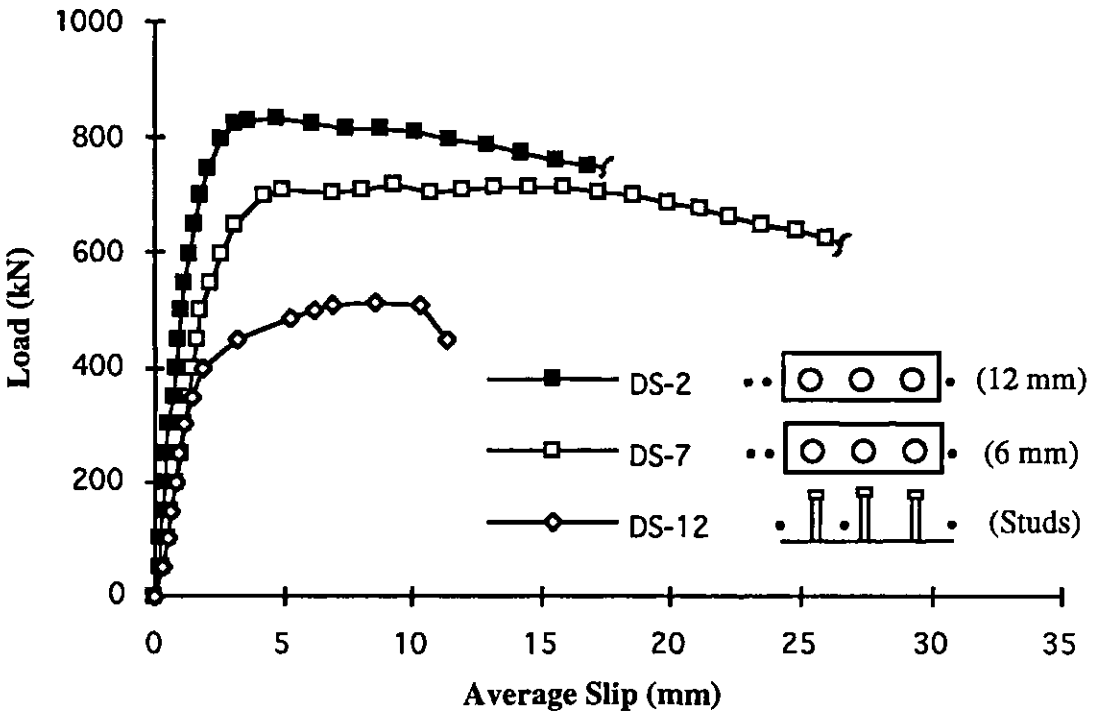

Fig. 3.23 Load-slip relationship of specimens DS-2, DS-7 and DS-12

A similar comparison between thick and thin perfobond rib connectors is presented in Fig. 3.24 which features the load-slip curves for specimens DS-1 and DS-6. These specimens had Type 1 perfobond rib connectors with four holes and were exactly the same in every respect except that the perfobond rib connectors in specimen DS-1 were 12 mm thick whereas those in specimen DS-6 were 6 mm thick. Once again, the increased ductility of the thinner perfobond rib connector was accomplished at the expense of a reduction in the ultimate shear strength. In this case, the drop in strength was

approximately 22%. Because of the additional dowel area in the perfobond rib connectors with four holes, there is no significant difference in the stiffness values of the two specimens.

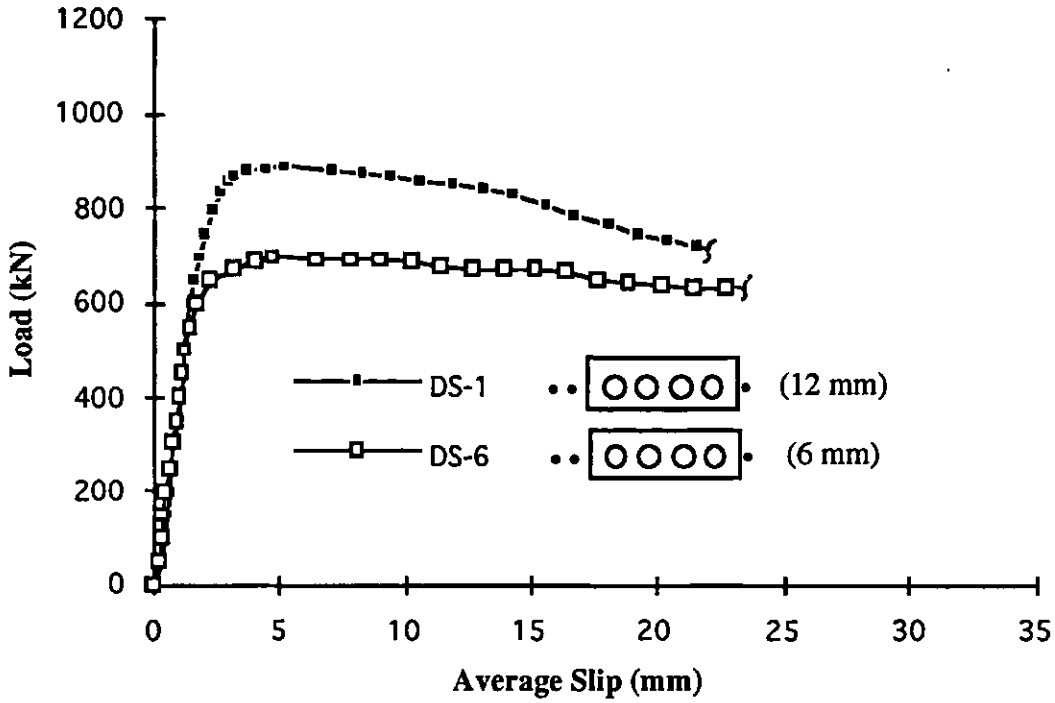

Fig. 3.24 Load-slip relationship of specimens DS-1 and DS-6

A comparison between thick and thin slotted perfobond rib connectors is presented in Fig. 3.25 which features the load-slip curves for specimens BS-10 and CS-10. The load-slip curve for specimen CS-11, which had four headed studs in each slab, is also included. In this plot, the load values have been normalized to a concrete strength f'_m = 26.2 MPa which is the mean concrete strength value. This was done by multiplying the load values by the factor k, where $k = \sqrt{(f'_m/f'_c)}$. This factor is based on the findings of a number of researchers (Viest 1960; Davies 1967; Slutter and Driscoll 1961; and Ollgaard et al. 1971) who dicovered that the ultimate capacity of a shear

connector increases with the increase in the compressive cylinder strength of concrete and that this increase is approximately proportional to the square-root of the compressive cylinder strength, $\sqrt{f_c}$. Normalization of the test results minimizes the effect of the difference in the concrete strengths of the specimens.

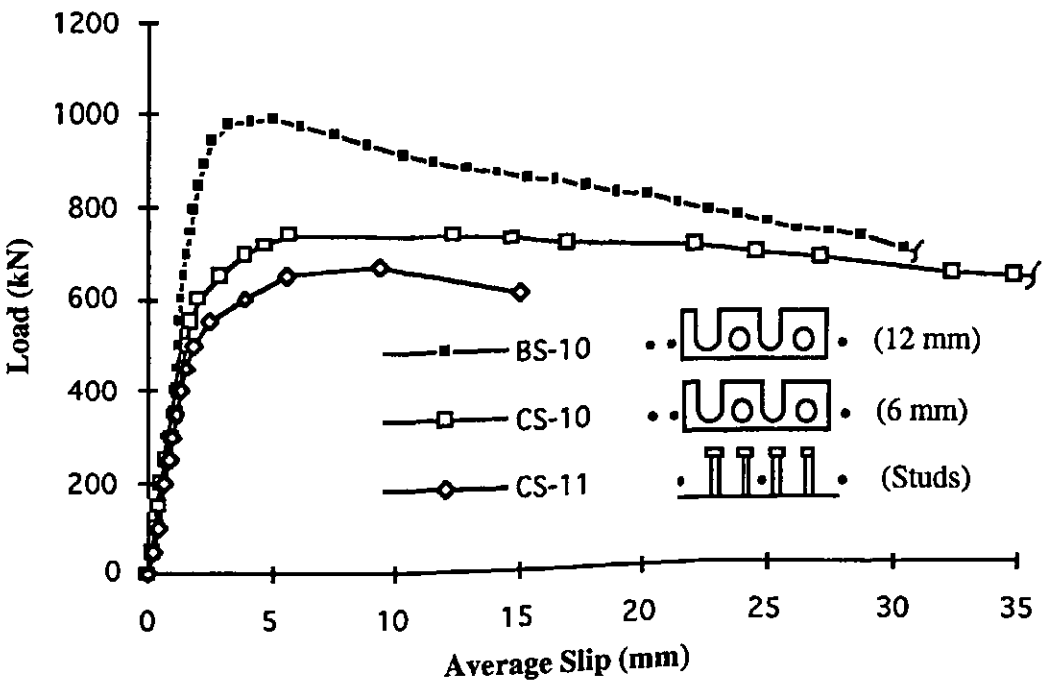

Fig. 3.25 Load-slip relationship of specimens BS-10, CS-10 and CS-11

As indicated in the inset to Fig. 3.25, both specimens featured Type 5 perfobond rib connectors. However, the perfobond rib connectors in specimen BS-10 were 12 mm thick whereas those in specimen CS-10 were 6 mm thick. Once again, the specimen with thinner perfobond rib connectors exhibited considerable ductile behavior although at the expense of a reduced ultimate load. The ultimate capacity of specimen CS-10 was 742 kN

compared to 988 kN for specimen BS-10; therefore, the reduction in strength was almost 25%. However, the observed ultimate load for specimen CS-10 was approximately 10% higher than that of specimen CS-11 which featured four headed studs. The ductility of these two specimens was similar but the load retaining capability of specimen CS-10 was much higher.

As shown in Fig. 3.26, a similar behavior was also observed for specimens with Type 3 slotted perfobond rib connectors. In this case, the reduction in strength for the specimen with a 6 mm thick perfobond rib connector was approximately 27 %.

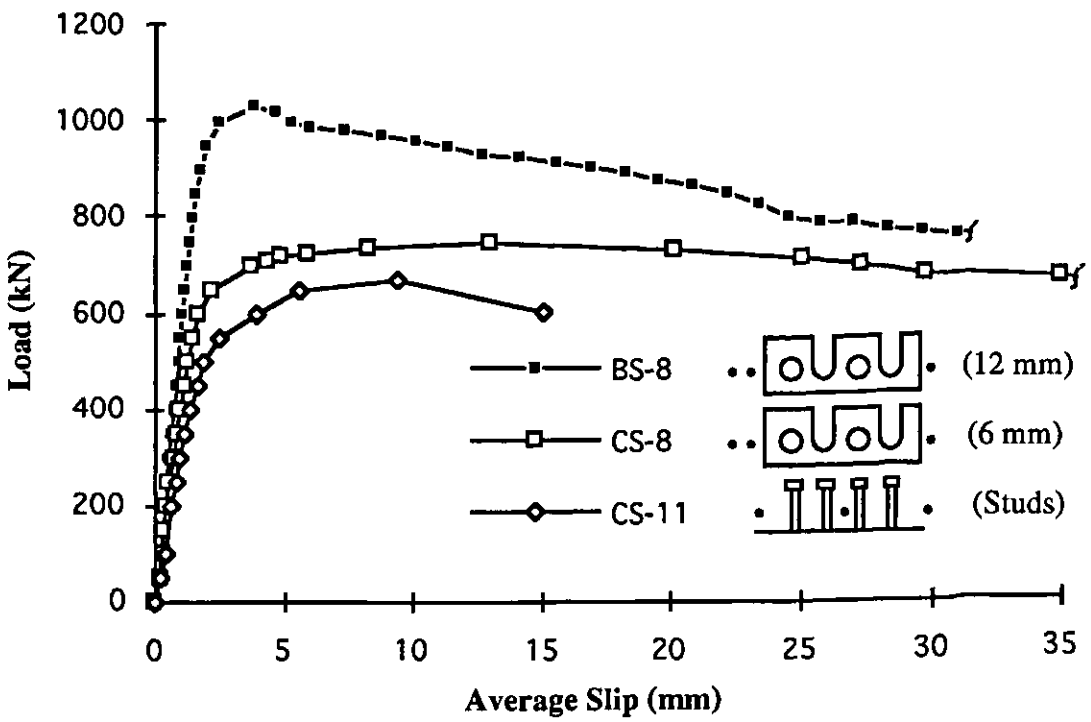

Fig. 3.26 Load-slip relationship of specimens BS-8, CS-8 and CS-11

The comparative load-slip curves for other specimens with both slotted and unslotted perfobond rib connectors are presented in Appendix A.

3.2.3 Contribution of concrete dowels

The load-slip curves for specimens DS-1, DS-2 and DS-5 are presented in Fig. 3.27. These specimens featured 12 mm thick perfobond rib plates. As shown in the inset, DS-1 had four holes, DS-2 had three holes, and DS-5 had no holes at all. Specimens DS-2 and DS-5 carried 833 kN and 608 kN, respectively. This means that the three concrete dowels in the perfobond rib connector were responsible for an additional 225 kN. In other words, roughly 27% of the ultimate strength is contributed by the concrete dowels formed within the holes of the perfobond rib connector. Specimen DS-1, with four holes, supported an ultimate load of 889 kN. The additional concrete dowel increased the strength by about 5%.

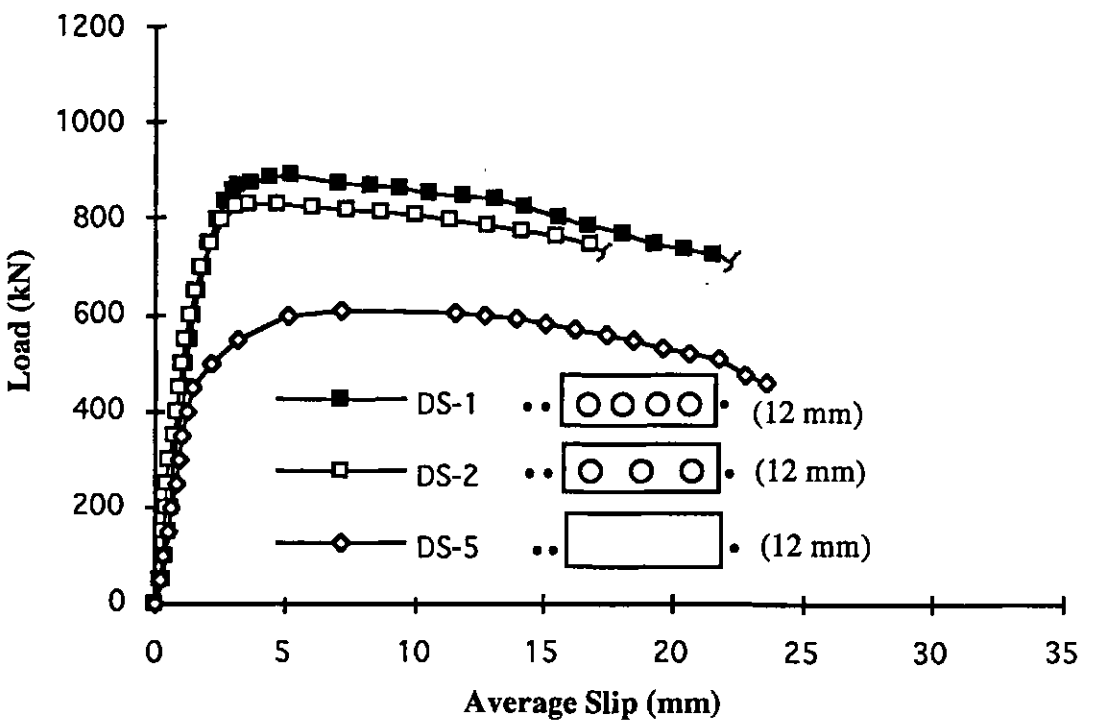

Fig. 3.27 Load-slip relationship of specimens DS-1, DS-2 and DS-5

The load-slip curves for specimens DS-6, DS-7 and DS-10, with 6 mm thick perfobond rib plates, are presented in Fig. 3.28.

As shown in the inset, DS-6 had four holes, DS-7 had three holes, and DS-10 had no holes at all. Except for the plate thickness, these specimens were identical to specimens DS-1, DS-2 and DS-5, respectively. Specimens DS-7 and DS-10 carried 719 kN and 444 kN, respectively. In other words, the three concrete dowels contributed an additional 275 kN or approximately 38% of the total strength. Unlike specimen DS-1, specimen DS-6 carried a slightly smaller load (695 kN) although it had four holes. Instead of increasing the total strength, the additional hole in the thin perfobond rib connector reduced its structural integrity to such an extent that the contribution of the additional concrete dowel was overshadowed. The reduction in strength was approximately 3%.

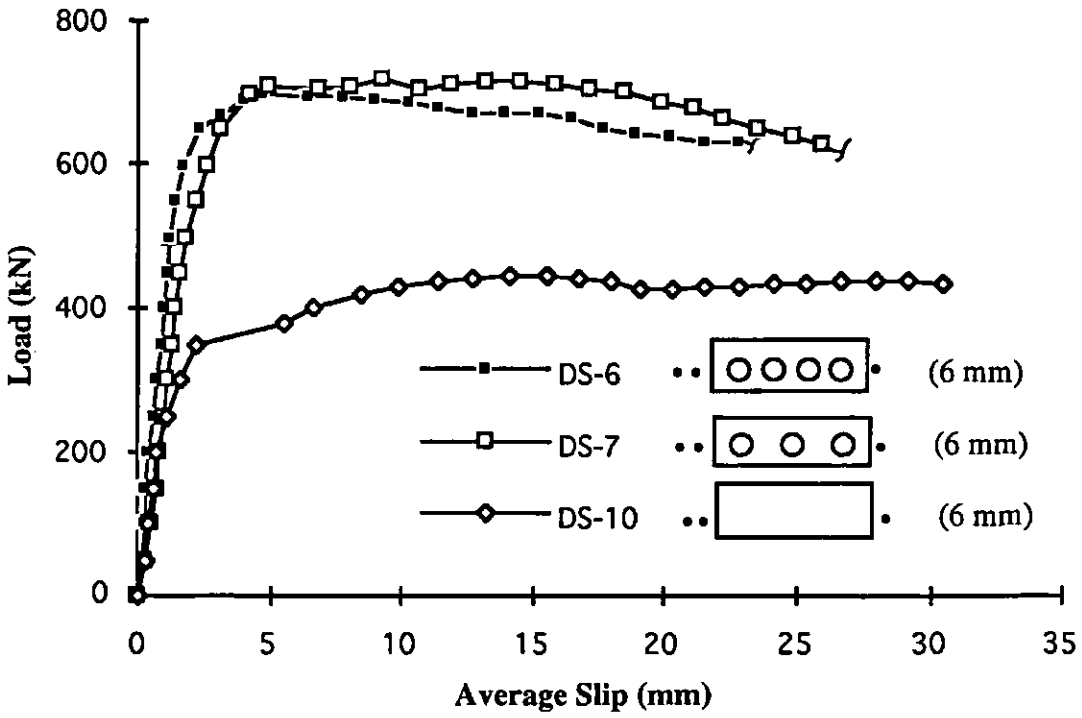

Fig. 3.28 Load-slip relationship of specimens DS-6, DS-7 and DS-10

The same trend was observed for specimens ES-1, ES-2 and ES-9 which also featured 6 mm thick perfobond rib plates. Their load-slip curves are presented in Fig. 3.29. In this case, the contribution of the three concrete dowels in specimen ES-2 was 34% of the total strength and reduction in strength for specimen ES-1 was approximately 6%.

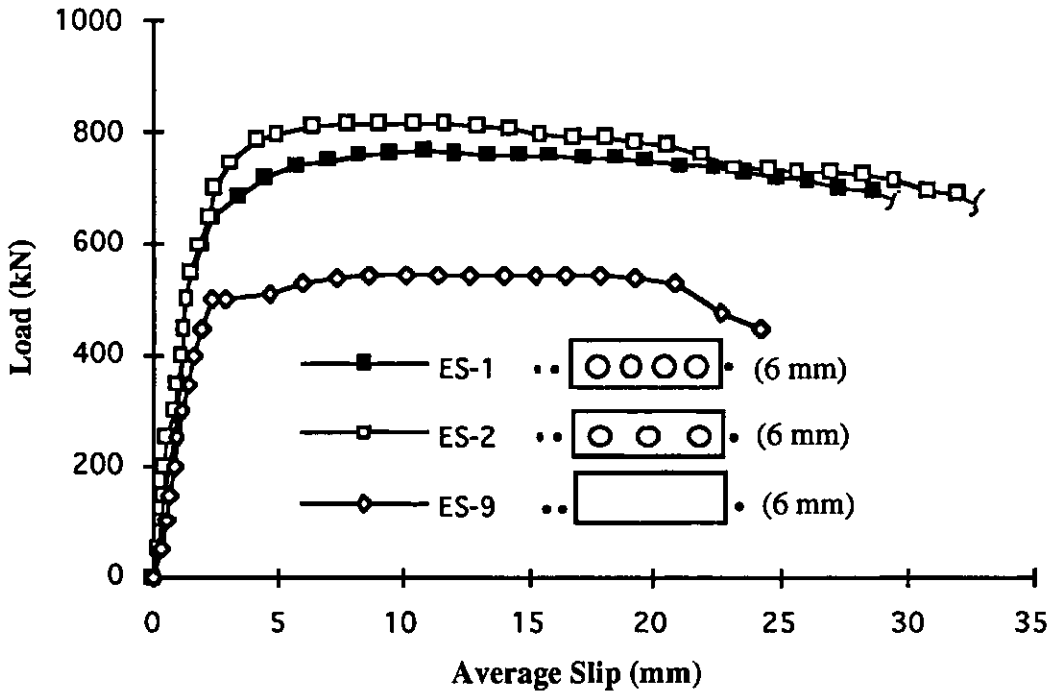

Fig. 3.29 Load-slip relationship of specimens ES-1, ES-2 and ES-9

The contribution of concrete dowels in the specimens with slotted perfobond rib connectors is illustrated in Figs. 3.30 to 3.32. The load-slip curves for specimens FS-1, FS-3 and FS-9, with 12 mm thick perfobond rib plates, are presented in Fig. 3.30. As shown in the inset, FS-1 had four holes, FS-3 had two holes and two slots, and FS-9 had no holes at all. The total loads carried by specimen FS-1 and FS-9 were 1024 kN and 689 kN, respectively. In other words, the contribution of the four concrete dowels in

specimen FS-1 was 33% of the total strength. Although the concrete dowel area is higher in specimen FS-3, it carried a slightly less ultimate load of 984 kN. The contribution of the concrete dowels for this specimen was approximately 30%. The reduction in the ultimate strength was probably due to the fact that slotted connectors are more susceptible to deformation under higher loads.

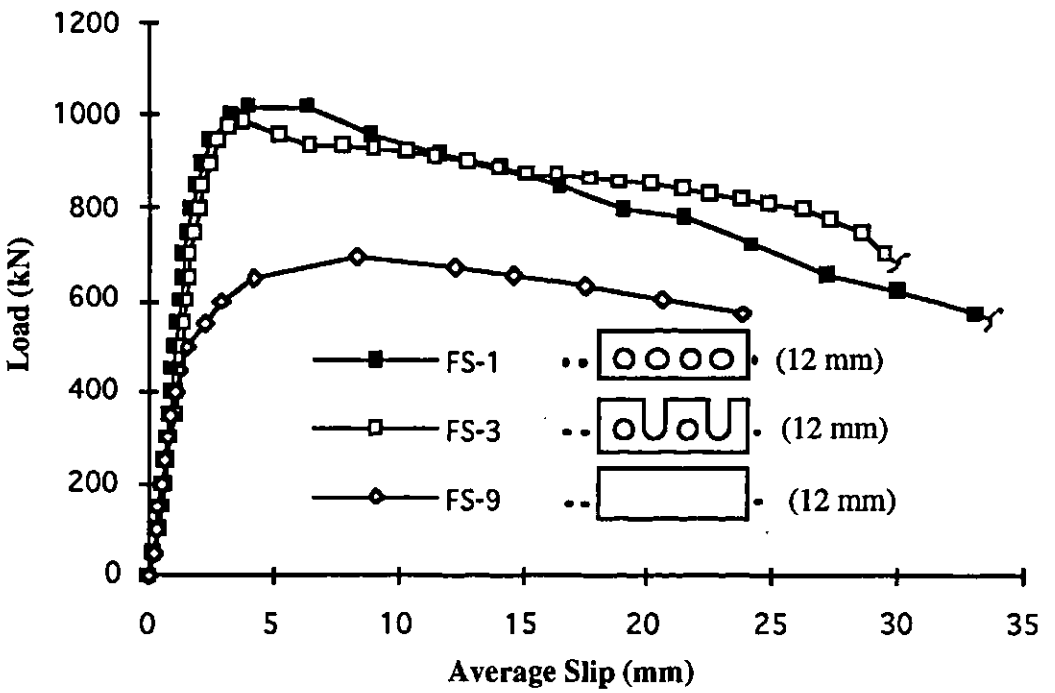

Fig. 3.30 Load-slip relationship of specimens FS-1, FS-3 and FS-9

The load-slip curves for specimens FS-2, FS-4 and FS-9, also with 12 mm thick perfobond rib plates, are presented in Fig. 3.31. As shown in the inset, FS-2 had 3 holes, FS-4 had one hole and two slots, and once again FS-9 had no holes. The total load carried by specimen FS-2 was 917 kN compared to 689 kN for specimen FS-9, as indicated earlier. This translates to a 25%

contribution by the three concrete dowels in specimen FS-2. Once again, specimen FS-4 carried a slightly smaller load (867 kN), although the concrete dowel area in this specimen was higher than that of specimen FS-2. As before, the slight reduction in the ultimate strength is attributed to the susceptibility of slotted connectors to deformation under higher loads.

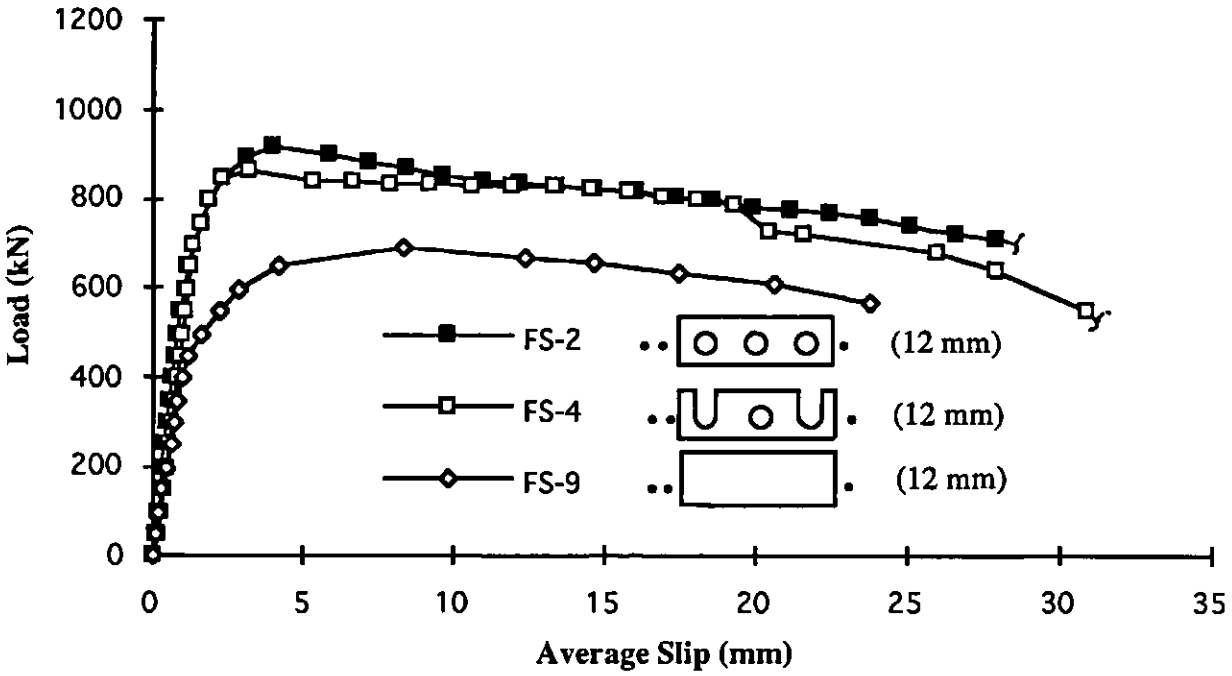

Fig. 3.31 Load-slip relationship of specimens FS-2, FS-4 and FS-9

The load-slip curves for specimens ES-2, ES-4 and ES-9, with 6 mm thick perfobond rib plates, are presented in Fig. 3.32. Except for the plate thickness, these specimens were identical to specimens FS-2, FS-4 and FS-9, respectively. Specimens ES-2 and ES-9 carried 817 kN and 542 kN, respectively. The three concrete dowels contributed an additional 275 kN or approximately 34% of the total strength. Specimen ES-4 carried a smaller

load (719 kN) than ES-2 although, with two slots, its concrete dowel area was higher than that of specimen ES-2. As indicated earlier, the additional hole in the thin perfobond rib connector tends to reduce its structural integrity. The reduction in ultimate strength was approximately 12%.

Additional load-slip curves for other specimens with both slotted and unslotted perfobond rib connectors are presented in Appendix A.

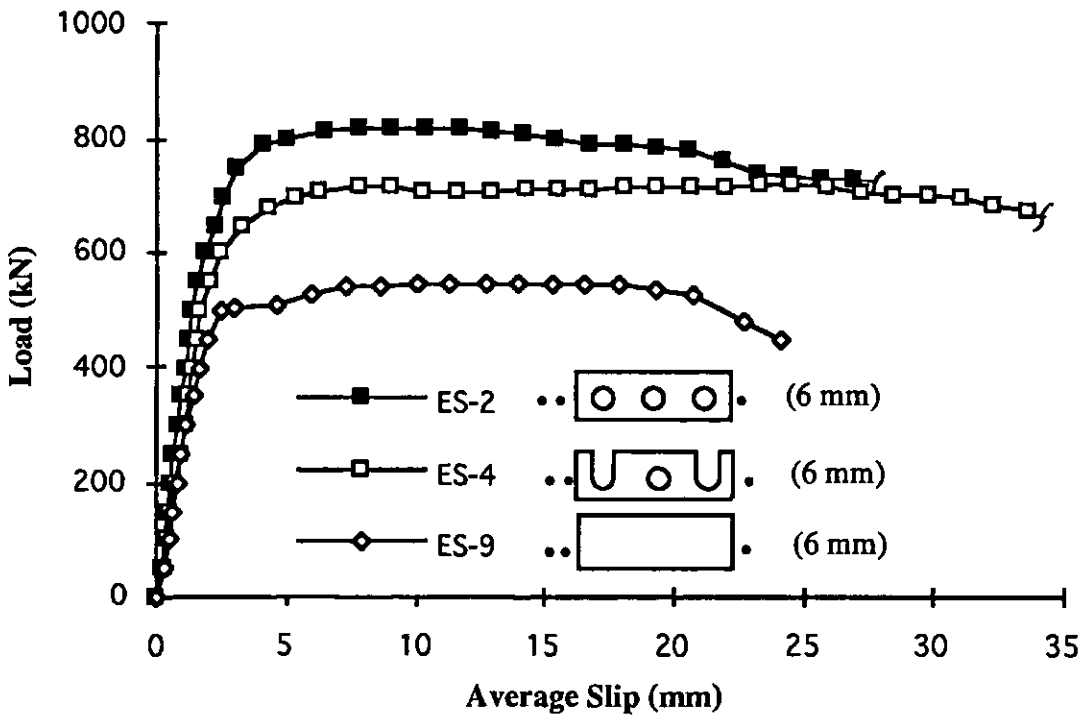

Fig. 3.32 Load-slip relationship of specimens ES-2, ES-4 and ES-9

3.2.4 Effect of Concrete Strength

In order to study the effect of concrete strength on the capacity of the perfobond rib shear connector, specimens with different concrete strengths were tested. The load-slip curves of specimens BS-1 and DS-1 are shown in Fig. 3.33. Specimens BS-1 and DS-1 were identical except for the concrete

strengths which were 27.2 MPa and 20.6 MPa, respectively. For these specimens, with four holes in each perfobond rib connector, the ultimate loads were 1001 kN and 889 kN, respectively. The ratio of these two numbers is 1.13; slightly less than the expected value of $\sqrt{27.2}/\sqrt{20.6}$ which is approximately equal to 1.15. As indicated earlier, the ultimate capacity of a shear connector increases approximately in proportion to the square-root of the compressive cylinder strength, $\sqrt{f_c}$. The higher value for specimen BS-1 may be attributed to the higher shear capacity of the concrete dowels and the splitting resistance of the concrete due to a higher concrete strength.

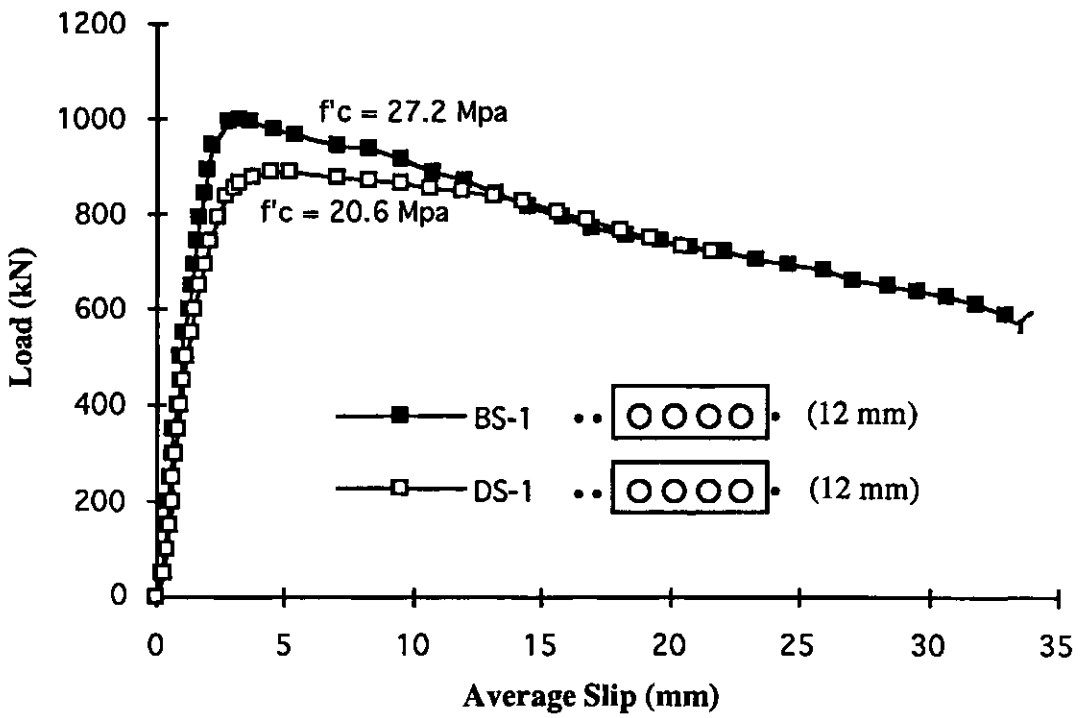

Fig. 3.33 Load-slip relationship of specimens BS-1 and DS-1

The load-slip curves of specimens BS-2 and DS-2 are presented in Fig. 3.34. Both specimens featured perfobond rib connectors with three holes and were identical in every respect except for the difference in the concrete strength, i.e. 27.2 MPa for specimen BS-2 and 20.6 MPa for specimen DS-2. Specimen BS-2 carried 994 kN compared to 832 kN carried by specimen DS-2. The ratio of ultimate loads comes to 1.19 which is somewhat higher than the expected value of 1.15 mentioned earlier. Both specimens featured Type 2 perfobond rib connectors.

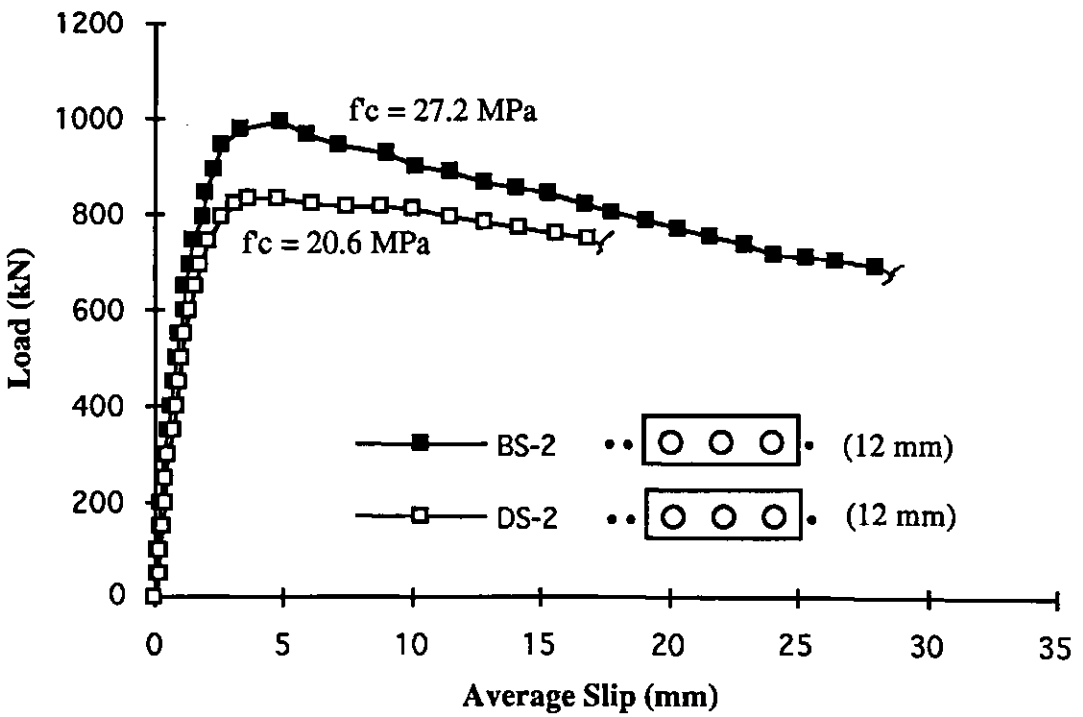

Fig. 3.34 Load-slip relationship of specimens BS-2 and DS-2

Similar results were also observed in specimens with stud shear connectors. As shown in Fig. 3.35, for specimens BS-11 and DS-11, with four headed studs in each slab, the ultimate loads were 741 kN and 614 kN, respectively. The increase in shear capacity was approximately 17% compared to 18.8% calculated according to the CSA S16.1 M89 standard (CSA 1989).

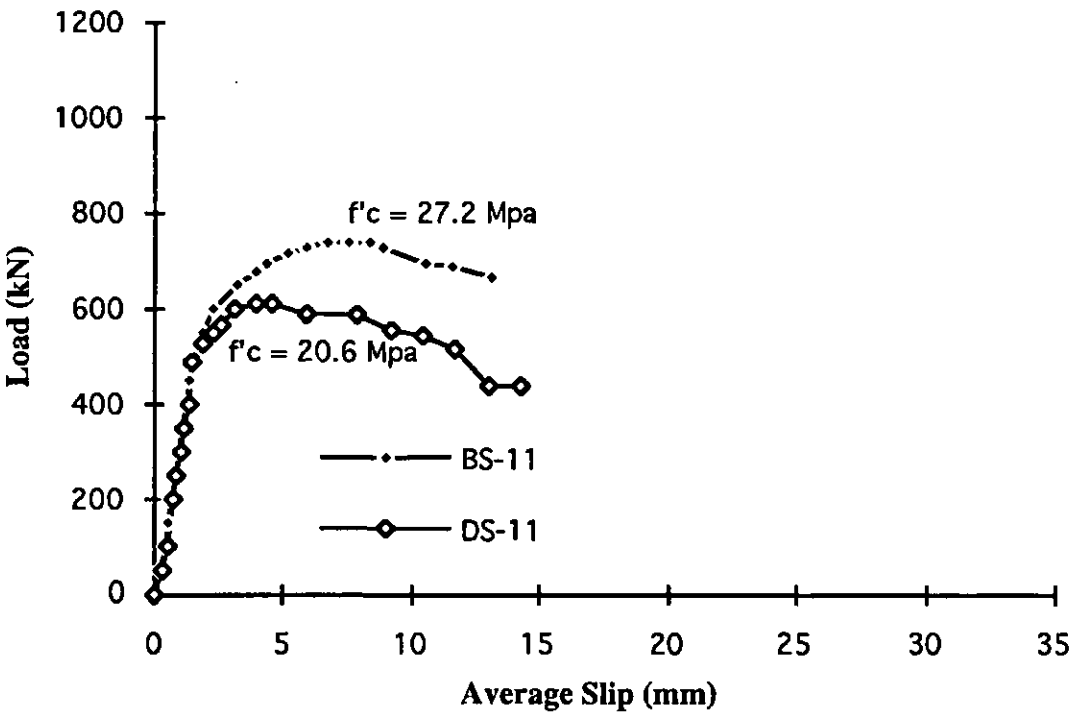

Fig. 3.35 Load-slip relationship of specimens BS-11 and DS-11

3.2.5 Effect of additional transverse reinforcement through the rib holes

In Series D, additional transverse reinforcing bars were passed through the rib holes of four specimens. Fig. 3.36 shows specimens DS-2 and DS-4, which formed the first companion pair. Both specimens featured 12 mm thick perfobond rib connectors with three openings and contained the usual

amount of transverse reinforcement, i.e. two No. 10 bars in the bottom and one at the top. However, three additional No. 10 bars were passed through the three openings of specimen DS-4. The load-slip curves for these specimens are presented in Fig. 3.37. The ultimate load carried by specimen DS-4 was 1156 kN compared to only 833 for specimen DS-2. In other words, the three additional reinforcing bars increased the ultimate load by 28%.

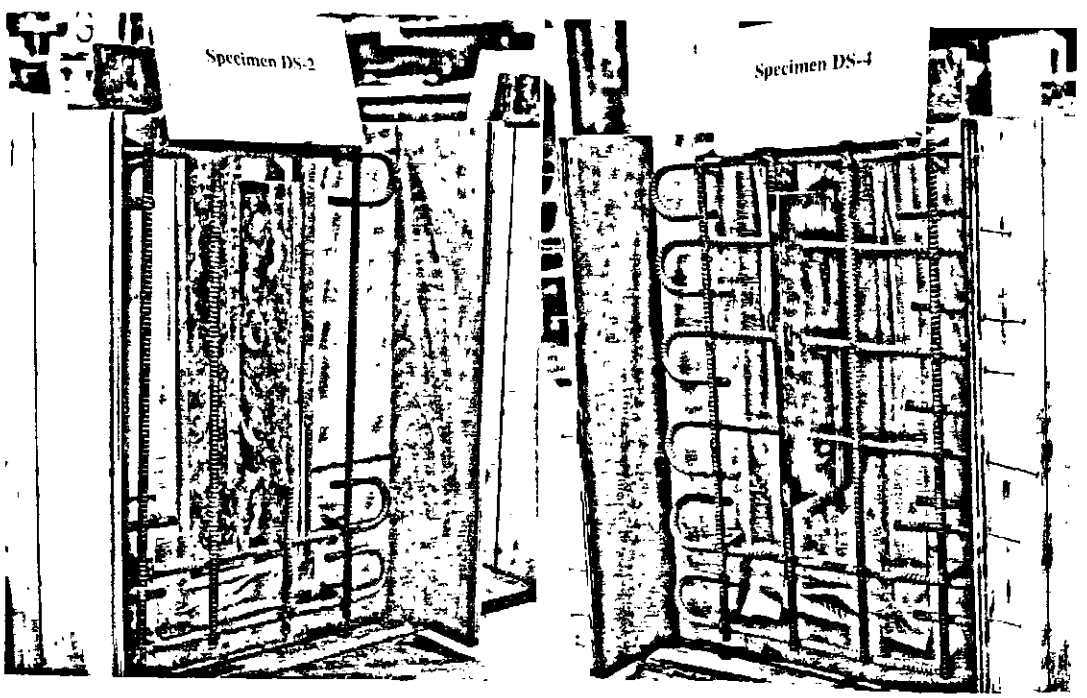

Fig. 3.36 Specimens DS-2 and DS-4 with additional reinforcement

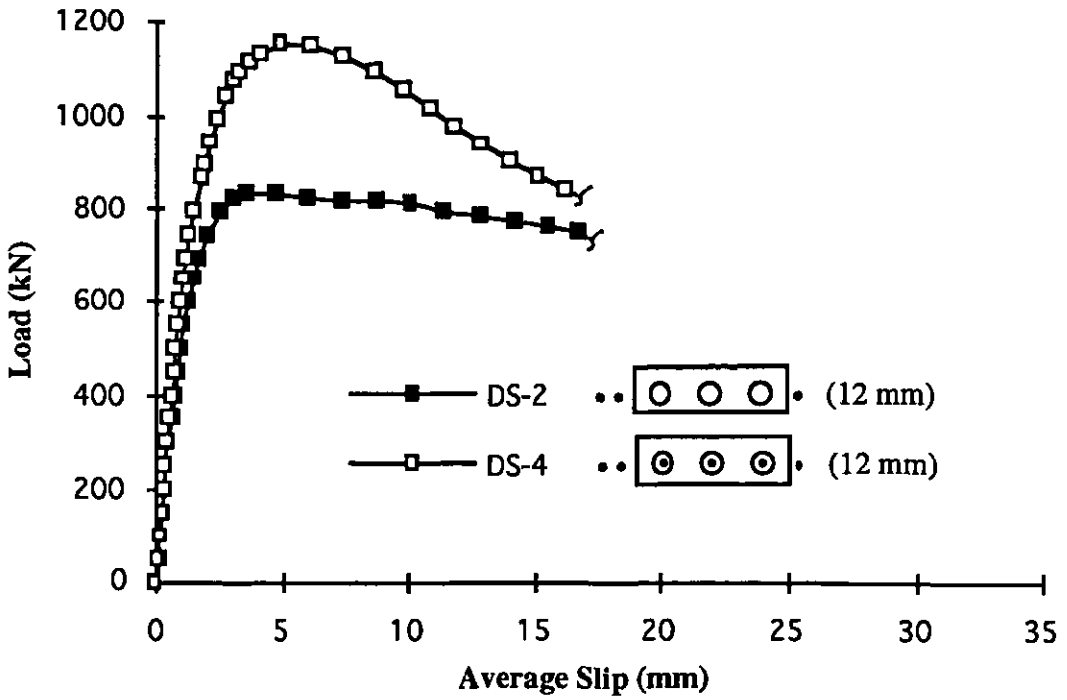

Fig. 3.37 Load-slip relationship of specimens DS-2 and DS-4

Fig. 3.38 presents the load-slip curves for specimens DS-1 and DS-3, the companion specimens with Type 1 perfobond rib connectors. In this case, the increase was 27%. These values are similar to those observed by Veldanda in an earlier test program (Veldanda 1991). Once again, the use of additional reinforcement through the openings added considerable ductility to specimen DS-3.

This behaviour adds to the advantages of perfobond rib connectors. If additional capacity is desired at a certain location, this option can be utilized.

Similar results were also observed for specimens with 6 mm perfobond rib connectors. The corresponding increases were 17% and 31% for the specimens with three-hole and four-hole connectors, respectively. The relevant load-slip curves are presented in Appendix A.

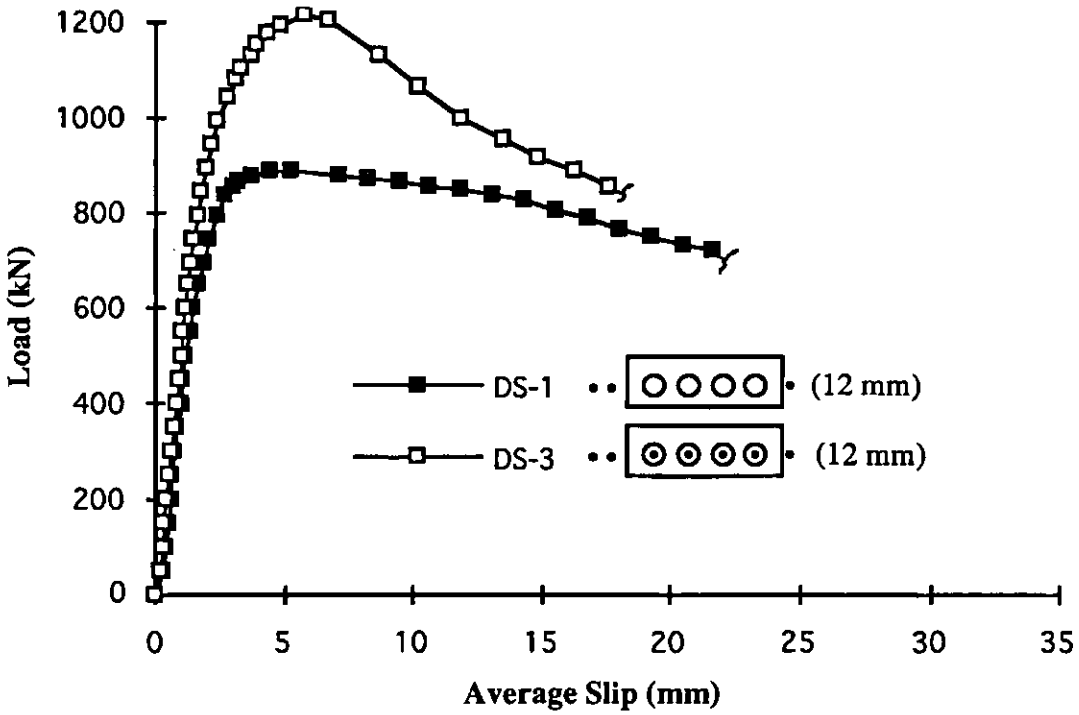

Fig. 3.38 Load-slip relationship of specimens DS-1 and DS-3

Table 3.1 Test Results - Series 1
$f'c = 26.3$ MPa, $f'_{ct} = 3.14$ MPa, slab without wire mesh

Specimen	Connector Geometry	Connector Type	Dimension (mm)	Ult. Load (kN)
AS-1	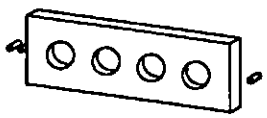	1	376x127x12	1016.33
AS-2	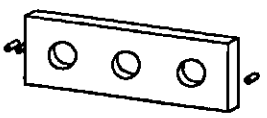	2	376x127x12	906.72
AS-3	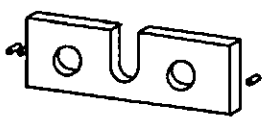	4	376x127x12	944.59
AS-4	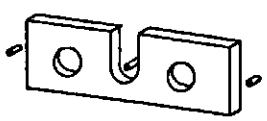	Type 4 with rebar	376x127x12	1032.27
AS-5	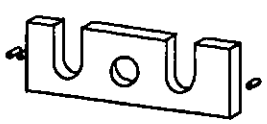	6	376x127x12	962.52
AS-6	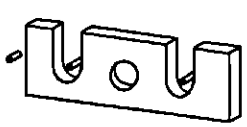	Type 6 with rebar	376x127x12	1058.18
AS-7	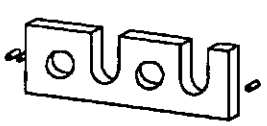	3	376x127x12	918.68
AS-8	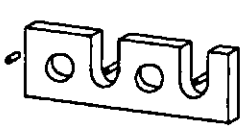	Type 3 with rebar	376x127x12	1160.81
AS-9	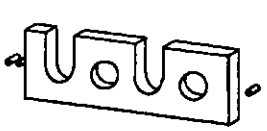	5	376x127x12	974.48
AS-10	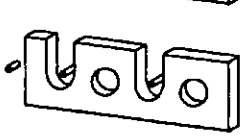	Type 5 with rebar	376x127x12	1159.81

Table 3.2 Test Results - Series 2
$f'c = 27.2$ MPa, $f'_{ct} = 3.20$ MPa, slab with wire mesh

Specimen	Connector Geometry	Connector Type	Dimension (mm)	Ult. Load (kN)
BS-1	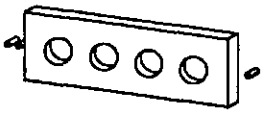	1	376x127x12	1001.38
BS-2	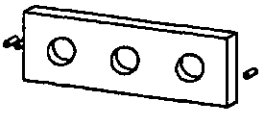	2	376x127x12	994.41
BS-3	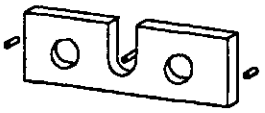	Type 4 with rebar	376x127x12	1074.12
BS-4	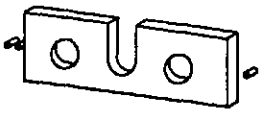	4	376x127x12	981.46
BS-5	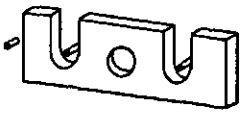	Type 6 with rebar	376x127x12	1029.28
BS-6	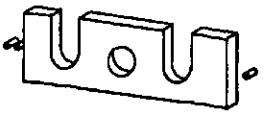	6	376x127x12	914.70
BS-7	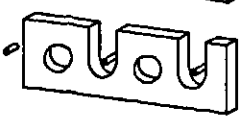	Type 3 with rebar	376x127x12	1143.87
BS-8		3	376x127x12	1031.28
BS-9	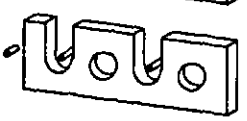	Type 5 with rebar	376x127x12	1210.62
BS-10	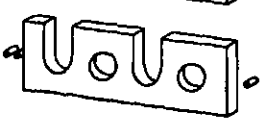	5	376x127x12	988.43
BS-11		Studs	19x125	741.32
BS-12		Studs	19x125	657.63

Table 3.3 Test Results - Series 3
$f'c = 25.2$ MPa, $f'_{ct} = 3.05$ MPa, slab with wire mesh

Specimen	Connector Geometry	Connector Type	Dimension (mm)	Ult. Load (kN)
CS-1	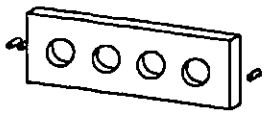	1	376x127x6	730.36
CS-2	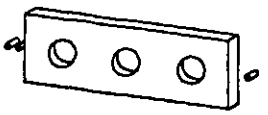	2	376x127x6	727.37
CS-3	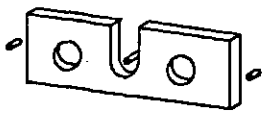	Type 4 with rebar	376x127x6	800.11
CS-4	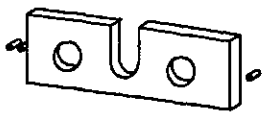	4	376x127x6	760.25
CS-5	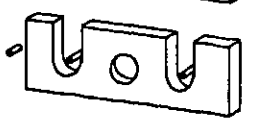	Type 6 with rebar	376x127x6	742.32
CS-6		6	376x127x6	661.61
CS-7		Type 3 with rebar	376x127x6	836.98
CS-8		3	376x127x6	747.30
CS-9	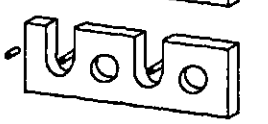	Type 5 with rebar	376x127x6	866.87
CS-10	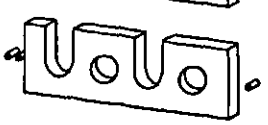	5	376x127x6	742.32
CS-11		Studs	19x125	671.57
CS-12		Studs	19x125	558.98

Table 3.4 Test Results - Series 4
$f'c = 20.6$ MPa, $f'_{ct} = 2.80$ MPa, slab with wire mesh

Specimen	Connector Geometry	Connector Type	Dimension (mm)	Ult. Load (kN)
DS-1	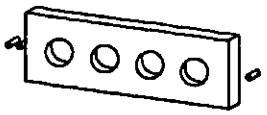	1	376x127x12	888.79
DS-2	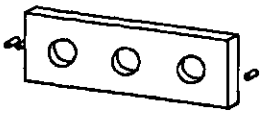	2	376x127x12	832.99
DS-3	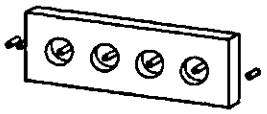	Type 1 with rebar	376x127x12	1251.61
DS-4	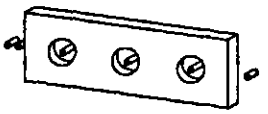	Type 2 with rebar	376x127x12	1155.83
DS-5	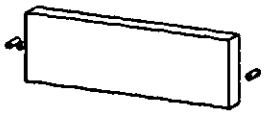	Solid	376x127x12	607.80
DS-6	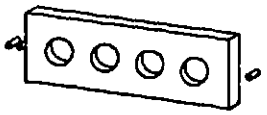	1	376x127x6	695.49
DS-7	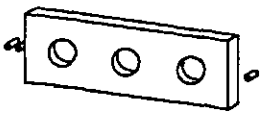	2	376x127x6	719.40
DS-8	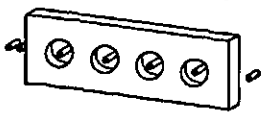	Type 1 with rebar	376x127x6	1002.38
DS-9	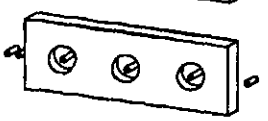	Type 2 with rebar	376x127x6	868.86
DS-10	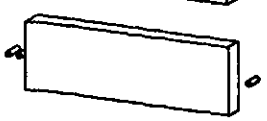	Solid	376x127x6	444.39
DS-11		Studs	19x125	613.78
DS-12		Studs	19x125	514.14
DS-13		Studs	19x125	609.80
DS-14		Studs	19x125	579.91

CHAPTER FOUR

EXPERIMENTAL RESULTS: PHASE TWO

4.1 Scope

As indicated in Chapter Three, two series of tests, Series 5 and Series 6, involving a total of 32 push-out specimens were tested to address a number of issues. The main objective was to study the effects of using a narrow plate in front of the perfobond rib connector. As shown in Table 4.1, Series 5 included ten specimens, five with and five without face plates, to serve this purpose. In two of these specimens, ES-9 and ES-10, unperforated plate connectors were used to evaluate the effects of the presence of a face plate on the contribution of the concrete dowels. Series 5 also included two specimens with headed studs, specimens ES-15 and ES-16, for comparison purpose. The remaining four specimens in Series 5 had perfobond rib connectors with rectangular openings instead of circular holes and rounded slots. The observed ultimate load values are listed in Table 4.1.

Series 6 also included a total of sixteen specimens. The first 14 specimens were identical to those of Series 5 except that the web thickness of the plate connectors was 12 mm. The last two specimens (FS-15 and FS-16) featured 75 mm and 100 mm wide face plates respectively. The observed ultimate load values are listed in Table 4.2 which is placed at the end of the chapter.

4.2 Behaviour of Perfobond Rib Connectors with Face Plates

The load-slip curves for specimens FS-1 and FS-5 are presented in Fig. 4.1. As shown in Fig. 4.2, these specimens featured 12 mm perfobond rib

connectors with four holes and were similar in every respect except that in specimen FS-5, a 12 mm thick face plate was attached. Specimen FS-5 carried a maximum load of 1457 kN compared to 1024 kN for specimen FS-1. In other words, the face plate was responsible for a 30% increase in strength. There is also an increase in the ductility although there is a decrease in the load retention capability.

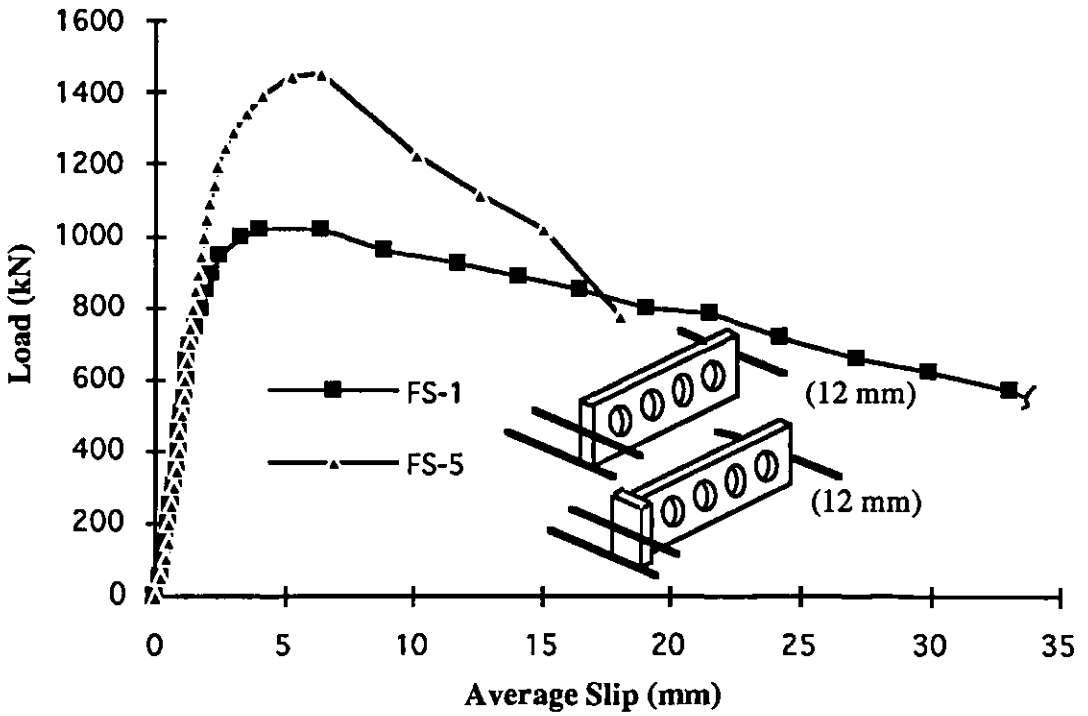

Fig. 4.1 Load-slip relationship of specimens FS-1 and FS-5

Table 4.1 Test Results - Series 5
f'_c = 26.2 MPa, f'_{ct} = 3.11 MPa, slab with wire mesh

Specimen	Connector Geometry	Connector Type	Dimension (mm)	Ult.Load (kN)
ES-1	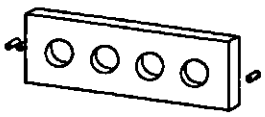	1	376x127x6	769.22
ES-2	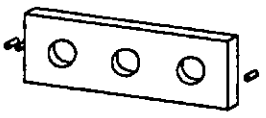	2	376x127x6	817.05
ES-3	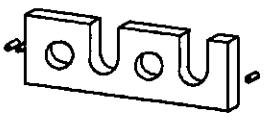	3	376x127x6	789.15
ES-4	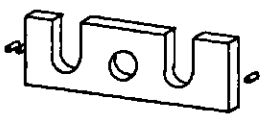	6	376x127x6	719.40
ES-5	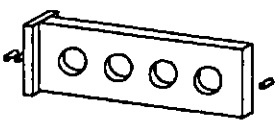	Type 1 with face plate	376x127x6 (50x127 face plate)	1200.66
ES-6	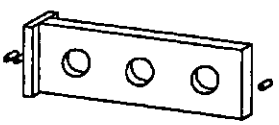	Type 2 with face plate	376x127x6 (50x127 face plate)	1209.63
ES-7	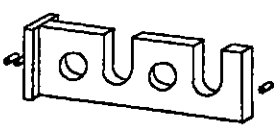	Type 3 with face plate	376x127x6 (50x127 face plate)	1173.76
ES-8	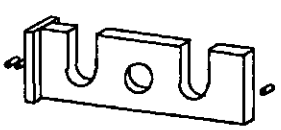	Type 6 with face plate	376x127x6 (50x127 face plate)	1094.05

Table 4.1 (Cont'd.) Test Results - Series 5
f'_c = 26.2 MPa, f'_{ct} = 3.11 MPa, slab with wire mesh

Specimen	Connector Geometry	Connector Type	Dimension (mm)	Ult.Load (kN)
ES-9	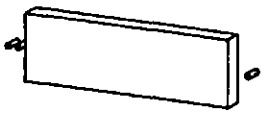	Solid	376x127x6	542.04
ES-10	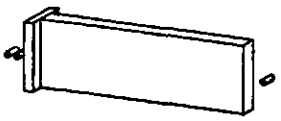	Solid with face plate	376x127x6 (50x127 face plate)	1041.24
ES-11	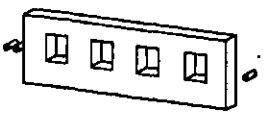	Type 1 with rectangular openings	376x127x6	775.20
ES-12		Type 2 with rectangular openings	376x127x6	795.13
ES-13	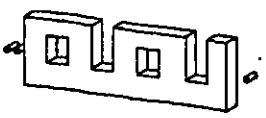	Type 3 with rectangular openings	376x127x6	741.32
ES-14	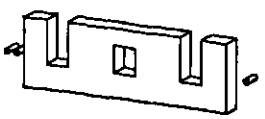	Type 6 with rectangular openings	376x127x6	697.48
ES-15		Studs	19x125	667.59
ES-16		Studs	19x125	617.77

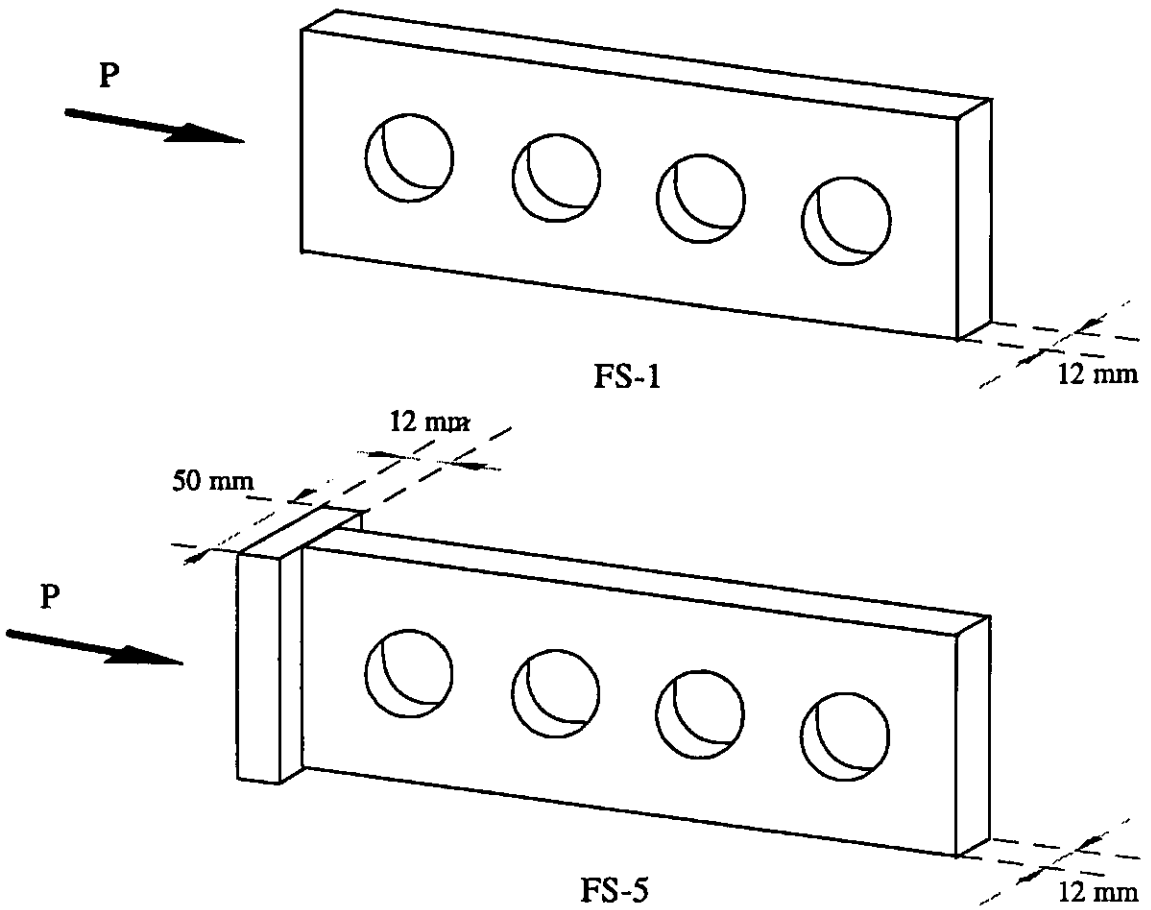

Fig. 4.2 Perfobond rib connector with and without face plate

For the corresponding pair with three holes, i.e. for specimens FS-2 and FS-6, the increase in ultimate load capacity for the specimen with a face plate was 34%. Once again, there is a substantial increase in ductility as can be seen in Fig. 4.3. There is however a decrease in the load retaining capability.

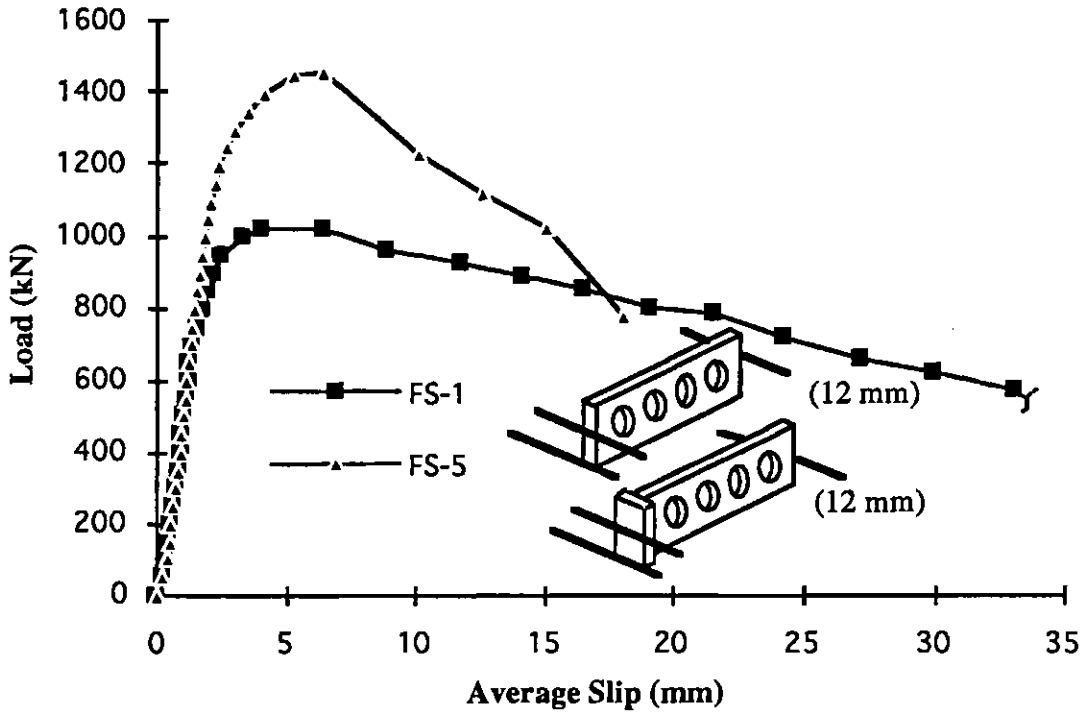

Fig. 4.3 Load-slip relationship of specimens FS-2 and FS-6

By distributing bearing force on a wider area, the face plate delayed the formation of longitudinal splitting and thereby enhanced the ultimate capacity. Failure was caused largely due to the crushing of concrete in front of the face plate as shown in Fig. 4.4. The failure mechanism appears to be dominated by crushing of the concrete instead of being predominantly splitting as before. Thus there is a decrease in the interlocking action between the split surfaces after failure occurs resulting in a rapid decrease in the load retaining capacity once the concrete crushes. The deformed face plates of specimens FS-5 and FS-6 are shown in Fig. 4.5. Photographs of other failed specimens from Series 5 and 6 are presented in Appendix B.

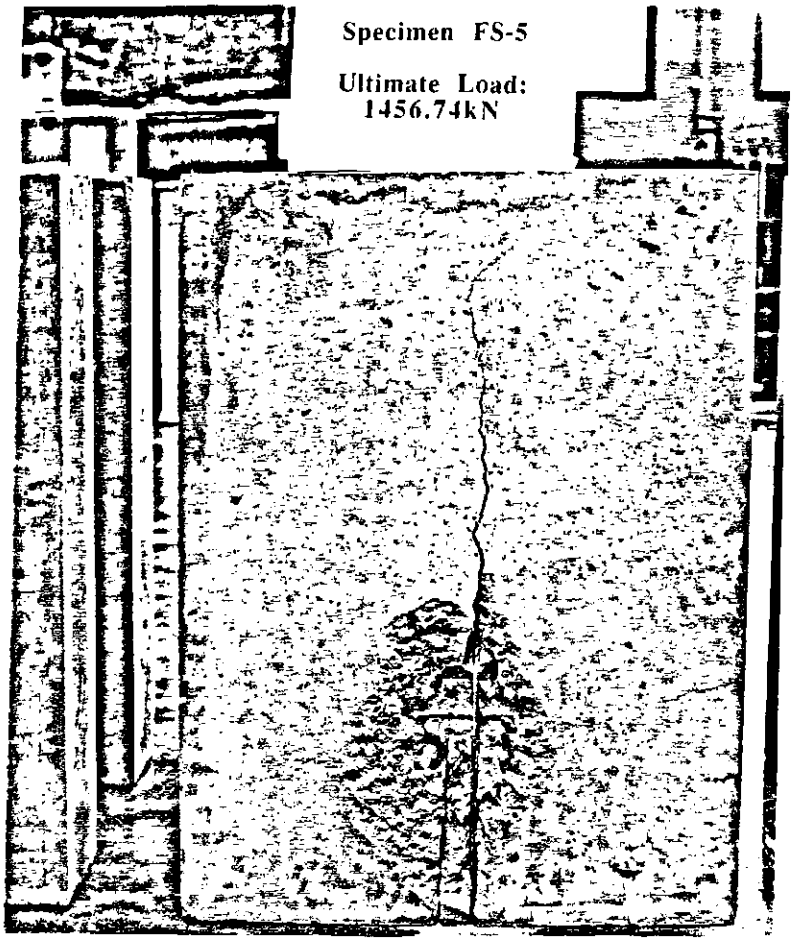

Fig. 4.4 Typical failure mechanism of specimens with face plates

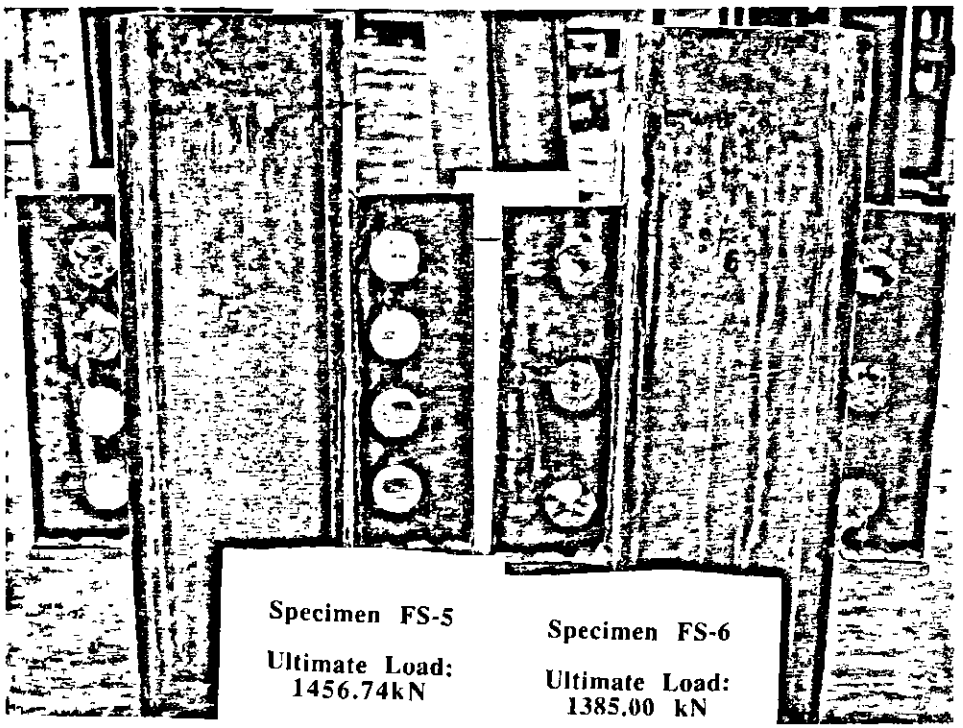

Fig. 4.5 Deformed perfobond rib connectors with face plates

Similar results were also observed for specimens with 6 mm thick perfobond rib connectors. The load-slip curves for specimens ES-1 and ES-5 are presented in Fig. 4.6. These specimens had perfobond rib connectors with four holes and were similar in every respect except that in specimen ES-5, a 6 mm thick face plate was attached. Specimen ES-5 carried a maximum load of 1201 kN compared to 769 kN for specimen ES-1. This translates into an increase of 36% in shear capacity due to the presence of the face plate. For the corresponding pair with three holes, i.e. specimens ES-2 and ES-6, the increase in ultimate load capacity for the specimen with a face plate was 32%.

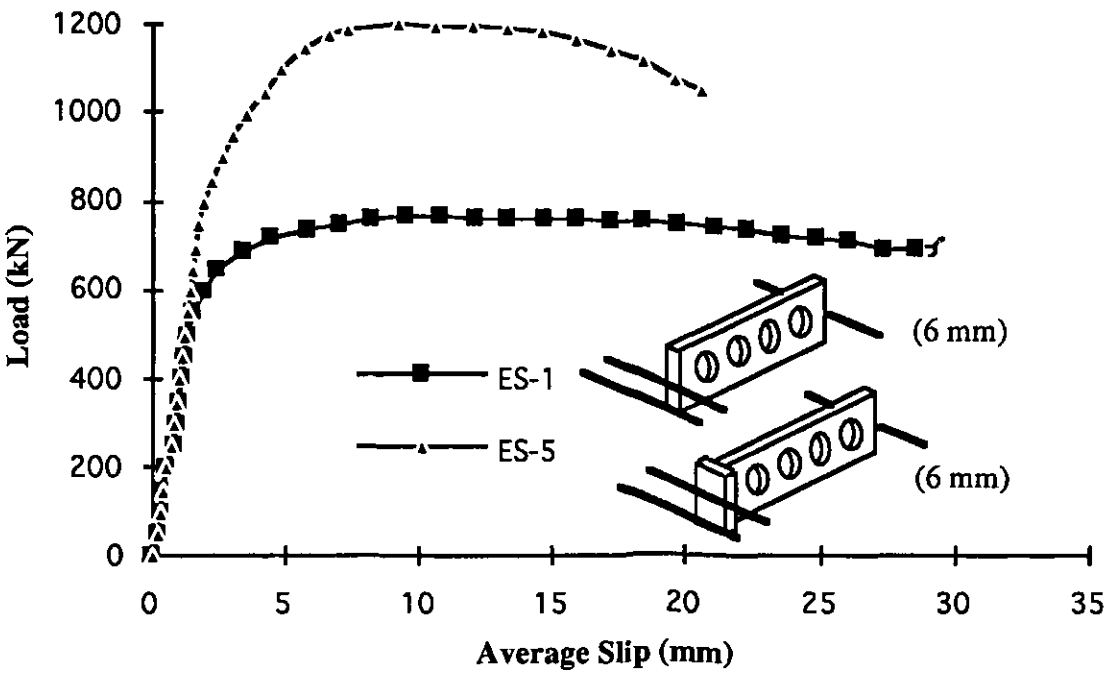

Fig. 4.6 Load-slip relationship of specimens ES-1 and ES-5

The load-slip curves for specimens ES-2 and ES-6, together with those of slotted specimens with and without face plates, are presented in Appendix A. For slotted specimens, the average increase in ultimate load capacity for the specimens with a face plate was approximately 34%.

The substantial increase in load carrying capacity as well as the enhancement in ductility would make the use of face plates a desirable option. In fact, this may turn out to be an entirely new area for further exploration. Due to the change in the failure mechanism as explained earlier, there may a diminishing role for the concrete dowels. This possibility will be investigated in the following section.

4.3 Contribution of the Concrete Dowels in Perfobond Rib Connectors with Face Plates

The load-slip curves for specimens FS-5, FS-6 and FS-10 are presented in Fig. 4.7. These specimens featured 12 mm thick perfobond rib connectors with face plates. As shown in Figs. 4.5 and 4.8, FS-5 had four holes, FS-6 had three holes, and FS-10 had no holes at all. Specimens FS-6 and FS-10 carried 1385 kN and 1154 kN, respectively. This means that the three dowels in the perfobond rib connector were responsible for an additional 231 kN. In other words, roughly 17% of the ultimate strength is contributed by the concrete dowels formed within the holes of the perfobond rib connector. As indicated in Chapter Three, specimens DS-2 and DS-5 (identical specimens without face plates) carried 833 kN and 608 kN respectively. The contribution of the concrete dowels in that case was roughly 27% of the ultimate strength.

As expected, there is a noticeable decrease in the contribution of the concrete dowels when a face plate is present. Specimen FS-5, with four holes, supported an ultimate load of 1457 kN. The additional concrete dowel increased the strength by about 5%.

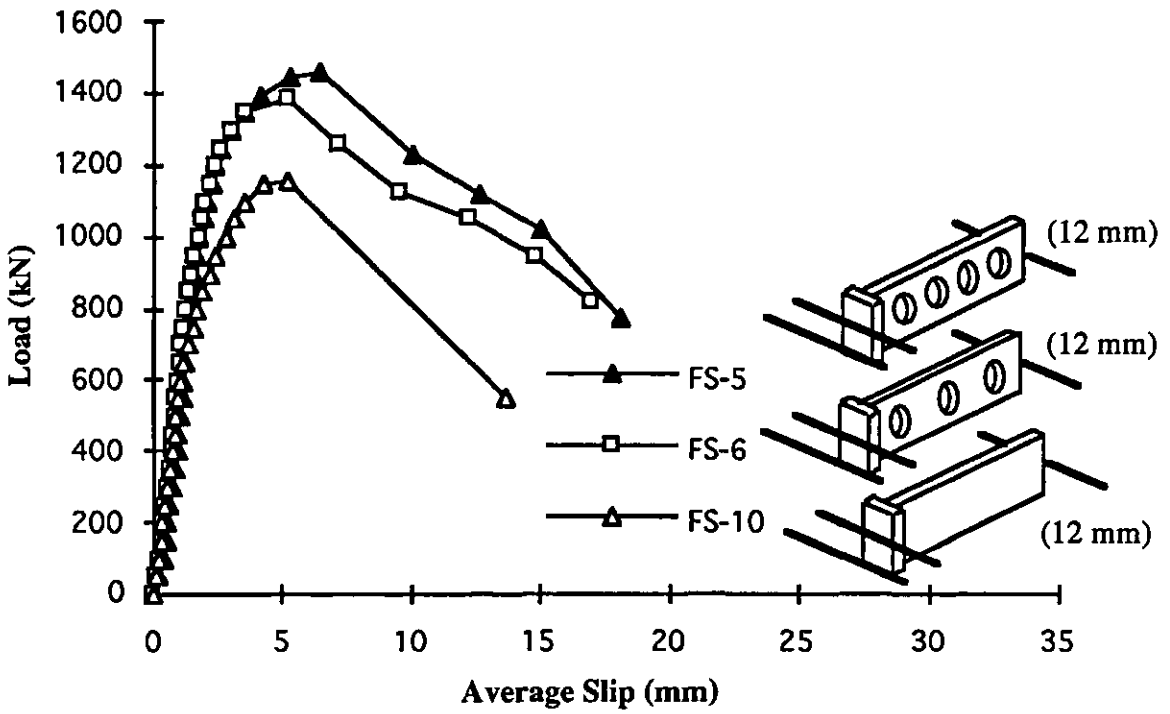

Fig. 4.7 Load-slip relationship of specimens FS-5, FS-6 and FS-10

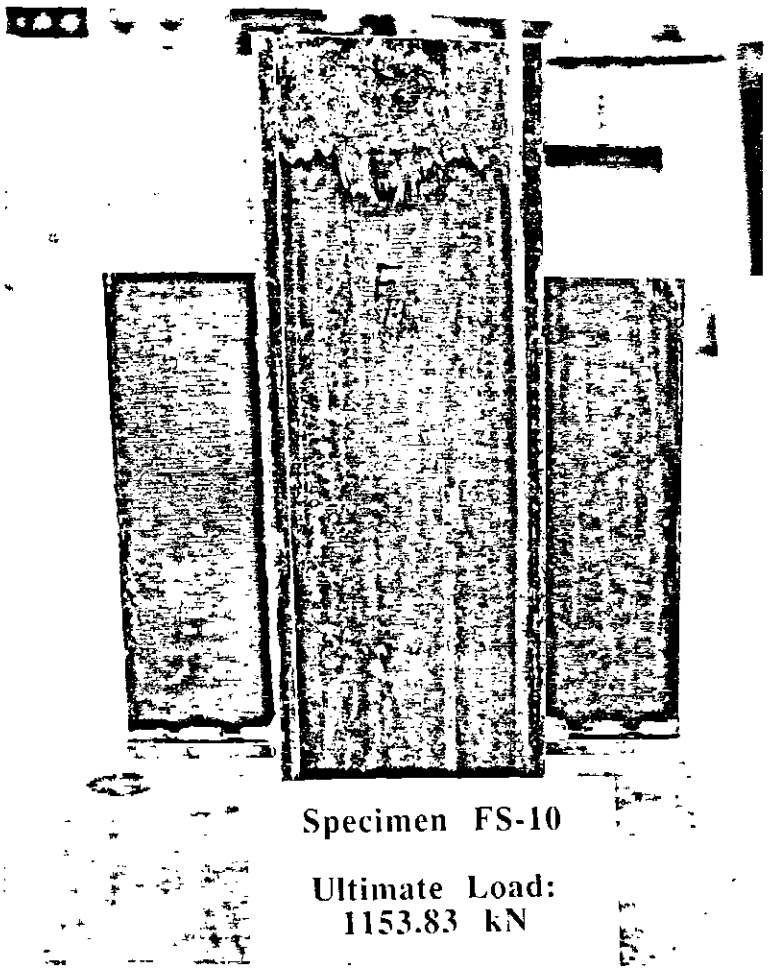

Fig. 4.8 Solid connector with face plate in specimen FS-10 after test

The load-slip curves for specimens ES-5, ES-6 and ES-10, with 6 mm thick perfobond rib connectors with face plates, are presented in Fig. 4.9. As shown in the inset, ES-5 had four holes, ES-6 had three holes, and ES-10 had no hole at all. Except for the plate thickness, these specimens were identical to specimens FS-5, FS-6 and FS-10, respectively. Specimens ES-6 and ES-10 carried 1210 kN and 1041 kN, respectively. In other words, the three concrete dowels contributed approximately 14% of the total strength. Once again, a diminished role for the concrete dowels is observed. The

corresponding value for identical specimens without face plates was 38%. Unlike specimen FS-5, specimen ES-5 carried a slightly smaller load (1201 kN) although it had four holes. The same behaviour was also observed for 6 mm thick perfobond rib connectors without face plates. As explained earlier in Chapter Three, the additional hole in a thin plate tends to make it very flexible to hold any additional load.

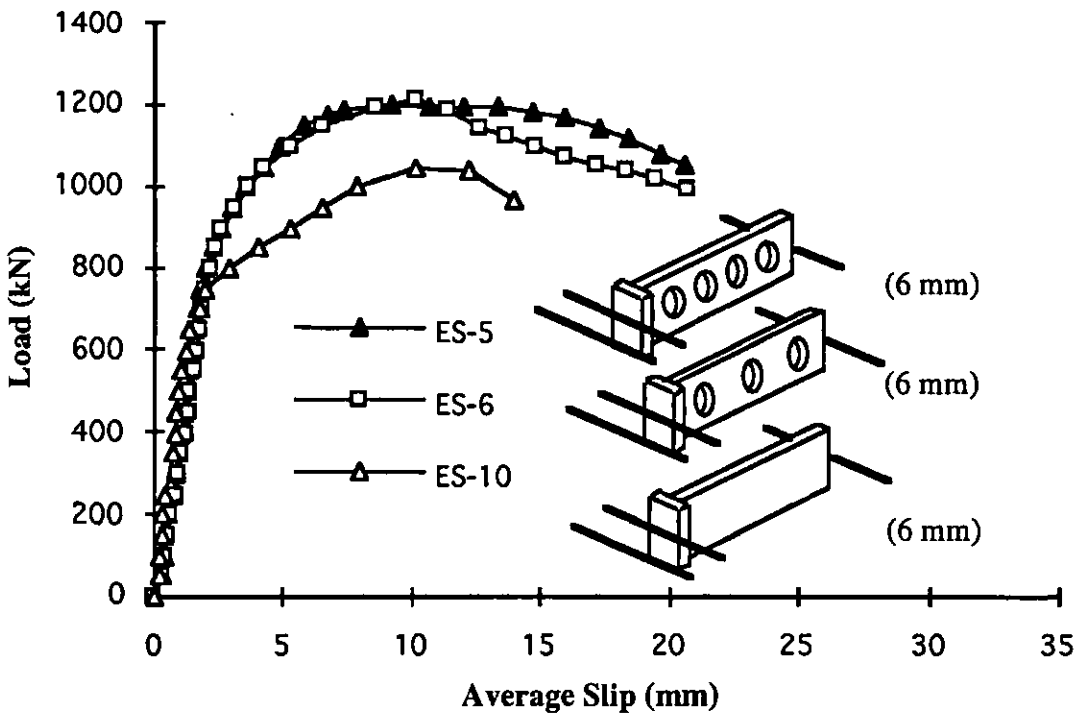

Fig. 4.9 Load-slip relationship of specimens ES-5, ES-6 and ES-10

4.4 Behaviour of Perfobond Rib Connectors with Rectangular Openings

The load-slip curves for push-out specimens FS-1 and FS-11, both from Series 6 and with 12 mm thick perfobond rib connectors, are presented in Fig. 4.10. As shown in the inset to this curve, specimens FS-1 and FS-11 were identical except for the shape of their openings. Specimen FS-1, with

circular holes, carried 1024 kN compared to 967 kN for specimen FS-11. The difference is approximately 6%. An examination of the failed specimens (Fig. 4.11) indicates that the concrete dowels in both specimens failed by double shear. Since the cross-sectional area of the circular opening in specimen FS-1 was approximately the same as that of the rectangular opening in specimen FS-11, the specimens were expected to carry approximately the same load.

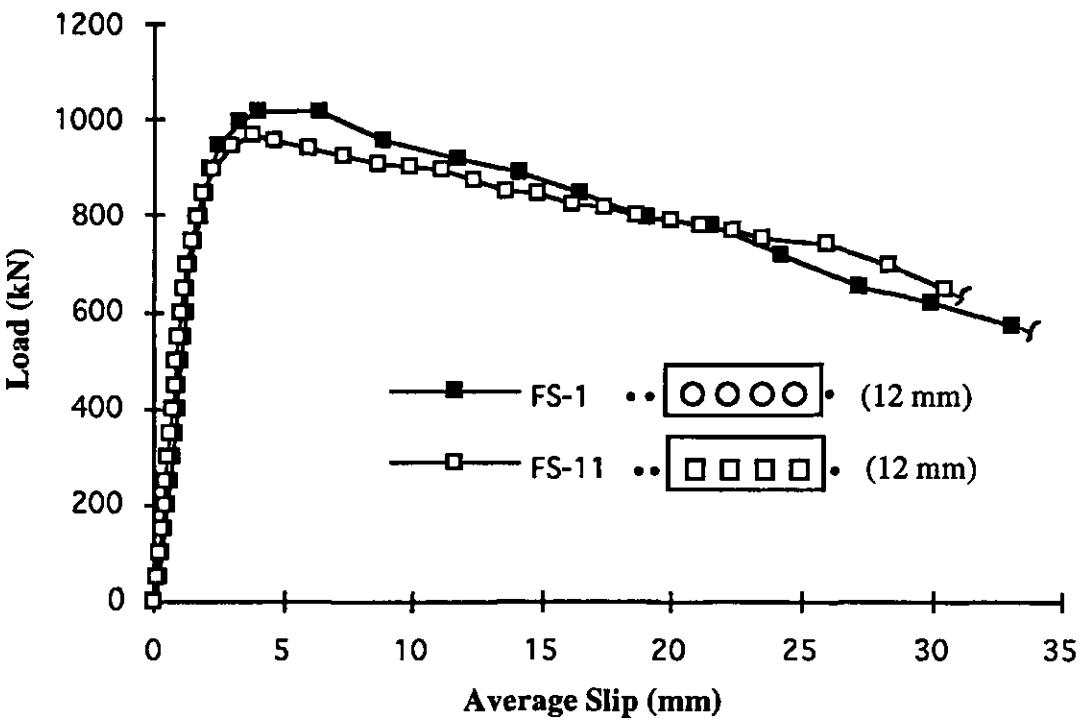

Fig. 4.10 Load-slip relationship of specimens FS-1 and FS-11

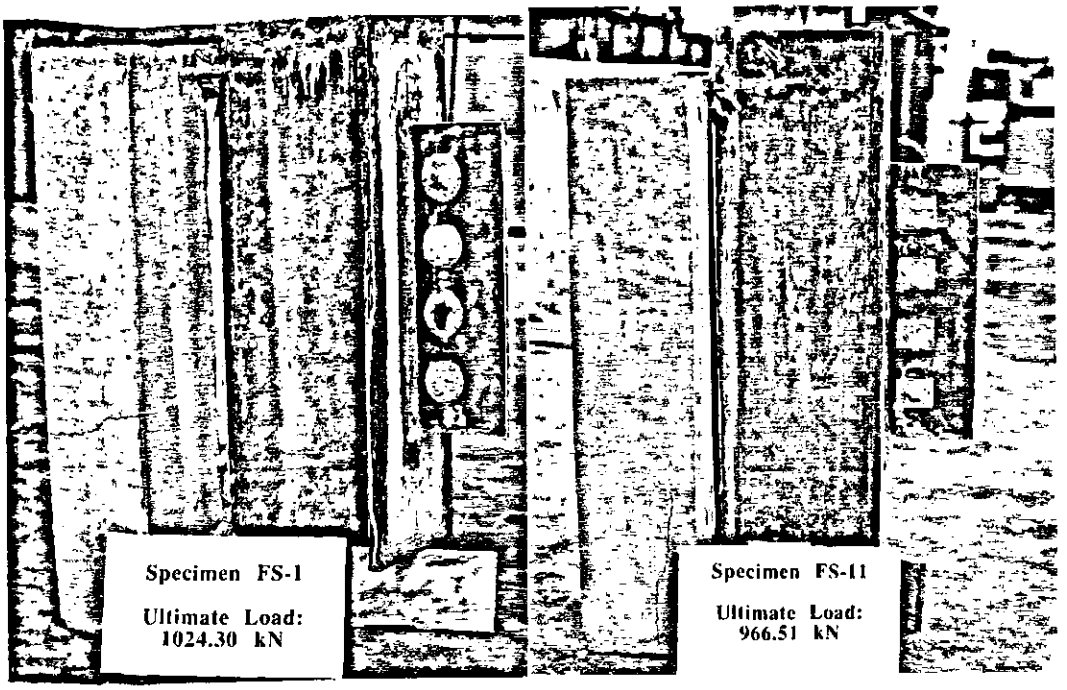

Fig. 4.11 Specimens FS-1 and FS-11 after failure

Fig. 4.12 presents the load-slip curves for push-out specimens FS-2 and FS-12, both with 12 mm thick perfobond rib connectors containing three openings. Once again, specimens FS-2 and FS-12 were identical except for the shape of their openings. As can be seen in Fig. 4.12, their behaviour was also very similar. Specimen FS-2, with circular holes, carried 917 kN compared to 961 kN for specimen FS-12, the difference being approximately 4% only.

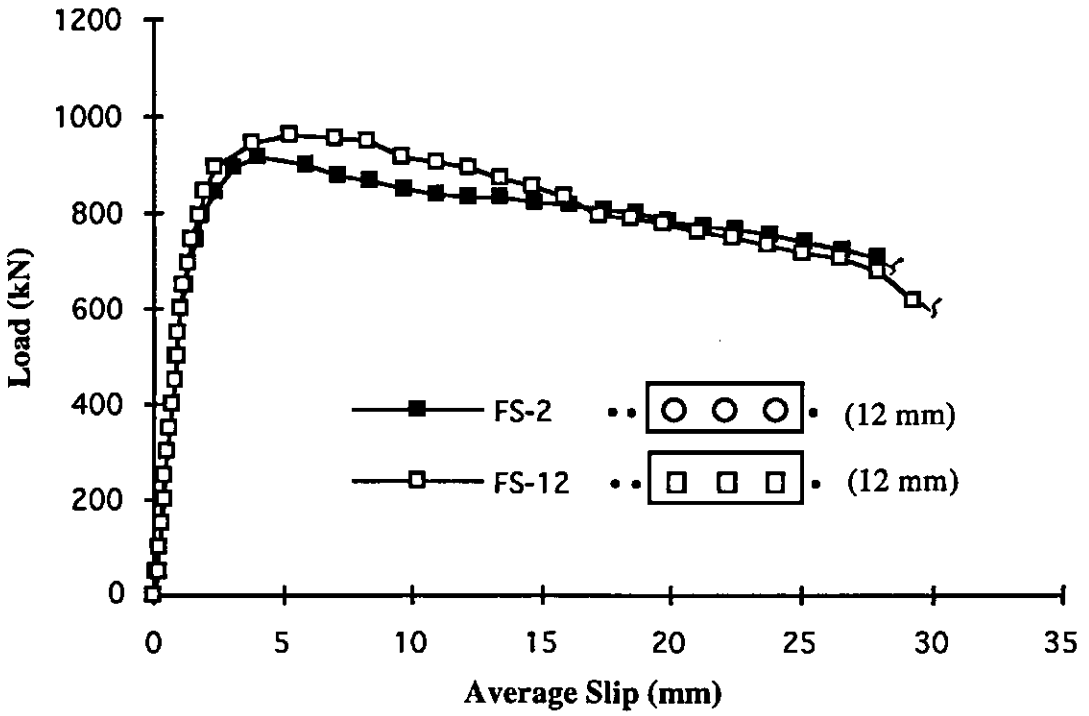

Fig. 4.12 Load-slip relationship of specimens FS-2 and FS-12

A similar trend was also observed for specimens with 6 mm thick perfobond rib connectors containing circular and rectangular openings. A comparison of the load-slip curves for specimens ES-1 and ES-11 and that of ES-2 and ES-12, shown in Figs. 4.13 and 4.14, respectively, indicates that their behaviour was almost identical to each other.

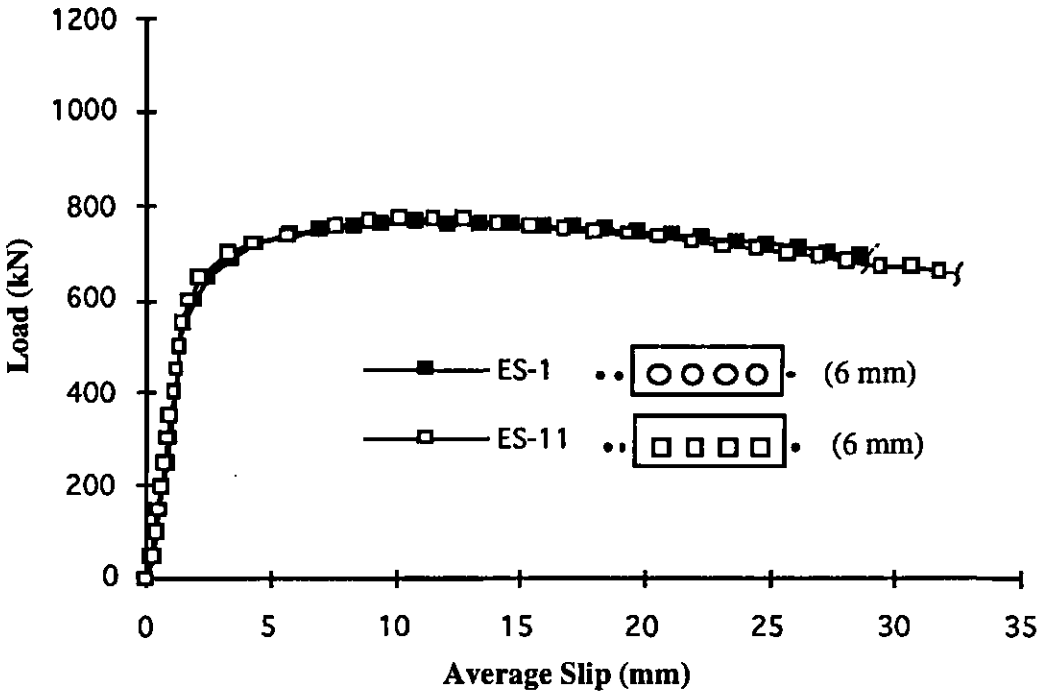

Fig. 4.13 Load-slip relationship of specimens ES-1 and ES-11

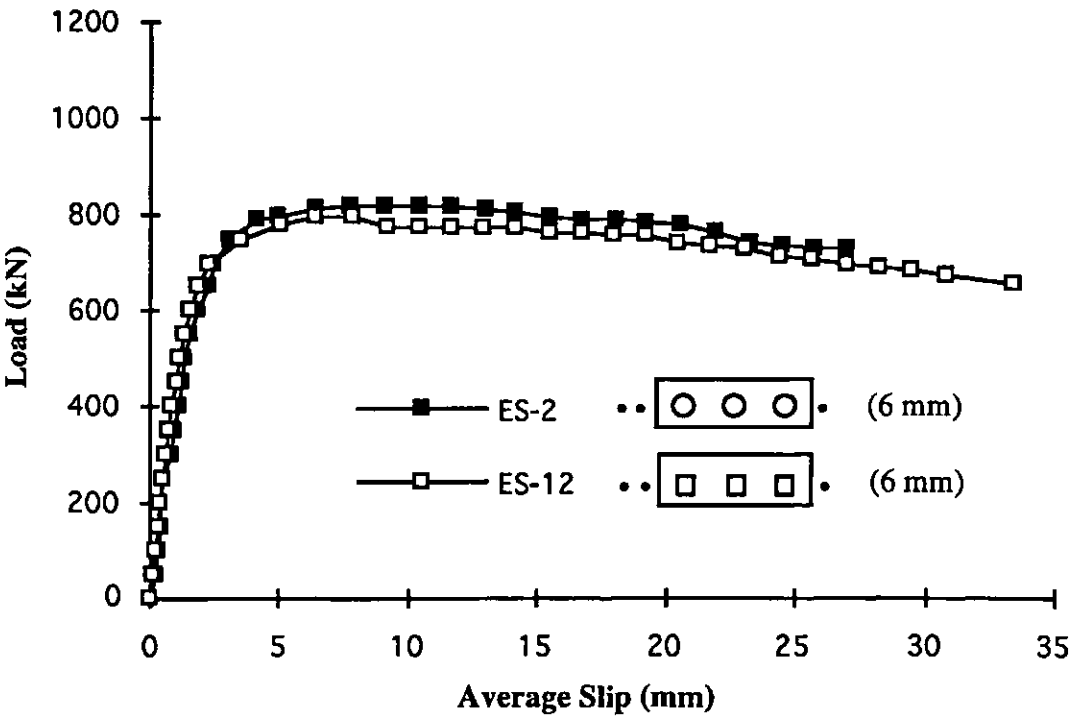

Fig. 4.14 Load-slip relationship of specimens ES-2 and ES-12

4.5 Behaviour of Slotted Perfobond Rib Connectors with Rectangular Openings

Fig. 4.15 presents the load-slip curves for push-out specimens ES-12 and ES-14, both with 6 mm thick perfobond rib plates and with rectangular openings. As shown in Figs. 4.16 and 4.17(a), specimens ES-12 and ES-14 featured unslotted and slotted perfobond rib connectors, respectively. The ultimate load of specimen ES-14 was approximately lower by 12% (695 kN compared to 795 kN for specimen ES-12). Although there is evidence of considerable deformation of the edge plates in specimen ES-14 (Fig. 4.17b), there is no sign of increased ductility. Since both specimens featured 6 mm thick rib plates, they were both naturally ductile.

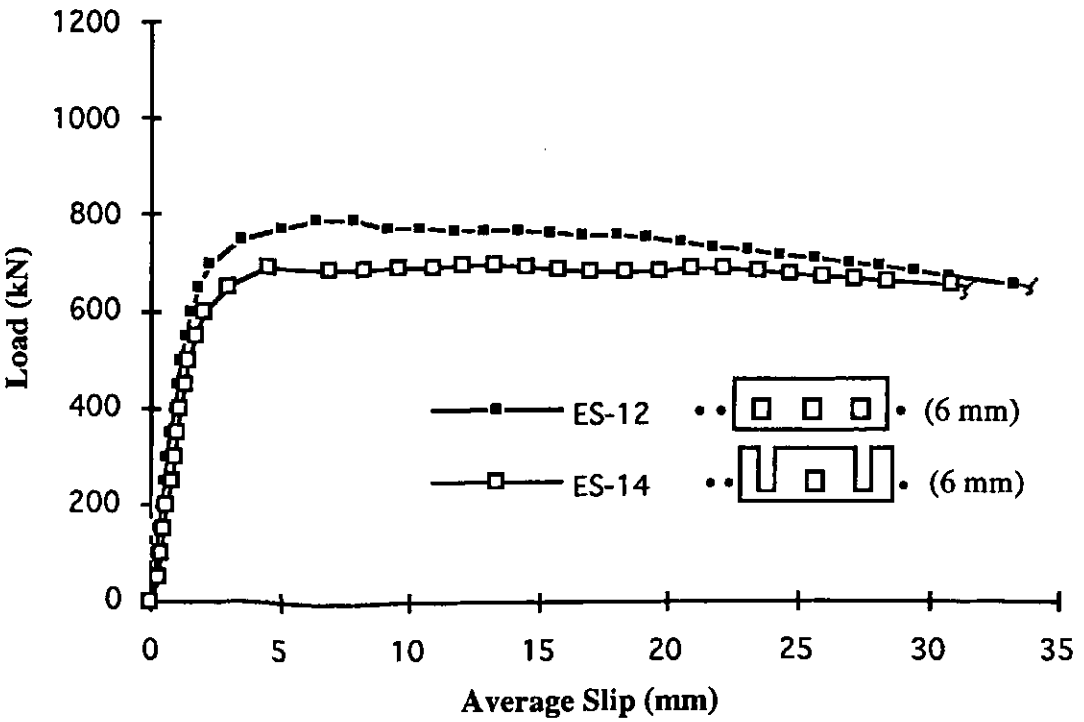

Fig. 4.15 Load-slip relationship of specimens ES-12 and ES-14

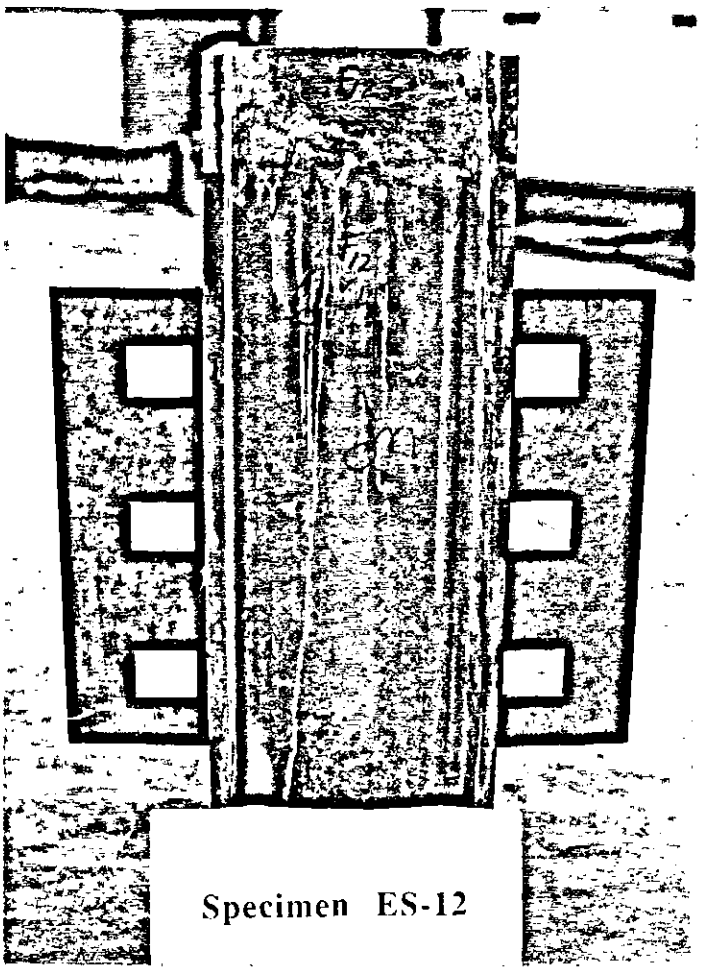

Fig. 4.16 Perfobond rib connector with rectangular openings

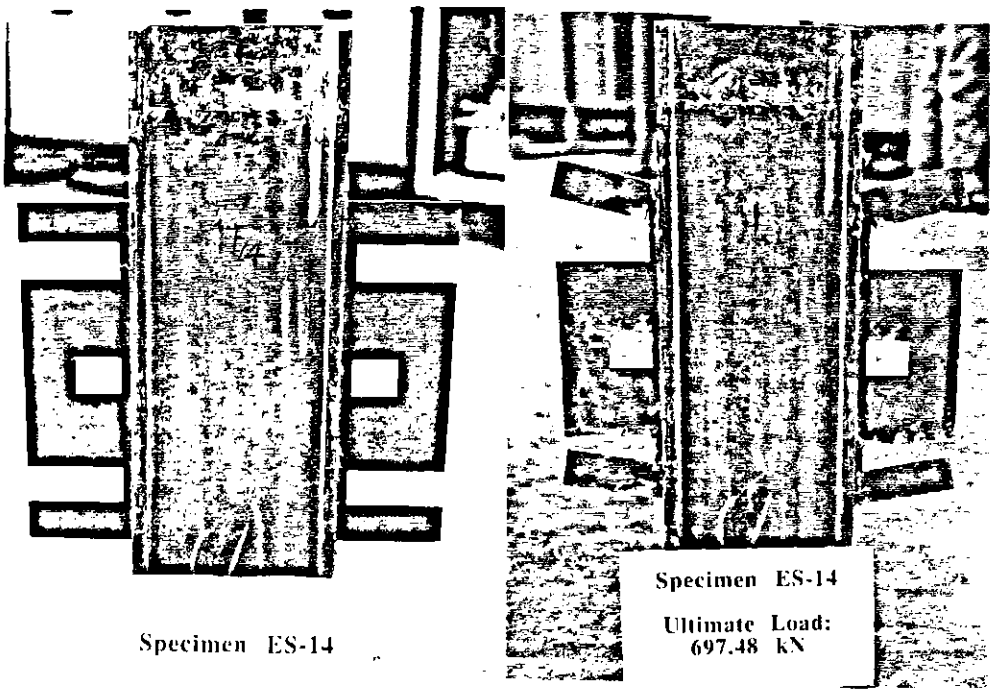

(a) Before test (b) After test

Fig. 4.17 Type 6 perfobond rib connector before and after test

Similar behaviour was also observed for specimens FS-12 and FS-14 which were identical to specimens ES-12 and ES-14 respectively except for the plate thickness (12 mm). In this case, the reduction in ultimate load for the specimen with slotted perfobond rib connector was approximately 6% although there was a slight increase in ductility. The load-slip curves for specimens FS-12 and FS-14 are presented in Appendix A.

Table 4.2 Test Results - Series 6
f'_c = 25.84 MPa, f'_{ct} = 2.93 MPa, slab with wire mesh

Specimen	Connector Geometry	Connector Type	Dimension (mm)	Ult. Load (kN)
FS-1	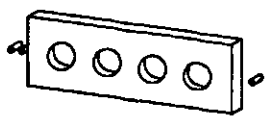	1	376x127x12	1024.30
FS-2	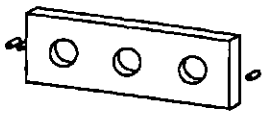	2	376x127x12	916.69
FS-3		3	376x127x12	984.44
FS-4	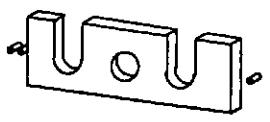	6	376x127x12	866.87
FS-5	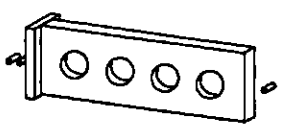	Type 1 with face plate	376x127x12 (50x127 face plate)	1456.74
FS-6	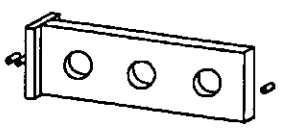	Type 2 with face plate	376x127x12 (50x127 face plate)	1385.00
FS-7	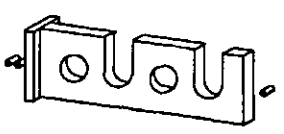	Type 3 with face plate	376x127x12 (50x127 face plate)	1414.89
FS-8	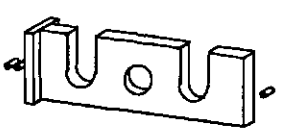	Type 6 with face plate	376x127x12 (50x127 face plate)	1245.50

Table 4.2 (Cont'd.) Test Results - Series 6
f_c = 25.84 MPa, f'_{ct} = 2.93 MPa, slab with wire mesh

Specimen	Connector Geometry	Connector Type	Dimension (mm)	Ult. Load (kN)
FS-9	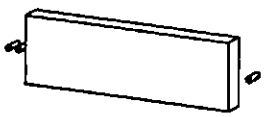	Solid	376x127x12	689.51
FS-10	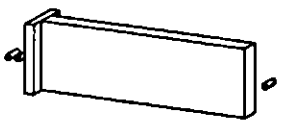	Solid with face plate	376x127x12 (50x127 face plate)	1153.83
FS-11	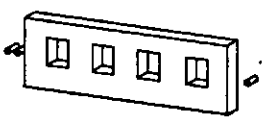	Type 1 with rectangular openings	376x127x12	966.51
FS-12	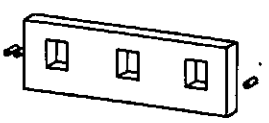	Type 2 with rectangular openings	376x127x12	960.53
FS-13	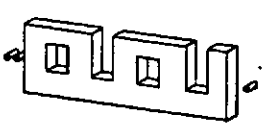	Type 3 with rectangular openings	376x127x12	974.48
FS-14	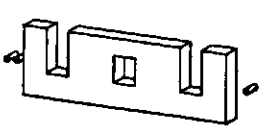	Type 6 with rectangular openings	376x127x12	898.75
FS-15	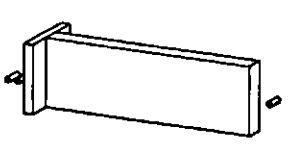	Solid with face plate	376x127x12 (75x127 face plate)	1434.82
FS-16	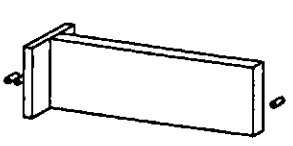	Solid with face plate	376x127x12 (100x127 face plate)	1564.35

CHAPTER FIVE

CONCLUSIONS AND RECOMMENDATIONS

5.1 Conclusions

This investigation led to the following main conclusions:

1. The test specimens with 12 mm slotted perfobond rib connectors exhibited slightly improved overall ductility compared to those featuring 12 mm normal perfobond rib connectors. However, the increased concrete dowel area provided by the slots in the perfobond rib connector tends to offset the increase in flexibility at low load levels.

2. The test specimens with 6 mm slotted perfobond rib connectors exhibited much improved overall ductility compared to those featuring unslotted connectors. Once again, there was no evidence of increased flexibility at low load levels.

3. As expected, specimens with 6 mm thick perfobond rib connectors indicated more ductility than those with 12 mm perfobond rib connectors. However, the increased ductility of the thinner perfobond rib connector was at the expense of the ultimate shear strength. The drop in strength, compared to that of a 12 mm thick perfobond rib connector, varied from 10 % to 22 % for normal connectors. For slotted connectors, the decrease was slightly higher. The specimens with 6 mm thick perfobond rib connectors exhibited more flexibility than those with 12 mm perfobond rib connectors. The flexibility of a 6 mm thick perfobond rib connector was very similar to that of a headed stud.

4. A significant portion of the ultimate shear resistance of a perfobond rib connector is provided by the concrete dowels. A 12 mm thick perfobond rib connector with three holes carried approximately 27% more load than that carried by a solid connector of the same size. There was a further increase in strength of approximately 5% when a fourth dowel was present. The contribution of three dowels in a 6 mm thick perfobond rib connector was approximately 34%. However, when a fourth hole was added there was a decrease in the shear capacity. The decline in shear capacity is attributed to the decrease in the structural integrity of the thin connector caused by the additional hole.

5. As expected, specimens with higher concrete strength provided higher ultimate shear capacity than identical specimens with concrete of a lower strength. The increase in shear capacity ranged from 11% to 16% when the concrete strength was increased from 20.6 MPa to 27.2 MPa. The higher values may be attributed to the higher shear capacity of the concrete dowels and the splitting resistance of concrete due to a higher concrete strength.

6. The addition of transverse reinforcement through the holes and slots increases the ultimate load of the specimens.

7. By distributing the bearing force on a wider area, a face plate placed in front of the perfobond rib connector delayed the formation of longitudinal splitting and thereby enhanced the ultimate capacity of the specimen. The increase in the ultimate load capacity was in excess of 30%. There was also a substantial increase in the ductility.

8. For the specimens with face plates, failure was caused largely due to the crushing of concrete in front of the face plates. Once the concrete crushed, the load carrying capacity went down quickly.

9. The load-slip behaviour of specimens featuring perfobond rib connectors with square and circular holes of equal area was almost identical. The sharp corners of the square hole did not produce any detrimental effects.

All in all, the results presented in this thesis indicate that thin and slotted perfobond rib connectors can be used effectively in composite beams with solid slab.

5.2 Recommendations for Further Research

1. The substantial increase in load carrying capacity as well as the enhancement in ductility would make the use of face plates a desirable option. In fact, this may turn out to be an entirely new area for further exploration. More work in this area is highly recommended.

2. To reduce the cost of fabrication, a standard tee section could be used instead of welding a face plate in front of a perfobond rib connector as illustrated in Fig. 5.1(a). Moreover, there may be no need to punch holes through the web plate as shown in Fig. 5.1(b), since the presence of the face plate diminishes the contribution of the concrete dowels. The possibility of using standard tee sections as shear connectors should also be investigated.

3. Although a number of specimens with unperforated plates have been tested to determine the contribution of the concrete dowels, no attempt has been made so far to isolate the effect of direct bearing stresses on the front end of the plate as shown in Fig. 5.2(a). It is recommended that a number of tests should be conducted on specimens containing a piece of foam in front of the plate, as illustrated in Fig. 5.2(b), to study this issue.

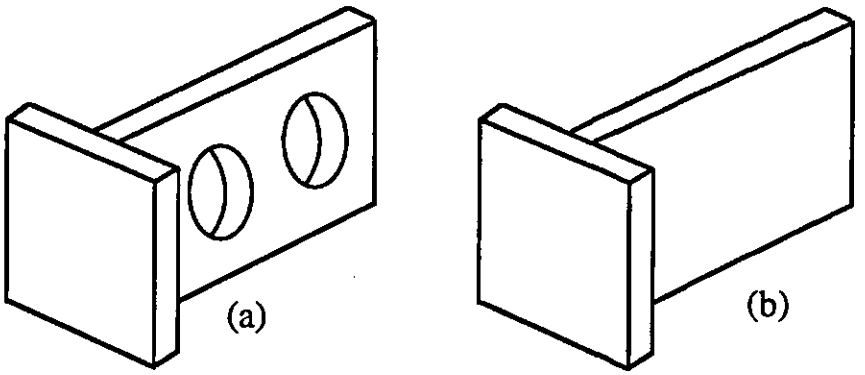

Fig. 5.1 Perforated and unperforated tee sections

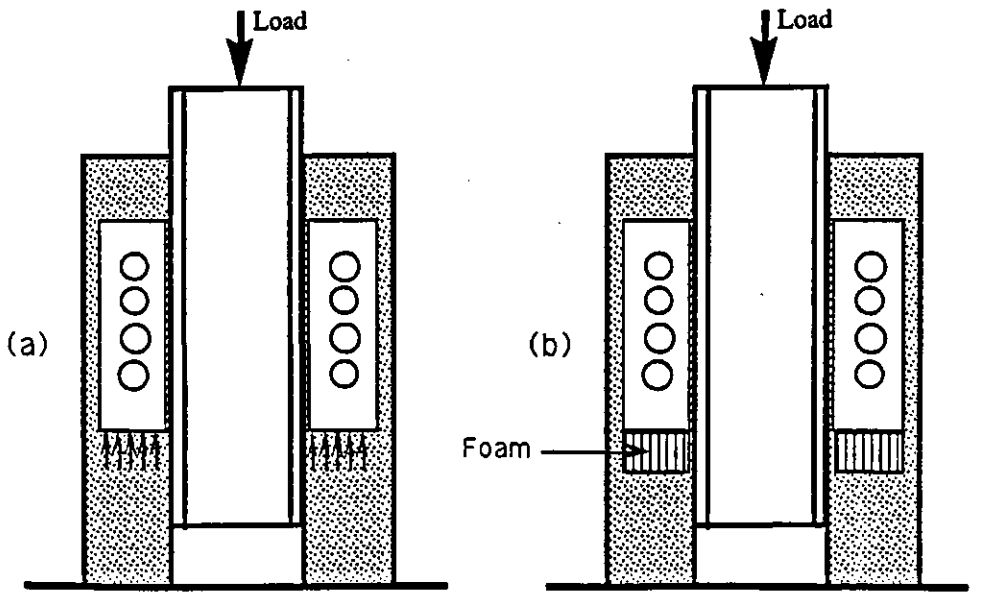

Fig. 5.2 Isolation of bearing stress on plate front ends

4. Although earlier test results indicated that the concrete dowels transfer load through double shear, it is recommended that a number of tests be carried out to lay the issue concerning transfer of load through a cone of compression to rest. This can be done by testing a number of push-out specimens featuring normal perfobond rib connectors of different thicknesses containing a piece of foam in front, as illustrated in Fig. 5.3. If load transfer occurs only through double shear, the thickness of the plate should not make any difference in the dowel capacity. If load transfer occurs through radiation, the specimens with thicker perfobond rib connectors should provide extra capacity. The presence of the foam block would eliminate the front end bearing stresses.

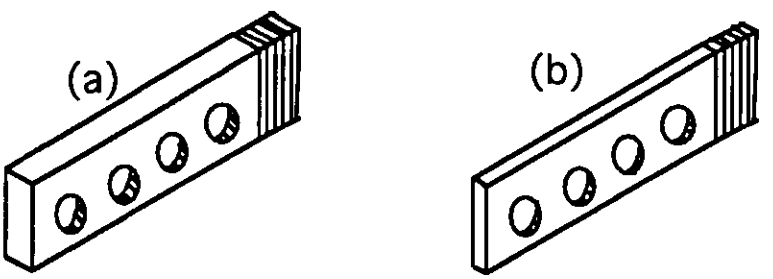

Fig. 5.3 Thick and thin perfobond rib connectors with foam blocks

As indicated earlier, this issue can also be resolved by testing a number of push-out specimens featuring perfobond rib with circular and rectangular openings of approximately the same cross-sectional areas, as illustrated in Fig. 5.4. If load transfer does occur through radiation, a rectangular hole with the larger contact area than that of a round one should provide higher resistance. However, the possibility of stress concentration at the corners of a rectangular hole makes this a less desirable option.

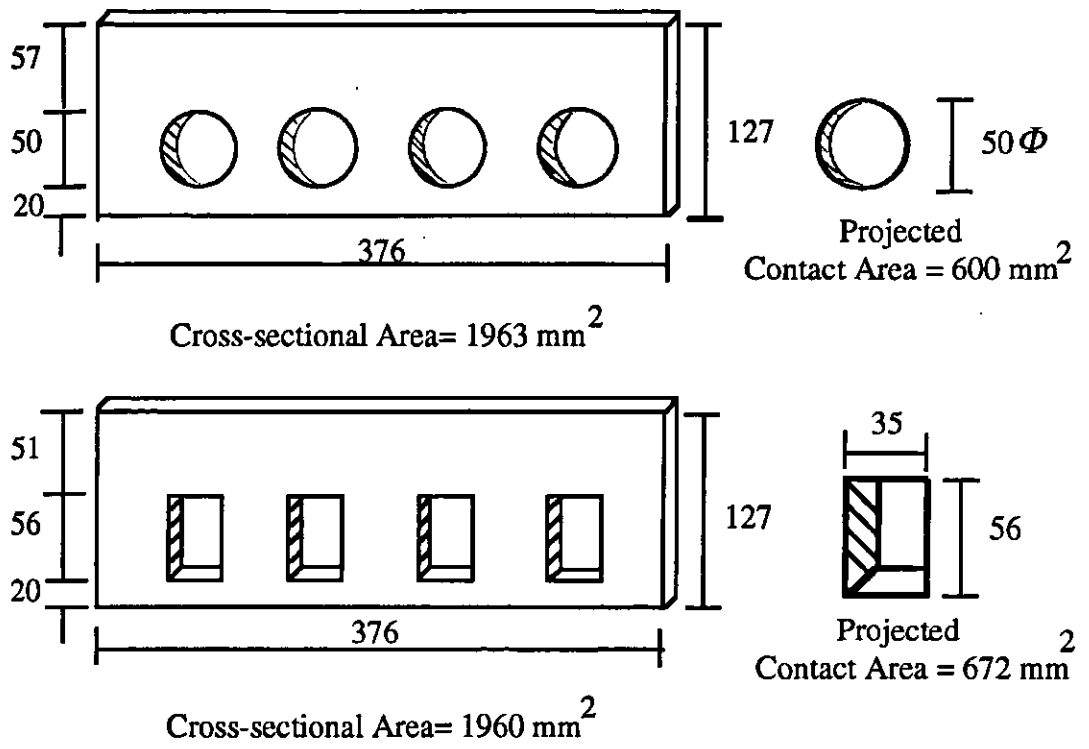

Fig. 5.4 Perfobond rib connectors with circular and rectangular openings

References

Antunes, P.J. 1988. Behavior of Perfobond Rib Shear Connectors in Composite Beams. B.Sc. Thesis, Department of Civil Engineering, University of Saskatchewan, Saskatoon, Canada.

Canadian Standard Association 1989. CAN3-S16.1-M89. Steel Structures for Buildings-Limit State Design, Rexdale, Ontario.

Davis, C. 1967. Small-Scale Push-out Tests on Welded Stud Shear Connectors, Concrete, September, 311-316.

Driscoll, Jr., G.C. and Slutter, R.G. 1961. Research on Composite Design at Lehigh University. Proceedings, National Engineering Conference, AISC, May.

Oguejiofor, E.C., and Hosain, M.U. 1994a. A Parametric Study of Perfobond Rib shear Connectors. Canadian Journal of Civil Engineering.[In Press].

Oguejiofor, E.C., and Hosain, M.U. 1994b. Tests of Full Size Composite Beams with Perfobond Rib Shear Connectors. Canadian Journal of Civil Engineering.[In Press].

Oguejiofor, E.C., and Hosain, M.U. 1994c. Perfobond Rib Shear Connectors: An Analytical Study. Proceedings of the CSCE Annual Conference, Winnipeg, June 1 - 4.

Oguejiofor, E.C., and Hosain, M.U. 1993. Shear Capacity of Perfobond Rib Connectors. Composite Construction in Steel and Concrete II. Special Publication of the ASCE Structural Division. New York, N.Y., pp. 883-898.

Oguejiofor, E.C., and Hosain, M.U. 1992. Behaviour of Perfobond Rib Shear Connectors in Composite Beams: Full Size Tests. Canadian Journal of Civil Engineering., 19(2), 224-235.

Oguejiofor, E.C., and Hosain, M.U. 1991. Perfobond Rib Shear Connectors: An Experimental Investigation. Proceedings of International Conference on Steel and Aluminum Structures, Singapore. May 22 - 24, 62 - 71.

Ollgaard, J.G., Slutter, R.G. and Fisher, J.W. 1971. Shear Strength of Stud Connectors in Lightweight and Normal-Weight Concrete, AISC Engineering Journal, vol. 8, 55-64

Quddusi F., and Hosain, M.U. 1993. Behaviour of Slotted and Flexible Perfobond Rib Shear Connectors. Proceedings of the CSCE Annual Conference, Fredericton, June 8-11, Volume II, pp. 629-638.

Roberts, W., and Heywood, R. 1992. Shear Connectors for Composite Structures. Physical Infrastructure Centre Digest, 1(4), Queensland Univ. of Tech., Brisbane, Australia, 4-5.

Veldanda, M.R., and Hosain, M.U. 1992. Behavior of Perfobond Rib Shear Connectors in Composite Beams: Push-out Tests. Canadian Journal of Civil Engineering., 19(1), 1-10.

Veldanda, M.R.1991. Behavior of Perfobond Rib Shear Connectors: Push-out Tests. M.Sc. Thesis, Department of Civil Engineering, University of Saskatchewan, Saskatoon, Canada.

Viest, I.M. 1960. Review of Research on Composite Steel-Concrete Beams. Journal of Structural Division, ASCE, Vol. 86,No. ST6, June,1-21

Zellner, W. 1987. Recent Designs of Composite Bridges and a New Type of Shear Connectors. Proceedings of the ASCE/IABSE Engineering Foundation Conference on Composite Construction, Henniker, New Hampshire, June 7-12, 240-252.

Appendix A

Comparative load-slip curves

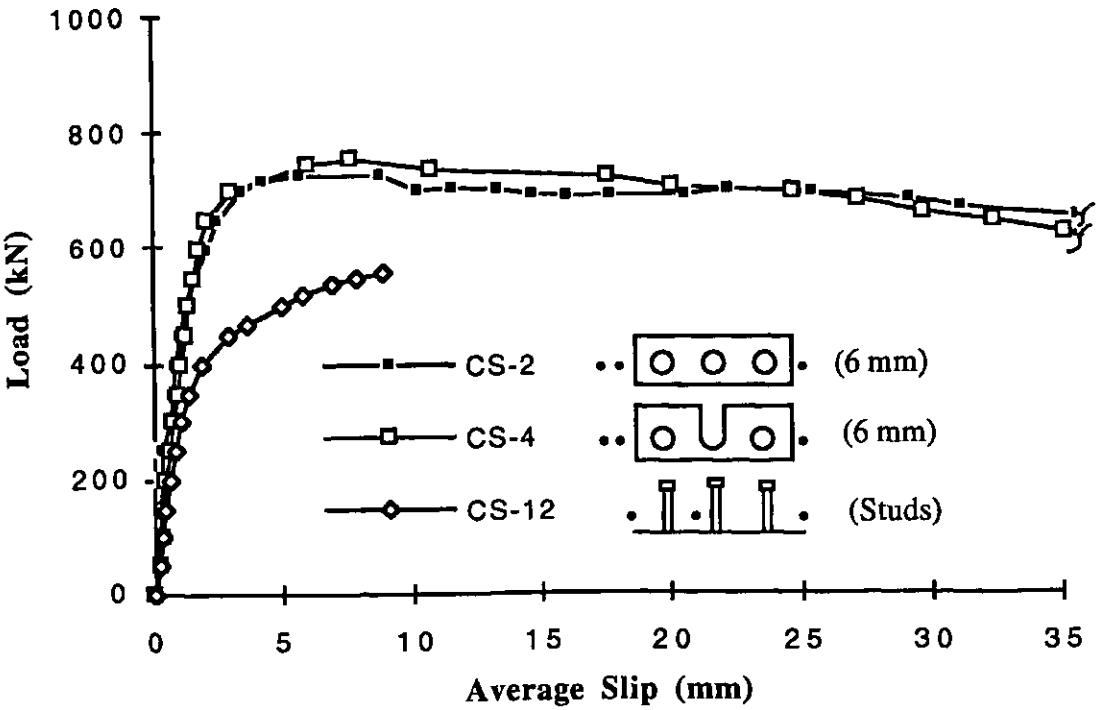

Fig. A.1 Load-slip curves for specimens CS-2, CS-4 and CS-12

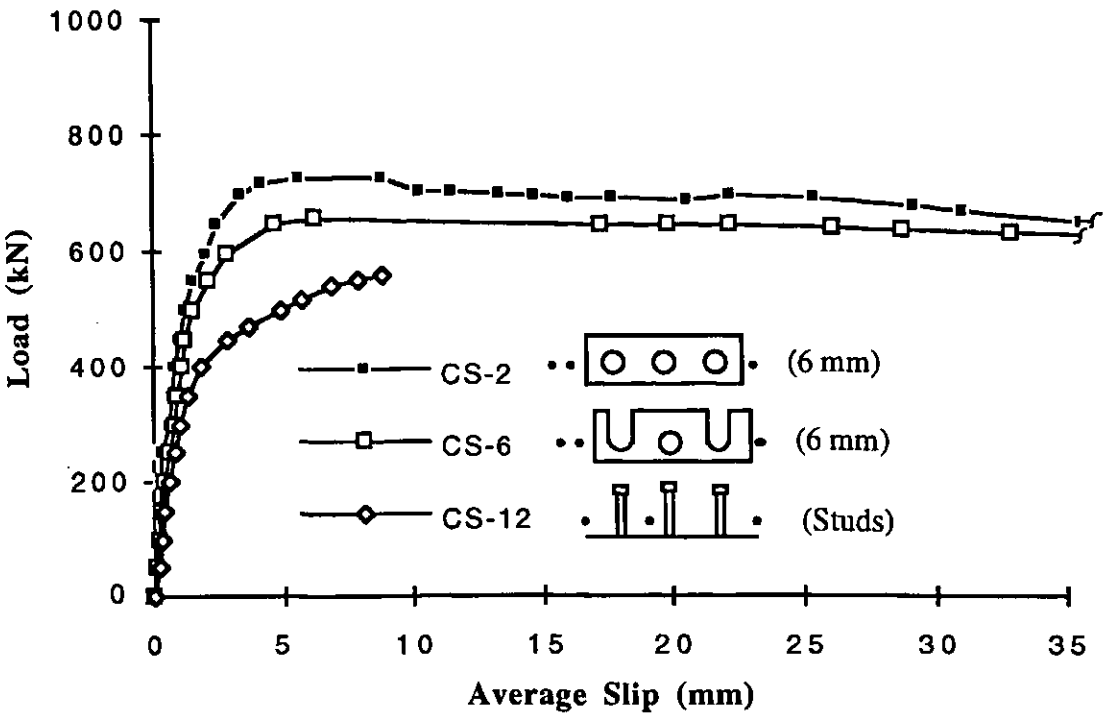

Fig. A.2 Load-slip curves for specimens CS-2, CS-6 and CS-12

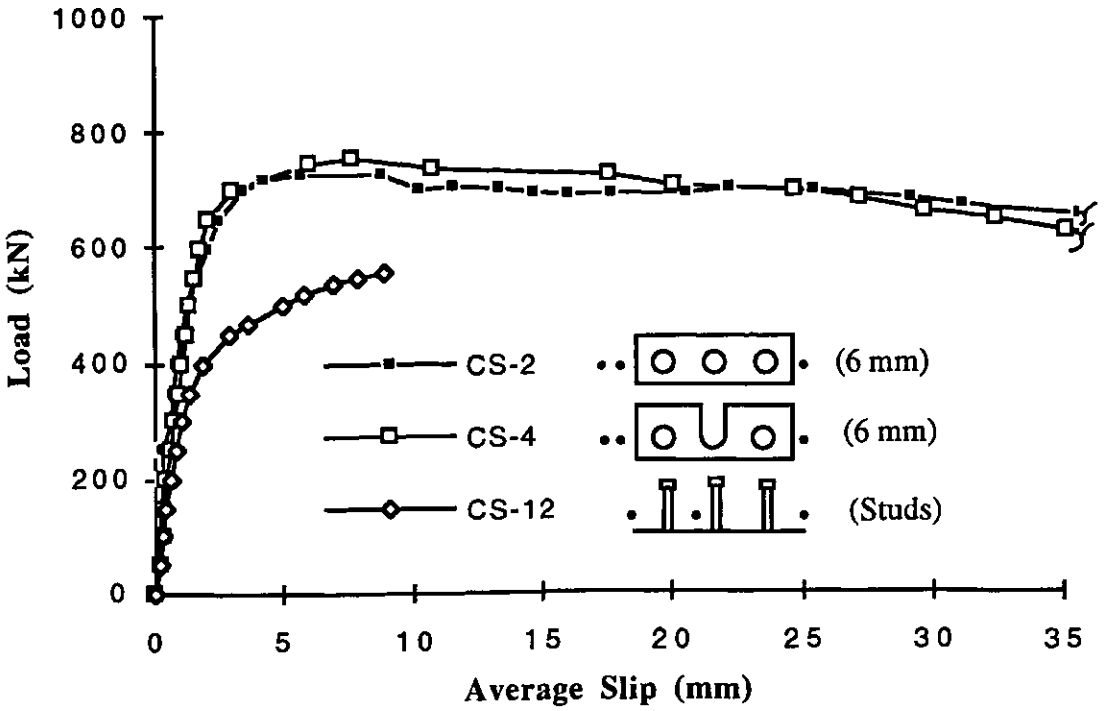

Fig. A.1 Load-slip curves for specimens CS-2, CS-4 and CS-12

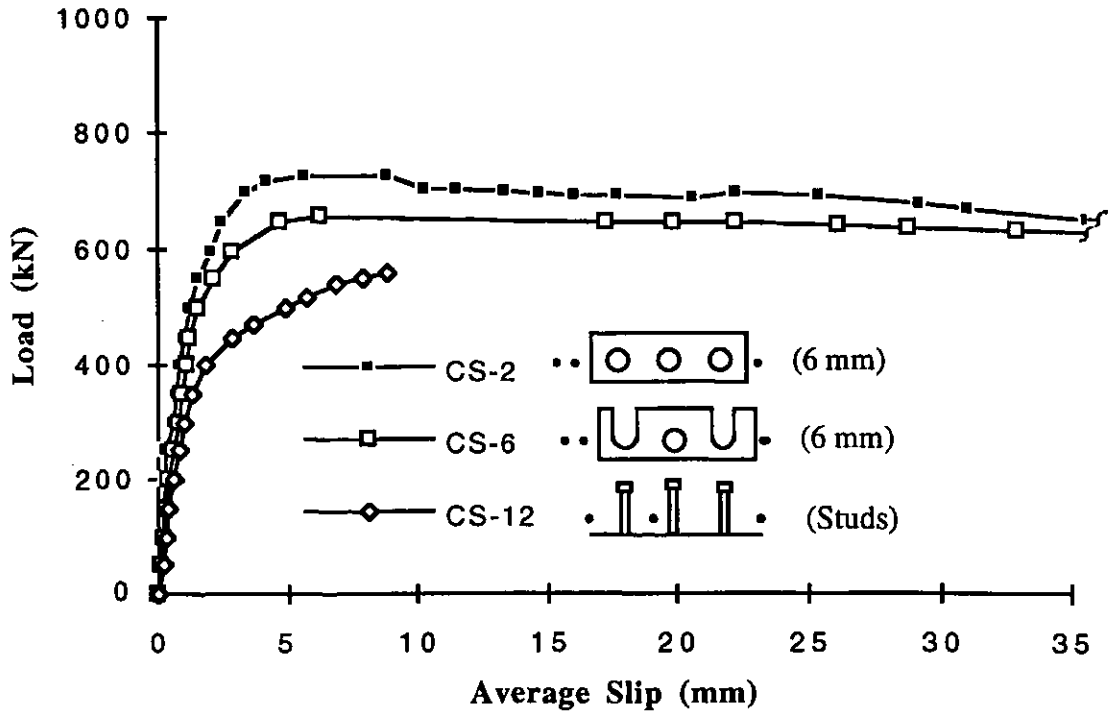

Fig. A.2 Load-slip curves for specimens CS-2, CS-6 and CS-12

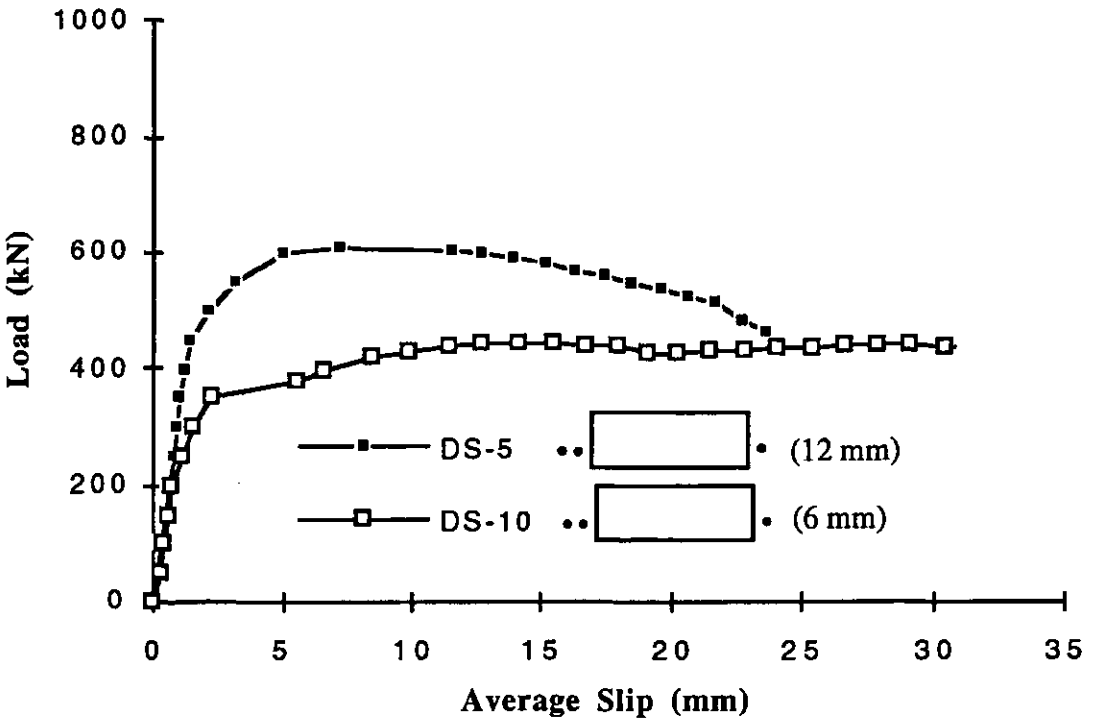

Fig. A.3 Load-slip curves for specimens DS-2 and DS-10

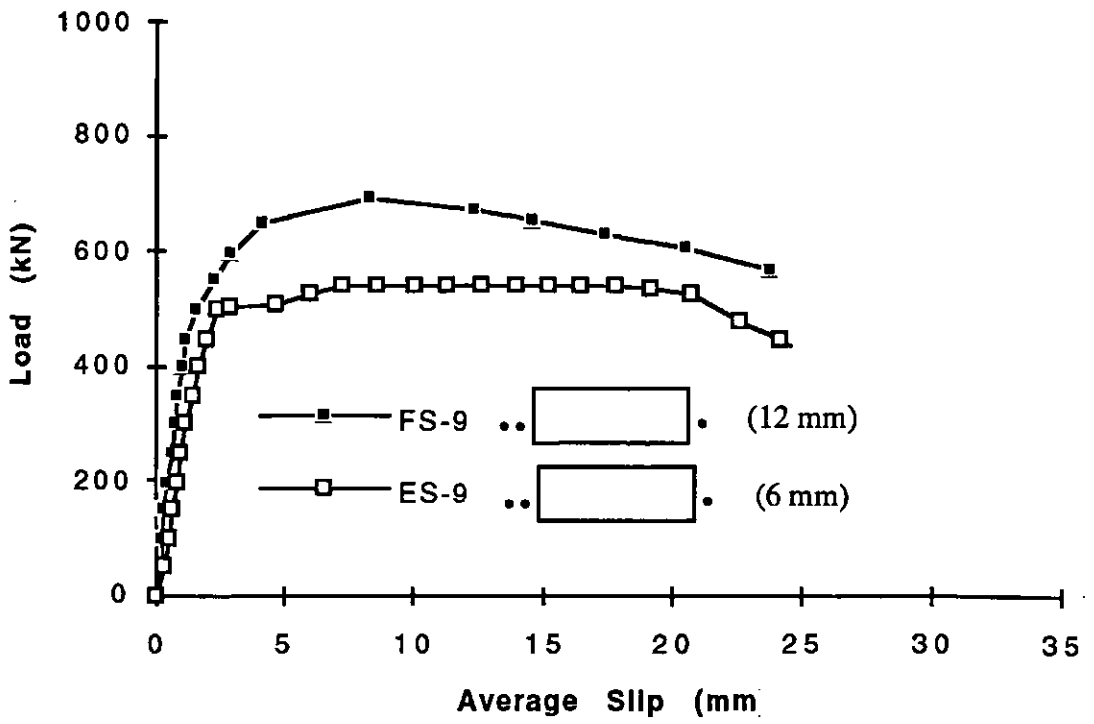

Fig. A.4 Load-slip curves for specimens FS-9 and ES-9

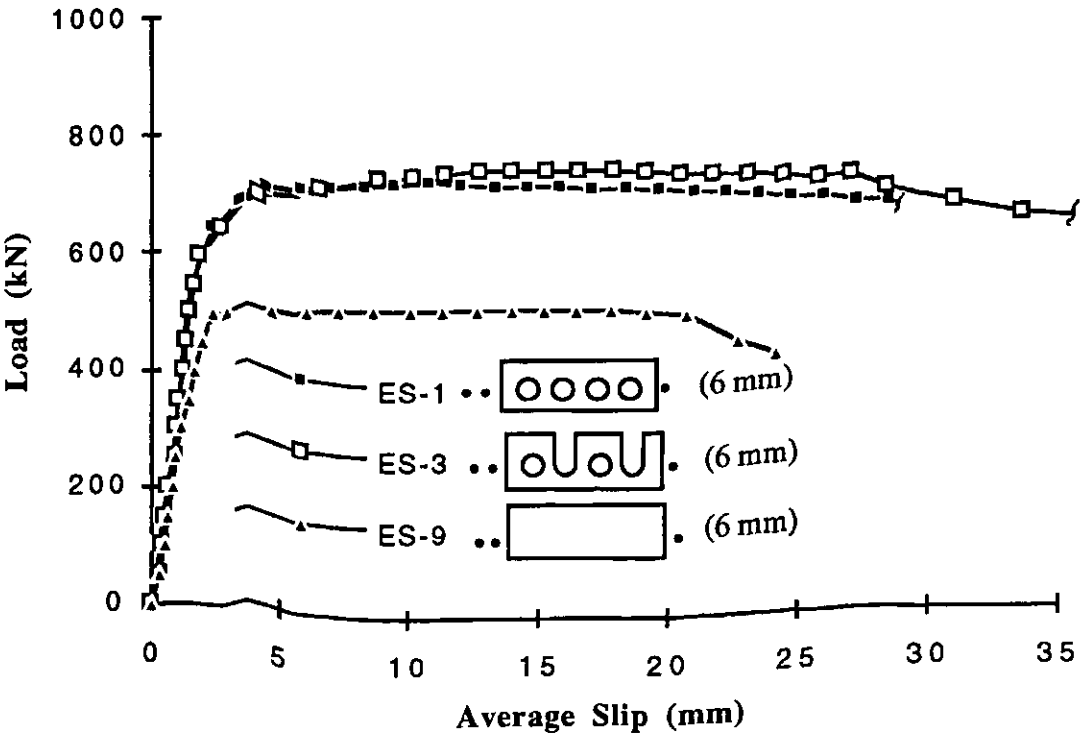

Fig. A.5 Load-slip curves for specimens ES-1,ES-3 and ES-9

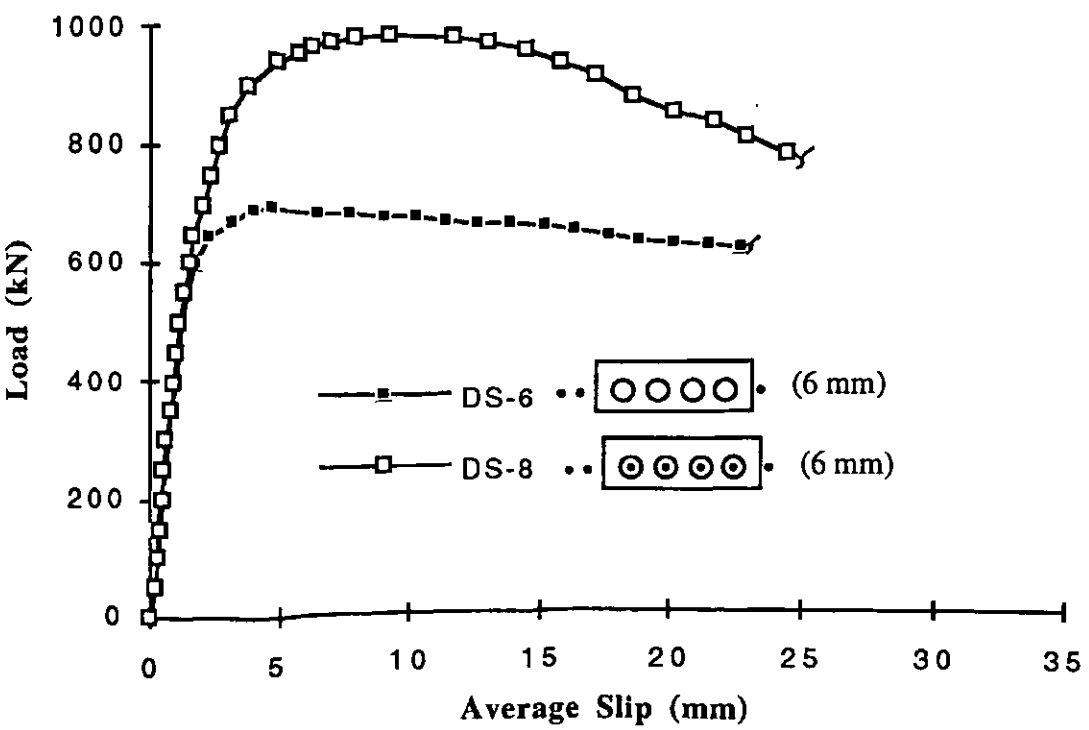

Fig. A.6 Load-slip curves for specimens DS-6 and DS-8

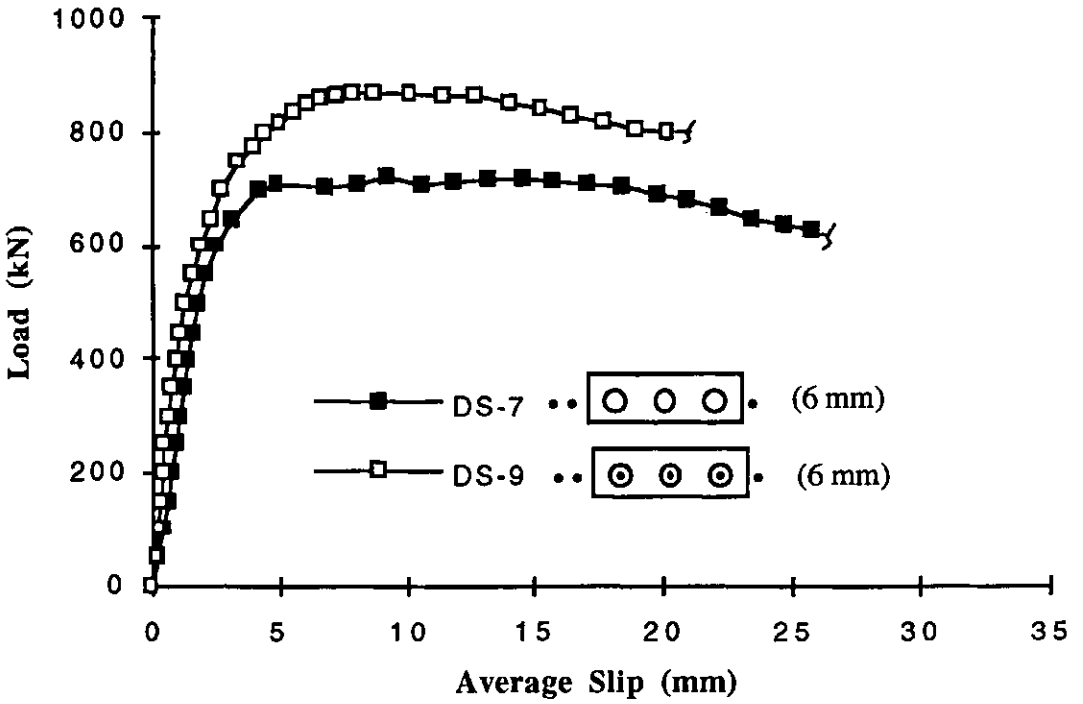

Fig. A.7 Load-slip curves for specimens DS-7 and DS-9

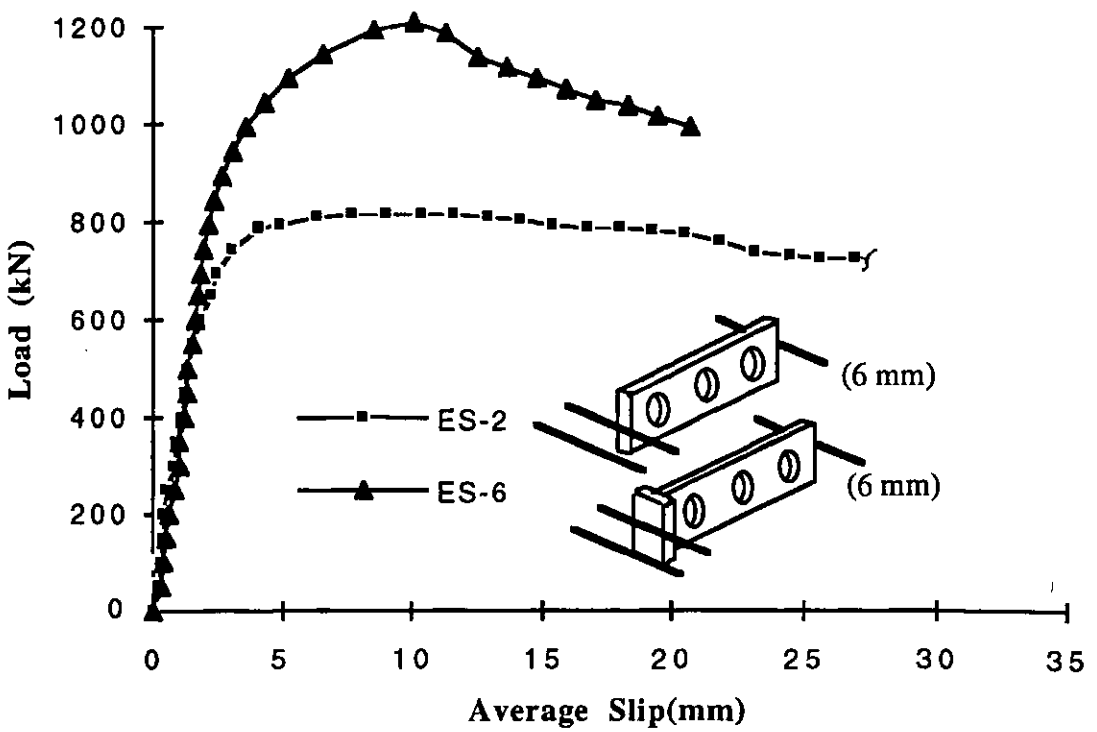

Fig. A.8 Load-slip curves for specimens ES-2 and ES-6

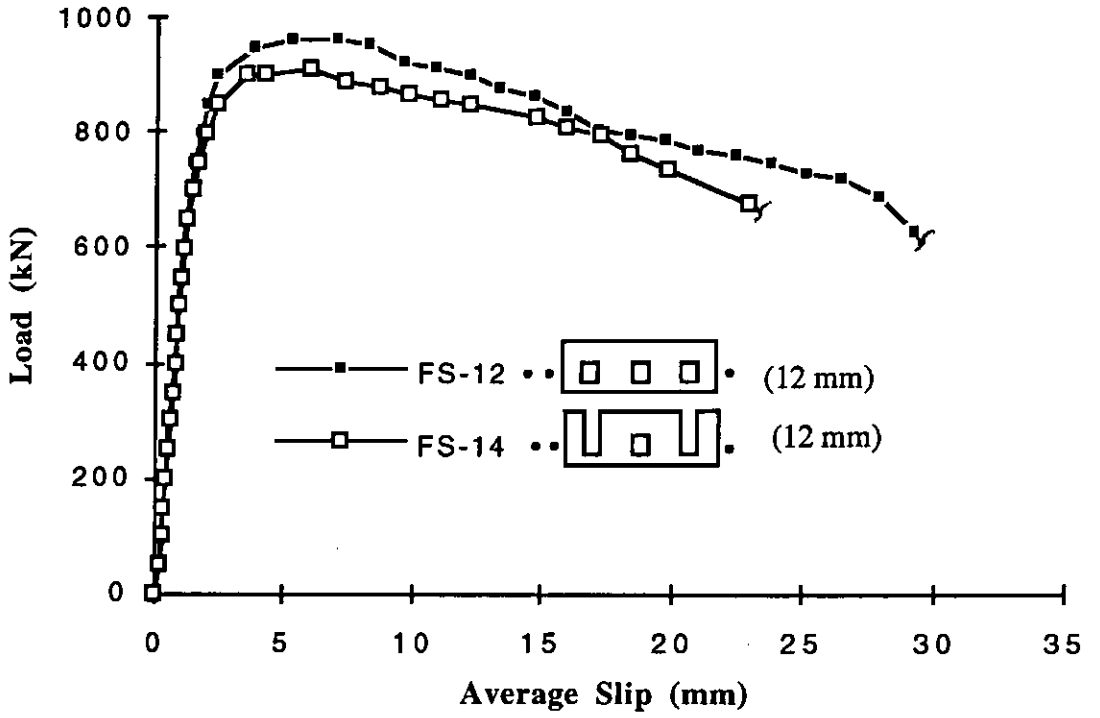

Fig. A.9 Load-slip curves for specimens FS-12 and FS-14

Appendix B

Photographs of some specimens after failure

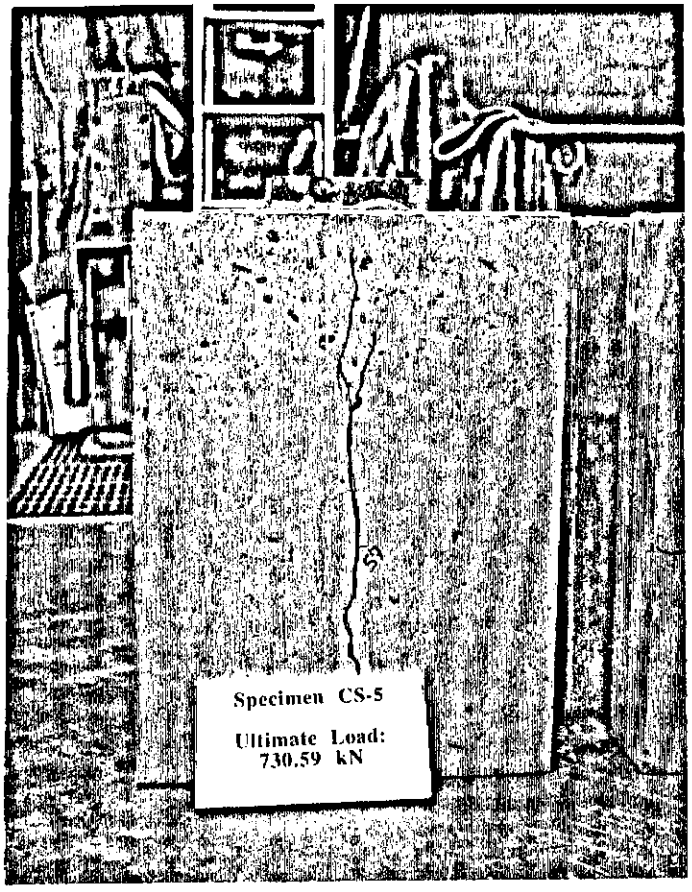

Fig. B.1 Type 6 perfobond rib connector after failure

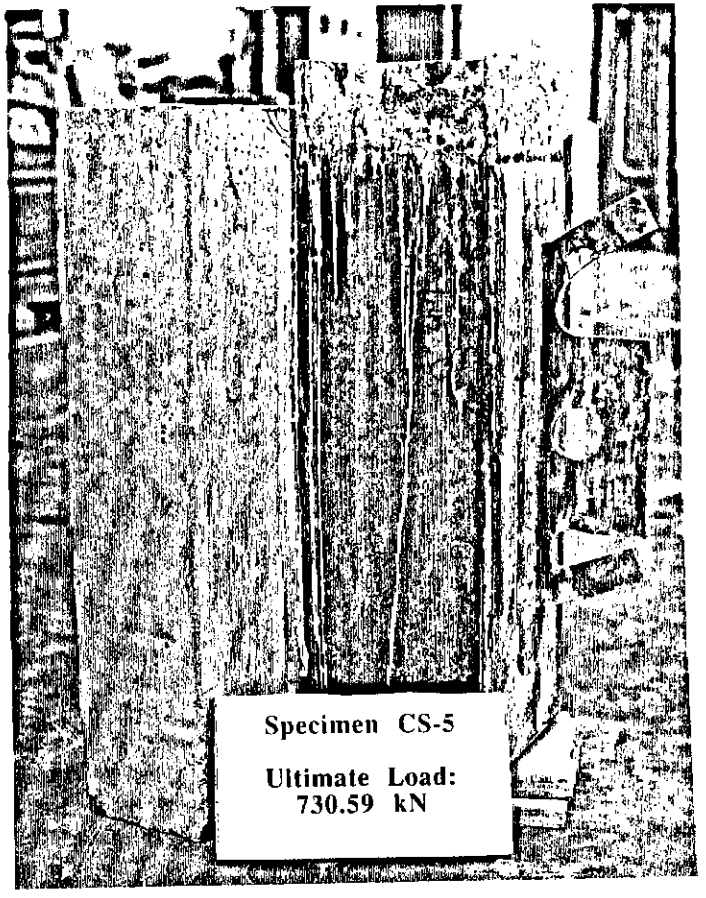

Fig. B.2 Specimen CS-5 after failure

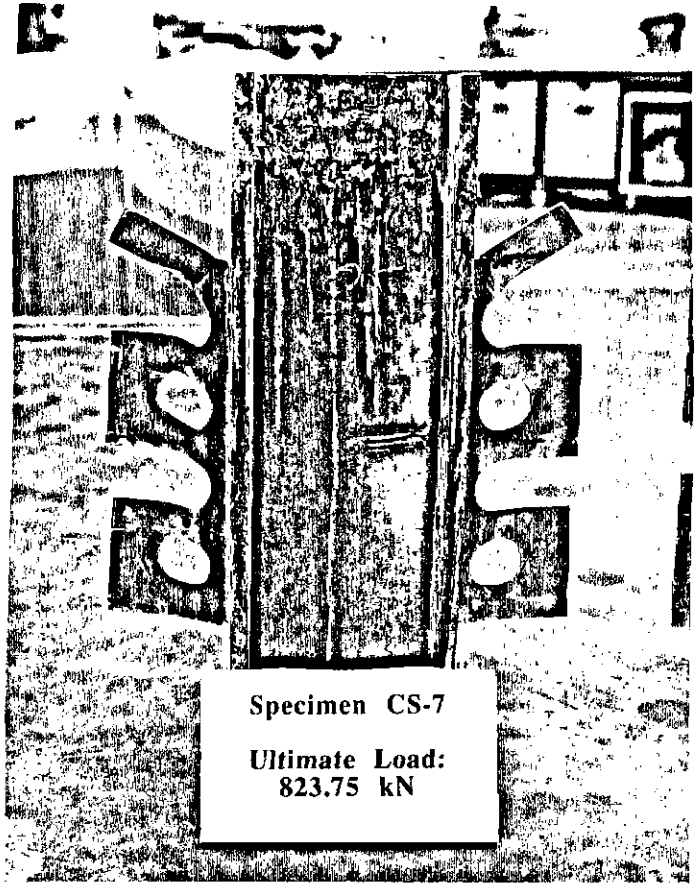

Fig. B.3 Type 3 perfobond rib connector after failure

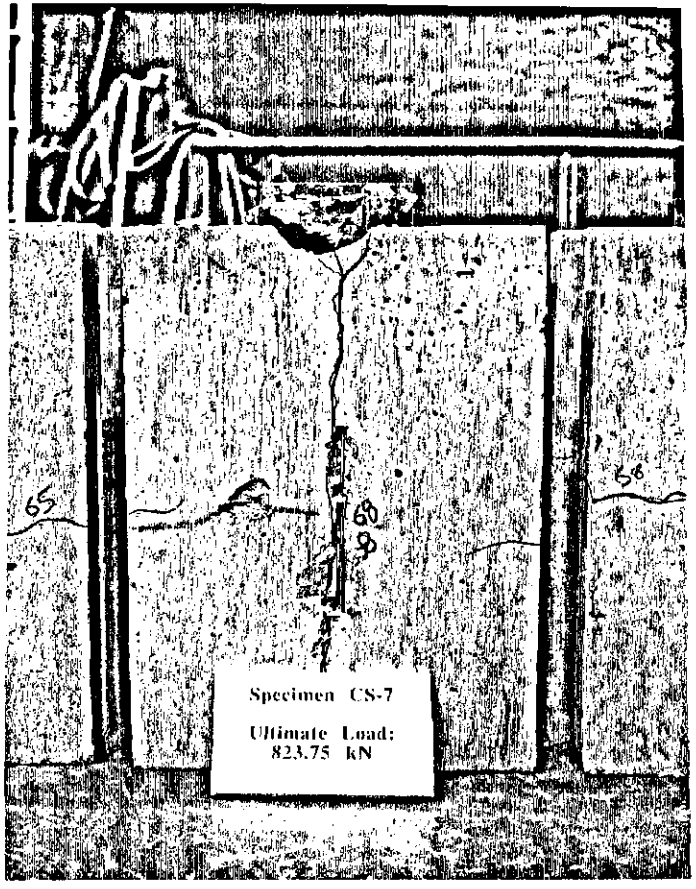

Fig. B.4 Specimen CS-7 after failure

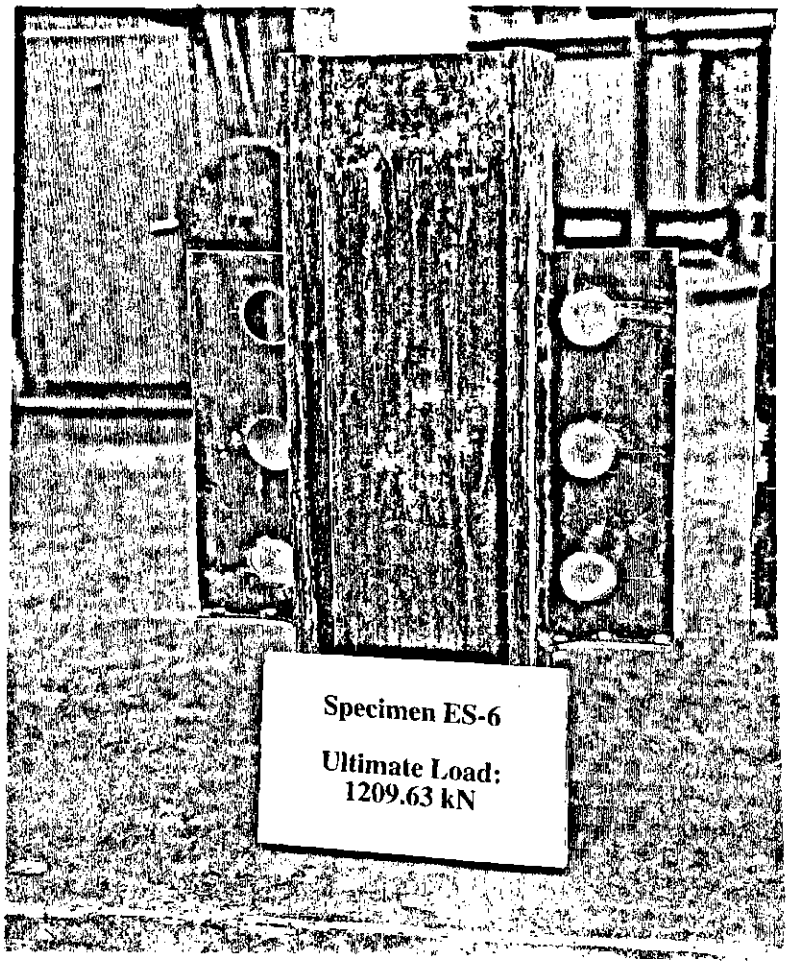

Fig. B.5 Type 2 perfobond rib connector with face plate after failure

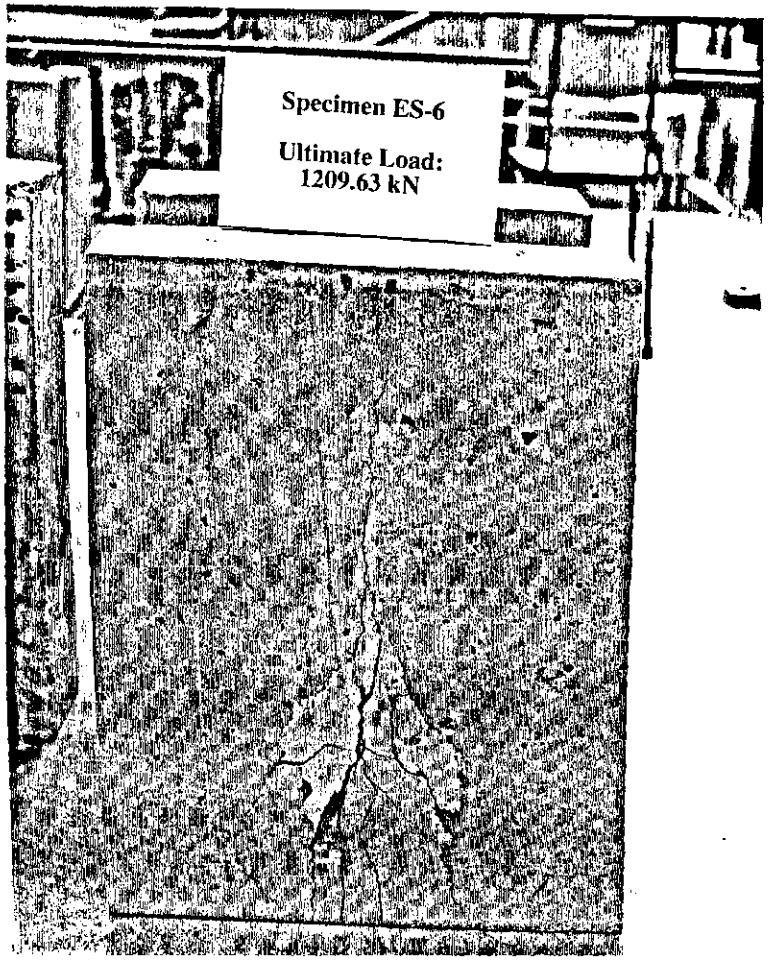

Fig. B.6 Specimen ES-6 after failure

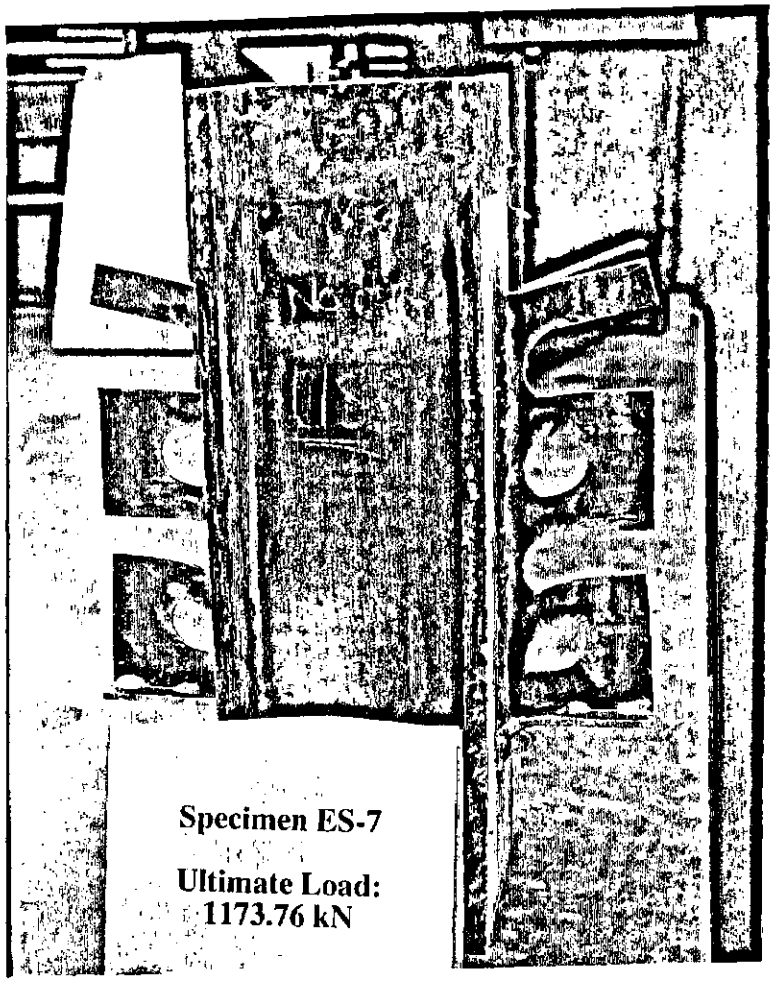

Fig. B.7 Type 3 perfobond rib connector with face plate after failure

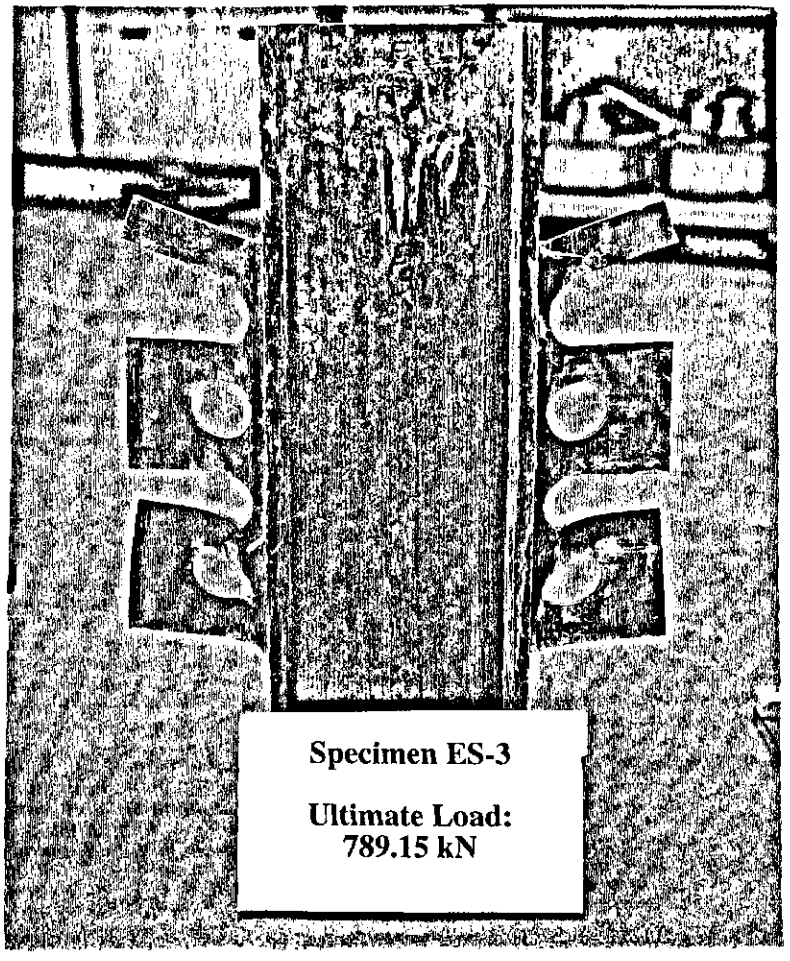

Fig. B.8 Type 3 perfobond rib connector after failure

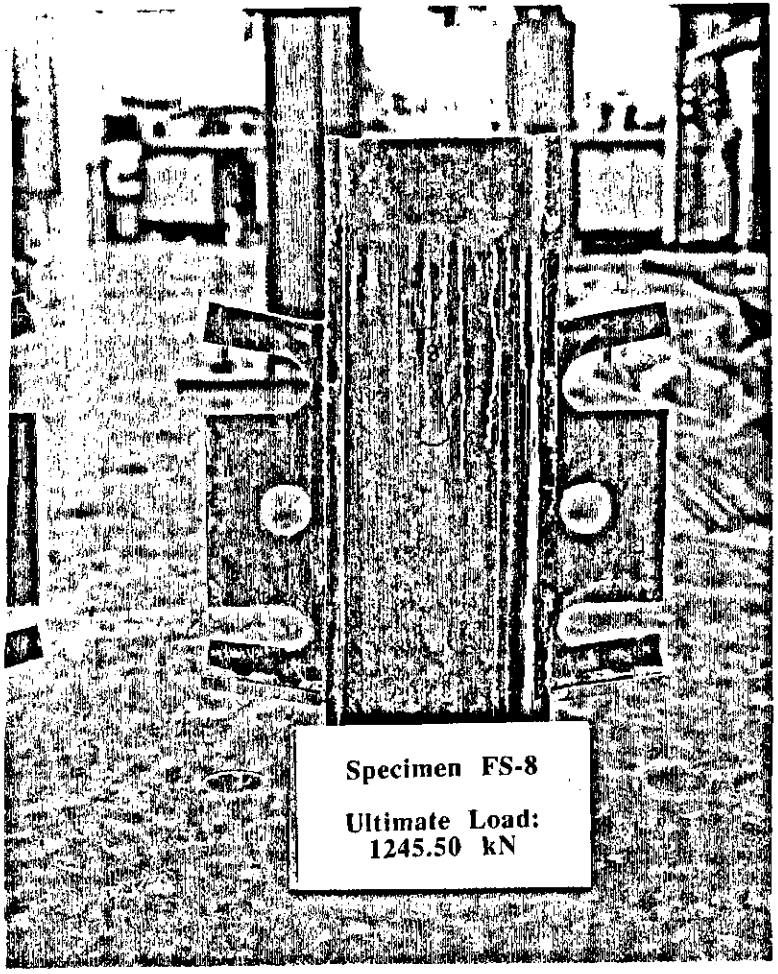

Fig. B.9 Type 3 perfobond rib connector with face plate after failure

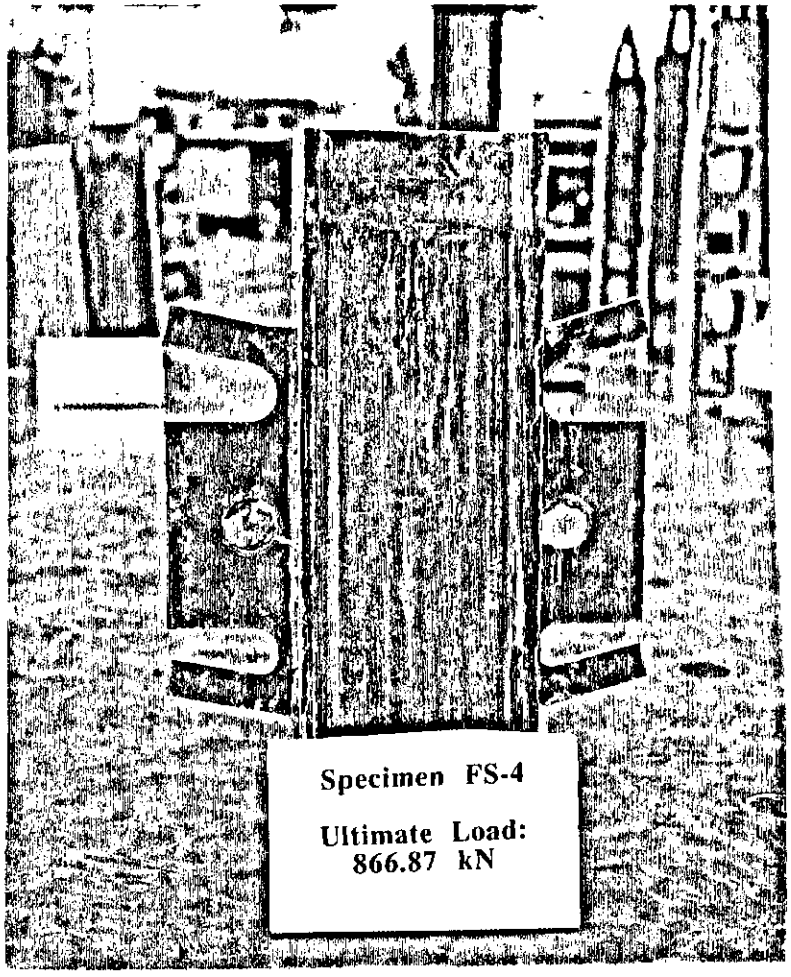

Fig. B.10 Type 6 perfobond rib connector after failure

Appendix C

Correspondance from Blackwell Consultilg Engineer

RODNEY BLACKWELL

CONSULTING ENGINEER

30 High Street, Stevenage, Herts. SG1 3EF

Tel: (0438) 743518
Fax: (0438) 315807

15th October 1992

M. R. Veldanda and M. U. Hosain
Department of Civil Engineering,
University of Saskatchewan,
Saskatoon, Sask
Canada
S7N 0W0

Dear Sir,

I am writing in response to your paper "Behaviour of perfobond rib shear connectors : push out tests" in the February 1992 edition of the Canadian Journal of Civil Engineering.
Unlike stud connectors, which have standard sizes, it appears that perfobond connectors could be designed to suit individual projects, in the same way as any other connection, provided that design rules can be established.
Can you please say what further tests are contemplated which would enable such rules to be formulated?
From the tests reported in your paper, the capacity of the concrete "dowels" does not appear to be directly related to the area of the holes. Between tests VSF-2 and VSF-4 there is an increase of 55KN capacity, from 380KN to 435KN, for one extra 35mm dia hole.
Between tests VDS-11 and VDS-10, the increase is 219KN, from 289KN to 508KN, for four extra 50mm dia holes, each of which has twice the area of a 35mm hole. So larger hole size alone does not give much benefit. Consider also the small difference between results VSF-2 (435KN) and VDS-7 (456KN).
Do you envisage that the load capacity is derived from a shear mechanism, or from a cone of compression radiating from the back surface of the hole, or some other means? In the first case, the thickness of the plate should make no difference to dowel capacity, whereas in the second case,the larger contact area within the hole should provide extra capacity (Apart from the extra plate front end contact area), and square holes would be better than round ones.
One other consideration is the load capacity with concrete only on one side of the plate. It may be that some beams do not need ribs or studs, just holes in the ends of the top flange.

Yours Sincerely

R A Blackwell, P.Eng

BLACKWELL B.A., M.I.C.E.

Appendix D

Tensile test procedure of headed studs

D.1 Description of the tensile test for studs

The studs were tested according to ASTM A-370. First the studs were machined to the specified dimensions. This resulted in specimens of 127 mm length with a 60 mm long reduced section. The diameter at the reduced section was 12.5 mm. The ends were threaded so that the specimen could be screwed on to the holders attached to the testing machine. Before positioning the specimen on the testing machine, a gauge length of 2 inches was marked on the specimen. After the specimen was placed on the testing machine, a dial gauge of 2 inches gauge length was attached to the specimen.

During testing, load and displacement readings were taken until the yield point was reached. The dial gauge was then removed and the specimen was loaded to failure. The maximum load attained was recorded. After the failure of the specimen, the final gauge length and the mean diameter of the specimen at the fracture point were measured. These measurements were used to calculate the percentage elongation and the percentage reduction in area. The yield stress of the specimen was determined using the 0.2% offset technique.